École Centrale de Lyon
TFE 2011

CSIRO Centre for Marine and Atmospheric Research
Hobart TAS Australia

End-of-studies final report

An approximate neutral density variable for the world oceans

Guillaume Sérazin

Supervisors :	*Option* : Aeronautics
ECL : Richard J. Perkins	*Filière* : Propulsion
Company : Trevor J. McDougall Paul M. Barker (Co-supervisor)	*Métier* : Research & Development

Abstract

Transport of heat, salt and other tracers in the ocean occurs principally along neutral surfaces. Due to the significant differences in mixing intensities between the exchanges that occur along and those that occur through these surfaces, it is crucial to be able to accurately determine neutral surfaces in order to describe flows inside the ocean. Because neutral surfaces are not mathematically well defined, several density variables have been introduced in order to approximate them. Potential density referenced to 2000 db is typically used in oceans models because it is fast compute. However, the results are close to being neutral only around the reference pressure. The two Neutral Density functions γ^n and γ^i currently provide the best approximation of neutral surfaces unfortunately they are not practical solutions for use in ocean models because they are very computationally intensive. Hence, this project aims to build an approximate form of Neutral Density, γ^{GP}, which is designed to replace the current variable σ_2 in ocean models. The world's oceans were decomposed into segments that covered each of the major oceanic basins. This allowed for accurate polynomial functions, γ^{poly}, to be fitted to a γ^i labelled version of the WOCE climatology. The global polynomial γ^{GP} is a result of combining each of the γ^{poly} functions. The polynomials have been built in terms of Practical Salinity S_P and potential temperature θ to be able be applied in current ocean models. The use of an approximate density surface introduces a fictitious diapycnal diffusivity (through the surface), D_f. If it is larger than $10^{-5}\, m^2.s^{-1}$, the error is significant describing neutral surfaces. Then, the γ^{poly} polynomials give 30% of improvement compared to σ_2 in the amount of fictitious dyapicnal diffusivity on the Southern Ocean and a least 40% on the other ocean basins. Performed on a snapshot of the ocean model MOM4, the global polynomial γ^{GP} has a 45% reduction in D_f greater than $10^{-5}\, m^2.s^{-1}$, when compared with those from σ_2.

Keywords

Physical oceanography, oceanic circulation, mixing, neutral surfaces, potential density, neutral density

Résumé

Les transports de chaleur, sel et autres traceurs dans l'océan se produisent principalement le long des surfaces neutres. Du fait de différences significatives au niveau de l'intensité des mélanges entre les échanges à travers et le long de ces surfaces, il est capital d'être capable de déterminer précisément ces surfaces neutres afin de décrire les écoulements au sein de l'océan. Comme il a été démontré que les surfaces neutres ne peuvent pas être correctement définies mathématiquement, des variables de densité ont été introduites afin de les approximer. La densité potentielle référencée à une pression de $2000\,db$, σ_2, est habituellement utilisée dans les modélisations numériques océaniques car elle est rapide à calculer. Cependant, les résultats ne sont proches d'être "neutre" seulement aux alentours de la pression de référence. Les deux fonctions γ^n and γ^i de Densité Neutre fournissent actuellement les meilleurs approximations des surfaces neutres, malheureusement, elles ne sont pas utilisables en pratique dans les modèles océaniques car elles requiert un temps de calcul trop important. Ce projet a donc pour but d'élaborer une forme approchée de Densité Neutre, γ^{GP}, conçue de façon à pouvoir remplacer la variable actuelle σ_2 dans les simulations océaniques. Les océans du monde ont été décomposés en différentes parties assimilées aux principaux bassins océaniques sur lesquels des fonctions polynomiales, γ^{poly}, ont pu être construites afin d'interpoler γ^i sur la climatologie WOCE. Le polynôme global γ^{GP} est le résultat de la recombinaison des fonctions γ^{poly}. Les polynômes ont été élaborés comme fonction de Salinité Pratique S_P et température potentielle θ afin d'être employés dans les modèles océaniques actuels. L'utilisation de surfaces approchées introduit une diffusivité diapycnale fictive (à travers la surface), D^f. Si cette valeur est supérieure $10^{-5}\,m^2.s^{-1}$, l'erreur n'est plus négligeable lors de la description des surfaces neutres. Les polynômes γ^{poly} montrent une amélioration de 30% en comparaison avec σ_2 en matière de diffusivité diapycnale fictive pour l'Océan Austral et d'au moins 40% pour les autres bassins océaniques. Appliqué sur un cliché du modèle océanique MOM4, le polynôme global γ^{GP} montre une réduction de 45% de D^f supérieur à $10^{-5}\,m^2.s^{-1}$ par rapport à celle introduite par l'usage de σ_2.

Mots-clés

Océanographie physique, circulation océanique, mélanges, surfaces neutres, densité potentielle, densité neutre.

Acknowledgements

To Trevor McDougall for having offered this opportunity and having been present all along this interesting project.

To Paul Barker for his help and having revised this report.

Contents

Introduction

The ocean is a stratified fluid medium whose thermodynamic properties are described by the equation of state of seawater. Stratification has an important role because it controls much of the flow in the ocean. Gradients in salinity and temperature generate the main oceanic circulation, called the thermohaline circulation. Since the beginning of the oceanographic science, it was noticed that the main flow is almost two-dimensional and occurs along specific surfaces due to the stratification. The mixing intensities between the exchanges that take place along these surfaces are a factor of eight orders of magnitude larger than those that occur through these surfaces. Thus, the ability to accurately define the surfaces where the strong exchange occurs in the ocean is crucial. However, this has proven to be a long and elusive problem. Historically, the first approximation was isobaric surfaces, i.e. surfaces of constant pressure, it was noticed that there were too many differences for this type of surface to be considered an accurate description. Wüst [1933] and Montgomery [1938] introduced the notion of potential density in order to counteract the effect of compressibility and better characterize the planes where the strong mixing occurs. The terms, commonly used in oceanography, of «isopycnal» and «diapycnal» were introduced to describe the flow along and through a density surface (Figure 1). Reid and Lynn [1971] used then the concept of patched potential density surfaces in an attempt to be more accurate, unfortunately this kind of surface has discontinuous properties with respect to height.

The investigation to obtain the correct description of the surfaces along which the strong mixing occur led to a milestone in oceanography with the mathematical definition of neutral surfaces or neutral tangent planes [McDougall, 1987a]. McDougall [1987a] also demonstrated that these surfaces cannot be constructed because of the non-linearity's of the equation of state of seawater. Neutral Density [Jackett and McDougall, 1997] was introduced to form approximations of neutral surfaces, and this proved to have good accuracy. The use of a surface which does not coincide exactly with the neutral tangent plane introduces a false diapycnal exchange through the approximate surface. This can be evaluated by the use of fictitious diapycnal diffusivity which is related to the slopes difference between an approximate neutral surface and the neutral tangent plane. Consequently, the outputs of ocean models are strongly dependent on the kind of surface used. The typical variable used in models is potential density referenced to 2000 db, σ_2. It is close of being neutral only around its referenced pressure, that is at 2000 db, and introduces unacceptable levels of false diapycnal exchanges at other pressures. Its computation is based on polynomials and it is fast to compute inside ocean models. However, the calculation of Neutral Density is based on a process that minimises the errors and requires several iterations. Although, it gives results that are close of being neutral, it is too time consuming to be computed in ocean models which run for millions of time steps.

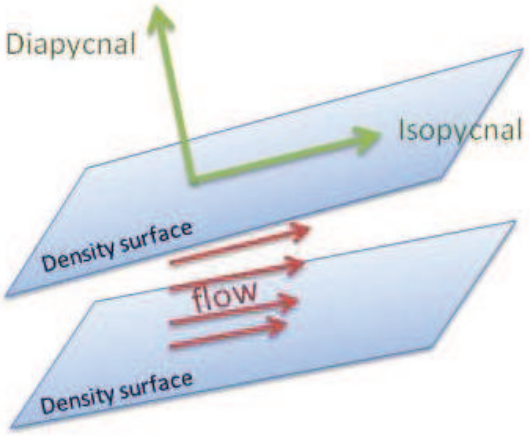

Figure 1: Flow between two density surfaces. "Isopycnal" and "diapycnal" describes the flow along and through a density surface respectively.

In order to improve the accuracy of ocean models, a density variable is needed that can be computed in a short time and is more accurate than σ_2. Therefore, this project was designed to find an approximate form of Neutral Density on the world oceans that is valid for a wide range of salinities and temperatures and is computationally efficient. McDougall and Jackett [2005a] showed that it was not possible to obtain a single rational function that successfully replicated Neutral Density (i.e. was close to being neutral) because of the hemispheric change in water-mass characteristics. Hence, this project is based on the construction of a polynomial γ^{poly} of Neutral Density for each ocean basin. Each γ^{poly} requires the two specifications which are (i) being only a function of salinity and temperature and (ii) being workable on a high range of these variables. The polynomial for the Southern Ocean proved to be the exception and required the addition of a pressure dependent term. Every function is fitted in a least-square sense on the WOCE climatology [Gouretski and Koltermann, 2004], that had been labelled with the improved Neutral Density γ^i. Due to the limited salinity and temperature range of the data, two processes have been developed that are designed to extrapolate the dataset and thus increase the range of the validity of the polynomials. A global polynomial γ^{GP} is achieved by gathering each of the γ^{poly} functions and joining the polynomials of neighbouring basins by the use of weighting functions. All these functions have been built in respect of Practical Salinity and potential temperature using the equation of state EOS-80 [Unesco, 1983]. These variables are currently used in ocean models. Recent breakthroughs in thermodynamics of seawater were the introduction of Absolute Salinity, Conservative Temperature and a new equation of state TEOS-10 [IOC et al., 2010] which is based on Gibbs function. Over the next few years, these variables will replace Practical Salinity and potential temperature in observational, theoretical oceanography and in ocean models. Therefore, the theory and the processes developed here for fitting a polynomial form of Neutral Density are valid for the new equation of state and γ^{poly} and γ^{GP} will be able to be constructed such

that they are a function of the latest thermodynamic variables.

The improvement of γ^{GP} compared to the variable σ_2 that it aims to replace is shown for two types of data, (i) the WOCE ocean atlas and (ii) a snapshot from the ocean model MOM4. The map of the world oceans depicted by Figure 2 shows the different ocean basins and the main regions which are discussed and where the major improvements exist. The results of the γ^{poly} functions are studied on each ocean basin, and their properties on the salinity-temperature diagram are highlighted. The reduction in the amount of fictitious diapycnal diffusivity provides the most convincing evidence that γ^{poly} describes neutral surfaces more accurately than σ_2. The use of weighting functions in the zipping regions introduces quite high levels of fictitious diapycnal diffusivity. The zipping issues are discussed and an explanation is offered to describe the origin of the introduced error. Included in this discussion are some thoughts of the quality of the dataset and the γ^i label as each of the ocean basin functions when taken separately are close to being neutral. Even with this non-negligible effect, γ^{GP} gives a good improvement compared to σ^2. The results for the ocean model MOM4 prove to be better than those observed for the WOCE climatology, this suggests that the γ^{GP} function is valid for use in models.

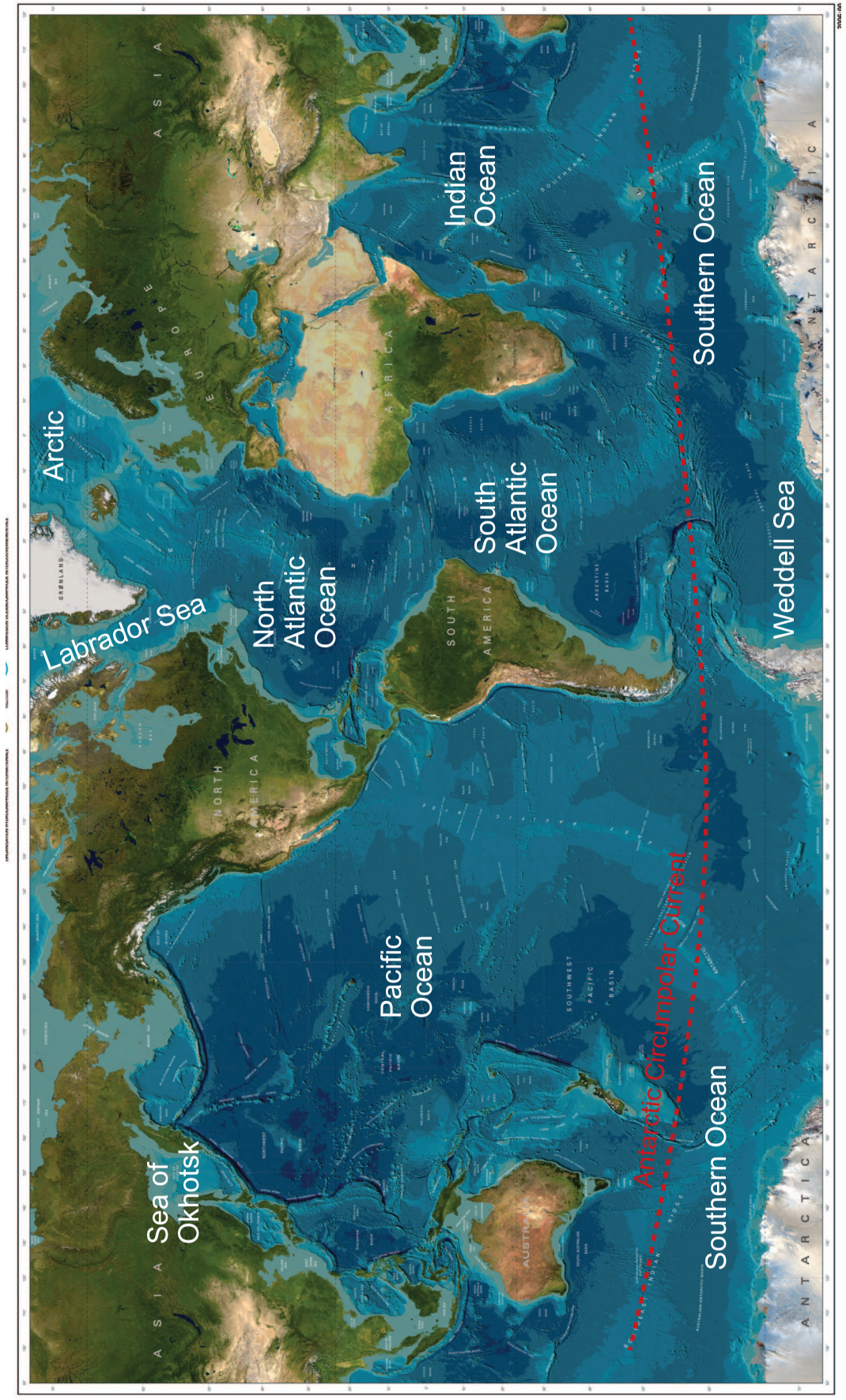

Figure 2: Map of the world oceans with the main notions used.

Chapter 1

Neutral physics in thermodynamics of seawater

1.1 Equations of state of seawater

In order to truly understand the concept of neutral tangent plane and take account of its importance in ocean circulation, a brief reminder of thermodynamics of seawater is necessary. A new equation of state has been recently designed approved by the scientific governing bodies (SCOR, IAPSO, IOC) which allows for a more accurate description of the ocean, as such this is a transition period for oceanographers in the use of thermodynamic variables. The global change could take at least five years, modifying an ocean model is not a trivial task. Thus, it is important to be precise which variables are used in this project. The project is to design a neural density function which can be used in the current ocean models. A second robust function based on the latest thermodynamic variables will have to be built for the next generation of ocean models and to provide the mechanism to label neutral density surfaces.

Introduced in 1980's, the old equation of state called *Equation of Seawater-1980* (EOS-80) [Unesco, 1983] was defined in terms of Practical Salinity S_P, *in situ* temperature t and pressure p. Versions designed in terms of potential temperature θ are currently implemented in ocean models and in the programs used in their analysis. Nevertheless, it lacks the ability to describe properly the properties of seawater such as a correct representation of the heat content or a real description of salinity. The SCOR/IAPSO Working Group 127 has recently published a new version of the equation of state, the *Thermodynamic Equation of Seawater-2010* (TEOS-10) [IOC et al., 2010], to overcome their limitations. The variables of Conservative Temperature Θ and Absolute Salinity S_A have replaced potential temperature and Practical Salinity. These new equations describe more accurately all thermodynamic properties of seawater (density, enthalpy, entropy, sound speed, etc...). Its innovation resides in the use of a Gibbs function which allow the derivation of all the variables in a thermodynamically consistent manner. The previous equation of state, EOS-80, was a collection of polynomials which were not consistent between the thermodynamic properties, and only allowed for the computation of the basics thermodynamic properties, but the new version possesses a lot of new functionalities. We invite the reader interested in the new thermodynamic properties of seawater to read *The international thermodynamics equation of seawater - 2010: Calculation and use of thermodynamic properties*

[IOC et al., 2010]. It is available on the website `http://www.teos-10.org/` as well as the Gibbs Seawater Oceanographic Toolbox for Matlab [McDougall and Barker, 2011] which allows the computation of many of these variables.

Because a parcel of seawater can be described as a trivariant system, the following part will focus on the three variables used to measure and characterize the ocean : pressure, salinity and temperature. The variable of density which is the link between thermodynamics and dynamics is derived by the equation of state. Understanding clearly these notions is fundamental for this study and the introduction of the concept of neutral surfaces.

1.1.1 Sea pressure

The sea pressure is defined to be the Absolute Pressure P less the Absolute Pressure of a standard atmosphere $P_0 = 101325Pa$

$$p = P - P_0 \tag{1.1}$$

The units commonly used in oceanography is the decibar ($dbar$) because the value is really close to the depth in metres. Pressure can be related to depth by the hydrostatic relation

$$g = -\nu\frac{\partial P}{\partial z} = -\frac{1}{\rho}\frac{\partial P}{\partial z} \tag{1.2}$$

Depending on the purpose, this relation can be easily integrated

$$p = \rho g h \tag{1.3}$$

Afterwards, we will need to accurately convert pressure differences into depth differences. Therefore, the function ***gsw_z_from_rho()*** from the GSW Oceanographic Toolbox for Matlab [McDougall and Barker, 2011] has been used for all the conversions of pressure into depth, which is based on the vertical integral of the hydrostatic equation:

$$\int_0^z g(z')dz = -\int_{P_0}^{P} \nu(p')dP' = -\int_{P_0}^{P} \hat{\nu}(S_{SO}, 0°, p')dP' + \Psi = -\hat{h}(S_{SO}, 0°, p') + \Psi \tag{1.4}$$

with the dynamic height anomaly Ψ defined in IOC et al. [2010], the Salinity of the Standard Ocean $S_{S0} = 35.165\,04\,g.kg^{-1}$.

1.1.2 Salinity

Practical Salinity

In the real life a lot of different species are dissolved in the ocean. Yet, it is not practical to study them with their own concentration and chemical potential. The physics can be described using one salinity variable that includes all these species. However, it is not possible to measure it in practice by evaporating a sample of seawater because volatiles components are lost during the process of drying when ones tries to evaporate seawater to get the mass of dissolved material. Salinity is currently determined by measurements of

electrical conductivity, which varies with the ionic content. The relationship between conductivity Λ and a so-called Practical Salinity $S_P(\Lambda, t, p)$ in Standard Seawater is specified by the "Practical Salinity Scale of 1978" (PSS-78):

$$\begin{aligned} &S_P = f(K_{15}) \\ &K_{15} = \Lambda(S, 15, 0)/\Lambda(KCl, 15, 0) \\ &2 <= S_P <= 42 \end{aligned} \tag{1.5}$$

Where K_{15} is the conductivity ratio which is the electrical conductivity of the sample (S) at temperature $t = 15°C\,(IPTS - 68)$ and pressure equal to one standard atmosphere, divided by the conductivity of a standard potassium chloride (KCl) solution at the same temperature and pressure. The salinity variable S_P is therefore directly related to measurements and it is under this form that measured salinity is currently stored.

Reference Salinity

The previous definition was actually based on the first scale with the definition of evaporated seawater which is in fact incorrect. As seen previously this definition is not true due to volatile components lost in the drying process. That's why, Millero et al. [2008b] defined the reference composition of seawater with the exact mole fractions of each species. It is based on seawater samples from the surface water of a certain region of the North Atlantic. They were analysed using mass spectrometry and/or ion chromatography. Consequently, Millero et al. [2008a] recently introduced a correction factor for Practical Salinity in order to take into account of chlorides missing. The corrected Practical Salinity is called Reference Salinity S_R. For the range of salinities where Practical Salinities are defined (that is $2 < S_P < 42$), it was shown that

$$S_R = \frac{35.16504\, g.kg^{-1}}{35} S_P \tag{1.6}$$

Absolute Salinity

The actual composition of seawater varies from one oceanic basin to another because of ocean circulation. This results in changes to the conductivity/salinity/density relationship, which is well defined only for the Standard Seawater obtained for a particular area in the North Atlantic [Pawlowicz et al., 2011]. Absolute Salinity is designed to take into account this spatial variation in seawater composition δS_A, due to small fluctuation in the silicate concentration. These variations while small, are a factor of about 10 larger than the accuracy with which scientists can measure salinity at sea. Absolute Salinity is related to a salinity anomaly δS_A and the Reference Salinity S_R:

$$S_A = S_R + \delta S_A = S_A(S_P, \phi, \lambda, p) \tag{1.7}$$

Figure 1.1 describes the method for forming Absolute Salinity which is the combination of reference composition and composition anomalies.

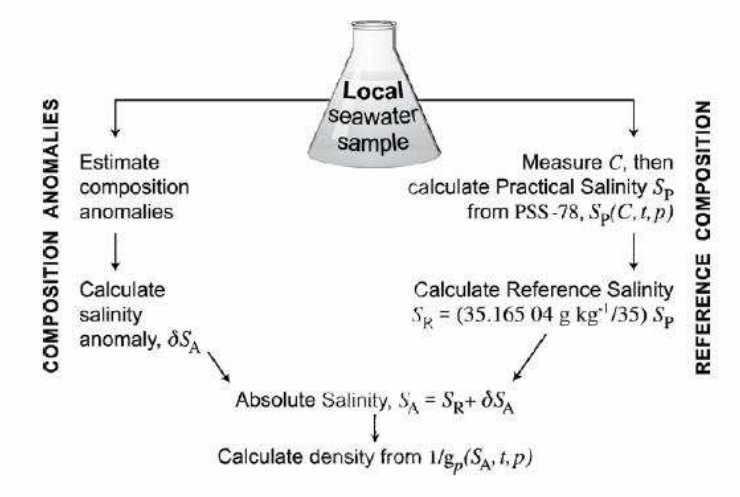

Figure 1.1: A sketch indicating how thermodynamics quantities such as density are calculated as functions of Absolute Salinity. Absolute Salinity is found by adding an estimate of the Absolute Salinity Anomaly δS_A to the Reference Salinity. [IOC et al., 2010]

1.1.3 Temperature

In situ temperature

Temperature has an important role in ocean processes. Several definitions can be used depending on the application. First, the absolute temperature T in Kelvin can be defined, which is a common thermodynamic variable. This is good for theory but in practice the measurement of temperature using a absolute scale is difficult. Thus, practical temperature scales were defined in laboratories for use in oceanographic sciences. For the ocean, the measuring device is a platinum-resistance thermometer. The most recent scale is the International Temperature Scale of 1990 (ITS-90). Oceanographers define in respect of this scale *in situ* temperature

$$t[^\circ C] = T[K] - 273,15 \tag{1.8}$$

Nevertheless, in physical oceanography it is useful to introduce temperature variables more appropriate to describe ocean processes in theoretical studies and in models.

Potential temperature

In order to discard the effect of compressibility and be more representative of the heat content, the concept of potential temperature, applied in the atmosphere originally by Helmotz (1888), was transfered to oceanography by Helland-Hansen (1912). The definition of potential temperature is the temperature that a fluid parcel would have if its pressure were changed to a fixed reference pressure p_r in an isentropic and isohaline manner. One can write potential temperature referred to a reference pressure p_r as the pressure integral of the adiabatic lapse rate

$$\theta = \theta(S_A, t, p, p_r) = t + \int_p^{p_r} \Gamma(S_A, \theta, p')dp' \tag{1.9}$$

Since its introduction to the field of oceanography, potential temperature has been treated as the variable representing the advection and diffusion of "heat". Ocean modellers have to date treated potential temperature as if it were a conservative variable. This assumption has been shown to be wrong because when fluids parcels mix at fixed pressure, non-conservative source terms of potential temperature arise because the isobaric heat capacity of seawater varies by up to 5% with salinity and also because enthalpy depends non-linearly with salinity [McDougall, 2003]. Note that this variable is still used by the modelling community in the equation of state EOS-80.

Conservative Temperature

Looking for a method capable of describing the heat content in the ocean accurately, McDougall [2003] introduced Conservative Temperature which is directly related to enthalpy in order to be as conservative as possible. Conservative Temperature Θ is similar to potential temperature in that the same artificial though experiment is involved. Conservative Temperature is directly related to potential enthalpy h^0 which is the enthalpy that a fluid parcel would have if its pressure was changed to a fixed reference pressure p_r in an isentropic and adiabatic way. As heat fluxes into and out of the ocean occur mostly near the sea surface, the reference pressure for potential enthalpy is always $p_r = 0\,dbar$. Hence, Conservative Temperature Θ is defined to be directly proportional to potential enthalpy according to

$$\Theta(S_A, t, p) = \tilde{\Theta}(S_A, \theta) = \frac{h^0(S_A, t, p)}{c_p^0} = \frac{\tilde{\Theta}^0(S_A, \theta)}{c_p^0} \tag{1.10}$$

where c_p^0 is defined in standard conditions, that is $S_A = 35,16504\,g.kg^{-1}$ and $\theta = 25°C$

$$c_p^0 = 3991,86795711963\,J.kg^{-1}.K^{-1} \tag{1.11}$$

It has been shown that the error incurred in ocean models by assuming that Conservative Temperature is 100% conservative is approximately 120 times smaller than the corresponding error for potential temperature [Graham and McDougall, 2012]. The air-sea heat flux is exactly proportional to the flux of Conservative Temperature and the meridional "heat" flux is very accurately given by the meridional heat flux of Θ. Figure 1.2 illustrates the non-conservative production of potential temperature θ in the ocean, it can. The difference between potential temperature and Conservative Temperature $\theta - \Theta$ can be as large as $-1.4°\,C$, but is more typically no more than $\pm 0.1°\,C$.

1.1.4 *In situ* Density

A parcel of seawater, being a trivariant system can be determined by three variables. Therefore, the knowledge of salinity, temperature and pressure, which can be easily measured by CTD probes (Conductivity, Temperature, Depth) allow the calculation of the seawater density. As water is weakly compressible, Absolute density is not really suitable to describe accurately a change in density. That's why oceanographers prefer using the relative density called *density anomaly* or *Sigma*:

$$\sigma = \rho - 1000\,kg.m^{-3} \tag{1.12}$$

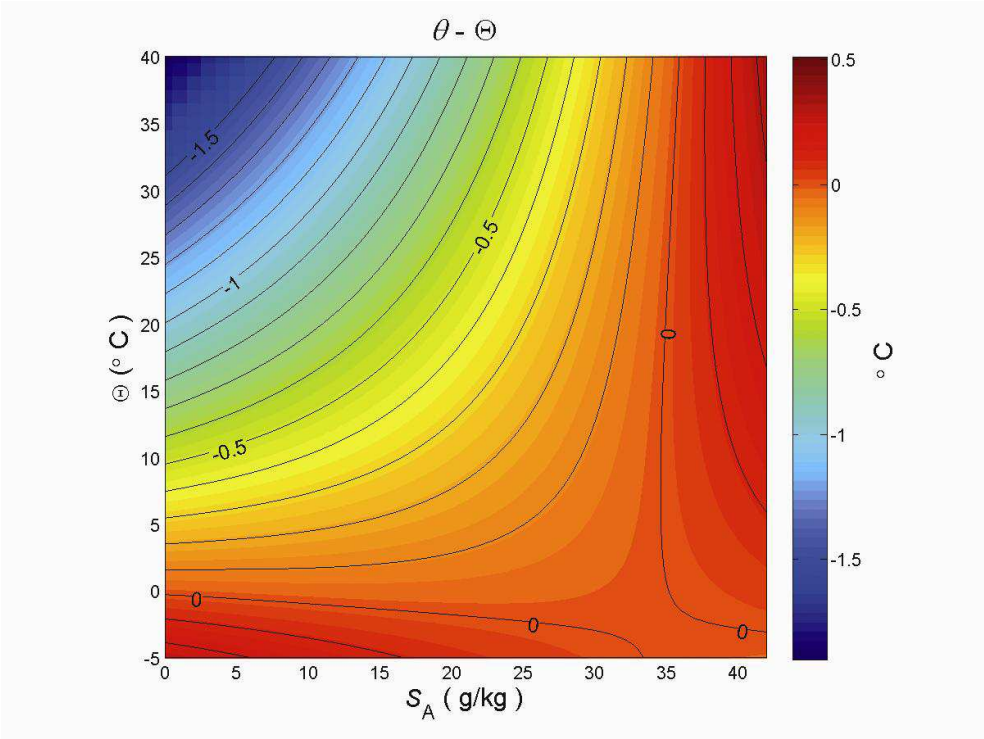

Figure 1.2: Contours (in $°C$) of the difference between potential temperature and Conservative Temperature $\theta - \Theta$. This plot illustrates the non-conservative production of potential temperature θ in the ocean. [McDougall and Barker, 2011]

1.2 Neutral tangent plane theory

Stratification in the global ocean has long been a difficult and elusive problem in physical oceanography. Wüst [1933] and Montgomery [1938] were the first to observe that the dominant flows in the ocean occurred along "isopycnals" that were not the same as density surfaces, as had been previously thought. They introduced the concept of potential density in order to describe these surfaces, but later Reid and Lynn [1971] demonstrated their faults showing that the same "isopycnal" can have density differences of $0.14\, g.kg^{-1}$ between the two hemispheres. In order to obtain a better description of these particular surfaces along which the strong exchanges occur, based on a theory of stability and not only on observations, McDougall [1987b,c] developed the theory of neutral surfaces and discussed the consequences of analysing oceanic motion with respect to neutral tangent planes, the other word to describe neutral surfaces. However, this kind of surface is not mathematically well defined it is impossible to build, which is proven by studying neutral helicity and neutral trajectories. Though, approximating these surfaces is achievable and is a real need in physical oceanography and can be used in many applications for describing flows. Neutral physics is then introduced in this part and seems necessary to truly understand the next concept of Neutral Density and the need to construct an approximate form of Neutral Density. It was chosen to write the equations in both forms of the equation of state, that is, EOS-80 [Unesco, 1983] with potential temperature θ and Practical Salinity S_P, and TEOS-10 [IOC et al., 2010] with Conservative Temperature Θ and Absolute Salinity S_A. As previously mentioned we are currently in a transition period while oceanographers change over to using TEOS-10. The current generation of ocean models have been written in terms of S_P, θ and rely on EOS-80, thus it is necessary

to develop γ^{GP} in the two versions of the equation of state.

1.2.1 Buoyancy frequency

Commonly used in geophysics, the buoyancy frequency (called sometimes the Brunt-Väisälä frequency) quantifies the stability of a stratified medium. Its magnitude has an important role in defining energetic exchanges in geophysical flows, particularly in atmospheric dynamics and physical oceanography. Therefore, in a stable stratified medium, if a fluid parcel is moved from is equilibrium position, its density will be modified and it will experience a buoyancy restoring force tending to bring it back to its initial position as represented on the figure 1.3. It follows that the parcel oscillates around its equilibrium position at the frequency N. The buoyancy frequency is then mathematically defined by

$$N^2 = \frac{g}{\rho}\left(-\frac{\partial \rho}{\partial z} + \left.\frac{\partial \rho}{\partial z}\right|_{isentropic,adiabatic}\right) \tag{1.13}$$

Here the first term is the vertical gradient of *in situ* density, and the second term repre-

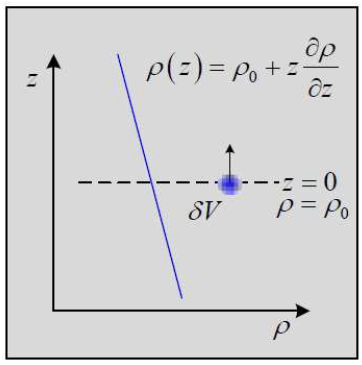

Figure 1.3: In a stable stratified middle, a parcel of fluid moved from its equilibrium position experiences a buoyancy restoring force [Perkins, 2011]

sents the change in *in situ* density that the fluid parcel would experience during vertical movements isentropically and adiabatically. The isentropic and isohaline compressibility is defined by

$$\kappa = \frac{1}{\rho}\left.\frac{\partial \rho}{\partial p}\right|_{S_P,\theta} = \frac{1}{\rho}\left.\frac{\partial \rho}{\partial p}\right|_{S_A,\Theta} \tag{1.14}$$

Then the equation of the buoyancy frequency (1.13) can be rewritten using the previous equation (1.14)

$$N^2 = -\frac{g}{\rho}\frac{\partial \rho}{\partial z} + \kappa g \frac{\partial p}{\partial z} \tag{1.15}$$

N^2 can be any real number that's why a discussion on its sign seems to be necessary. One can distinguish three different cases:

- $N^2 < 0$, the system is unstable and it leads to vertical mixing because denser water lies on lighter water.
- $N^2 > 0$, the system is stable and oscillate at the frequency N

- $N^2 = 0$, the system is said neutral

The buoyancy frequency occurs in a lot of phenomenon in the ocean such as internal waves. The last case of $N^2 = 0$ is particularly noticeable and constitutes a fundamental property of neutral tangent planes.

1.2.2 Mathematical definition of neutral tangent planes

As a fluid parcel moves around the ocean and experiences a variety of pressures, its *in situ* density continually changes because of the compressibility of seawater. In order to reduce this variation of density, McDougall [1987b] introduced the concept of neutral tangent plane or neutral surface in physical oceanography. Then, a neutral surface is defining so that infinitesimal isentropic and adiabatic displacements of a parcel of seawater do not produce a buoyant restoring force. In other words, it is a plane of neutral buoyancy. In this way, fluid parcels can be exchanged and mixed over small distances in the neutral surfaces without having to supply gravitational potential energy (i.e. a buoyancy force). Following this definition, the normal vector of this plane is given by

$$\mathbf{n} = \frac{g}{N^2}\left(-\frac{1}{\rho}\nabla\rho + \kappa\nabla p\right) \tag{1.16}$$

The equation of state of seawater can be written in respect of Pratical Salinity S_P and potential temperature θ of EOS-80 [Unesco, 1983] or in respect of the last thermodynamic variables Absolute Salinity S_A and Conservative Temperature Θ of TEOS-10 [IOC et al., 2010].

$$\begin{aligned} \frac{1}{\rho}\nabla\rho &= \beta^\theta \nabla S_P - \alpha^\theta \nabla\theta + \kappa\nabla\rho \qquad \textit{(EOS-80)} \\ &= \beta^\Theta \nabla S_A - \alpha^\Theta \nabla\Theta + \kappa\nabla\rho \quad \textit{(TEOS-10)} \end{aligned} \tag{1.17}$$

where β is the saline contraction coefficient defined by

$$\beta^\theta = \frac{1}{\rho}\left.\frac{\partial\rho}{\partial\theta}\right|_{\theta,p} \text{ or } \beta^\Theta = \frac{1}{\rho}\left.\frac{\partial\rho}{\partial\Theta}\right|_{\Theta,p} \tag{1.18}$$

and α is the thermal dilatation defined by

$$\alpha^\theta = -\frac{1}{\rho}\left.\frac{\partial\rho}{\partial\theta}\right|_{S_P,p} \text{ or } \alpha^\Theta = \frac{1}{\rho}\left.\frac{\partial\rho}{\partial\Theta}\right|_{S_P,p} \tag{1.19}$$

Note that the equation of state of seawater is non-linear and the coefficients α and β do not not vary linearly. It will be seen in the next part the consequences on the definition of neutral surfaces. Then, using the two different equation of state, the normal vector can then be rewritten

$$\begin{aligned} \frac{N^2}{g}\mathbf{n} &= \alpha^\theta\nabla\theta - \beta^\theta\nabla S_P \\ &= \alpha^\Theta\nabla\Theta - \beta^\Theta\nabla S_A \end{aligned} \tag{1.20}$$

Combining in a second time the equation of buoyancy frequency (1.15) and the equation of state (1.17) one can obtain

$$\begin{aligned} \frac{N^2}{g} &= \alpha^\theta \left.\frac{\partial\theta}{\partial z}\right|_{x,y} - \beta^\theta \left.\frac{\partial S_P}{\partial z}\right|_{x,y} \\ &= \alpha^\Theta \left.\frac{\partial\Theta}{\partial z}\right|_{x,y} - \beta^\Theta \left.\frac{\partial S_A}{\partial z}\right|_{x,y} \end{aligned} \tag{1.21}$$

Therefore it is important to note that the z component of $\beta^\theta \nabla S_P - \alpha^\theta \nabla\theta$ (respectively $\beta^\Theta \nabla S_A - \alpha^\Theta \nabla\Theta$) is simply N^2/g. Remarking now that the three-dimensional gradient ∇ is related to the two-dimensional gradient ∇_n by

$$\nabla = \nabla_n + \left.\frac{\partial}{\partial z}\right|_{x,y} \mathbf{k} \tag{1.22}$$

Since the mathematical definition of a neutral surface, ie a plane of neutral buoyancy, is then given by the expression

$$\frac{1}{\rho}\nabla_n \rho = \kappa \nabla_n p \tag{1.23}$$

This previous definition is equivalent to

$$\begin{array}{c} \beta^\theta \nabla_n S_P = \alpha^\theta \nabla_n \theta \\ \beta^\Theta \nabla_n S_A = \alpha^\Theta \nabla_n \Theta \end{array} \tag{1.24}$$

This last form is the most commonly used to describe a neutral surface. It expresses in terms of gradients of Absolute Salinity S_A and Conservative Temperature Θ (respectively S_P and θ) which are both conservative thermodynamic variables, whereas the alternative definition (1.23) involves the non-conservative variable of *in situ* density.

1.2.3 Neutral helicity

The physics of neutral surfaces are well described by the equation (1.24), but the construction of these surfaces in the real ocean is a bit more complicated. A well-known property in vector geometry is that the surfaces normal to a vector $\mathbf{n}$ are well defined by the equality $\mathbf{n}.\nabla \times \mathbf{n} = 0$ everywhere. In analogy with fluid mechanics, the term $\mathbf{U}.\nabla \times \mathbf{U}$ is called helicity and represents the potential for helical flow to evolve. Therefore the flow follows the pattern of a corkscrew. Looking for a way to construct neutral surfaces, McDougall [1988] defined in a similar way the concept of neutral helicity in the ocean. Previously, it has been seen that the normal to a neutral tangent plane is in the direction $\alpha^\theta \nabla\theta - \beta^\theta \nabla S_P$ (respectively $\alpha^\Theta \nabla\Theta - \beta^\Theta \nabla S_A$). Hence neutral helicity can be written:

$$\begin{array}{rcl} H^n & = & (\alpha^\theta \nabla\theta - \beta^\theta \nabla S_P).\nabla \times (\alpha^\theta \nabla\theta - \beta^\theta \nabla S_P) \\ & = & (\alpha^\Theta \nabla\Theta - \beta^\Theta \nabla S_A).\nabla \times (\alpha^\Theta \nabla\Theta - \beta^\Theta \nabla S_A) \end{array} \tag{1.25}$$

It is now useful to introduce the thermobaric coefficient T_b^Θ because the ratio α/β of the thermal expansion coefficient and the saline contraction coefficient depends actually on pressure. The thermobaric coefficient [McDougall, 1987b] quantifies the rate of variation of that ratio.

$$\begin{array}{rcccccl} T_b^\theta & = & T_b^\theta(S_P,t,p) & = & \beta^\theta \left.\dfrac{\partial \alpha^\theta/\beta^\theta}{\partial p}\right|_{S_P,\theta} & = & \left.\dfrac{\partial \alpha^\theta}{\partial p}\right|_{S_P,\theta} - \dfrac{\alpha^\theta}{\beta^\theta}\left.\dfrac{\partial \beta^\theta}{\partial p}\right|_{S_P,\theta} \\ T_b^\Theta & = & T_b^\Theta(S_A,t,p) & = & \beta^\Theta \left.\dfrac{\partial \alpha^\Theta/\beta^\Theta}{\partial p}\right|_{S_A,\Theta} & = & \left.\dfrac{\partial \alpha^\Theta}{\partial p}\right|_{S_A,\Theta} - \dfrac{\alpha^\Theta}{\beta^\Theta}\left.\dfrac{\partial \beta^\Theta}{\partial p}\right|_{S_A,\Theta} \end{array} \tag{1.26}$$

In a lot of ocean application the thermobaric parameter can be considered constant with a value of $T_b = 2.7\,10^{-8}\,K^{-1}db^{-1}$ With this magnitude, it has been shown that Neutral helicity can be written as

$$\begin{array}{rcl} H^n & = & \beta^\theta T_b^\theta \nabla p.\nabla S_P \times \nabla\theta \\ & = & \beta^\Theta T_b^\Theta \nabla p.\nabla S_A \times \nabla\Theta \end{array} \tag{1.27}$$

Therefore it appears that this kind of surface is not mathematically well-defined because neutral helicity is not zero everywhere. The only way for neutral helicity to be null is that the intersection of the S_P and θ planes, $\nabla S_P \times \nabla\theta$ (respectively $\nabla S_P \times \nabla\theta$), must lie in the isobaric surface. Due to the non-linearities of the equation of state of seawater, this equality does not exist everywhere in the real ocean. As a result, it is not possible to construct such a surface and neutral tangent plane can only be defined locally by being plane of neutral static stability. Another illustration of the ill-defined nature of neutral surface is given by the helical shape of neutral trajectories (see Figure 1.4). In fact, helicity is path-dependent so that tracing a neutral trajectory around an ocean basin and returning to the original longitude and latitude gives a depth different from the starting point. This path-dependency is related to the thermobaric coefficient which varies non-linearly with pressure.

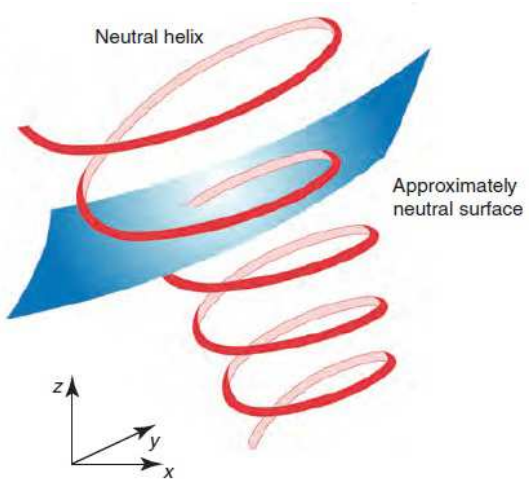

Figure 1.4: The neutral helix depicts a trajectory of the mean circulation such as would occur in the absence of interior diapycnal mixing. The helical nature of this Neutral trajectory means that mean vertical motion occurs through density surfaces [McDougall and Jackett, 2008]

1.2.4 Interest in neutral surfaces

Mesoscale turbulence in evaluating the circulation in the main ocean is well described by a model of eddy diffusion. The fact that strongest exchanges occur along neutral surface in the ocean is well characterized by the value of the lateral mixing diffusion coefficient $K = 1000\, m^2.s^{-1}$. On the contrary, it has been shown that the mean diapycnal diffusivity due to irreversible processes is roughly $10^{-5}\, m^2 s^{-1}$ in the ocean [Stewart, 2007]. A simple calculation gives that isopycnal mixing is eight orders better than diapycnal mixing. Therefore, neutral surfaces are an important concept in physical oceanography because their knowledge allows the correct describtion of where the strong lateral mixing occurs. The smallness of the rate of dissipation of mechanical energy in the ocean also confirms the common assumption that the strong lateral diffusion achieved by mesoscale eddies occurs along neutral tangent planes in the ocean interior. Consequently, it is necessary to be able to determine the slope of the neutral tangent plane to an accuracy of about 10^{-4} in order to separate and understand the different lateral and vertical mixing processes.

An example of such an importance in defining neutral surfaces is given by the "thermal wind" equation. This equation gives the vertical gradient of the horizontal velocity under the geostrophic approximation. It can be expressed by

$$f\frac{\partial \mathbf{v}}{\partial z} = \frac{N^2}{g\rho}\mathbf{k} \times \nabla_n p \tag{1.28}$$

With this form, the "thermal wind" is directly related to the pressure gradient in the neutral tangent plane. And it is possible to see that the knowledge of th pressure gradient along a neutral surface is sufficient to describe the "thermal wind".

Conservation equations can also be written in the frame of neutral surface in order to align the mixing tensors. An approximate turbulent-averaged form of the conservation equation of Absolute Salinity thickness-and-density-weighted on neutral surfaces [Graham and McDougall, 2012] is given by

$$\frac{DS_A}{Dt} = \left.\frac{\partial \widehat{S_A}}{\partial t}\right|_n + \hat{\mathbf{v}}.\nabla_n \widehat{S_A} + \tilde{e}\frac{\partial \widehat{S_A}}{\partial z} = \gamma_z^a \nabla_n . \left(\frac{1}{\gamma_z^a} K \nabla_n \widehat{S_A}\right) + \left(D\frac{\partial \widehat{S_A}}{\partial z}\right)_z + \hat{\boldsymbol{S}}^{S_A} \tag{1.29}$$

where $\hat{\mathbf{v}}$ is horizontal velocity, $\widehat{S_A}$ Absolute Salinity, the thickness-weighted, all thickness-and-density-weighted, $\tilde{e}$ is the temporally averaged dianeutral velocity, D is the dianeutral diffusivity and K the epineutral diffusivity, γ_z^a is the vertical gradient of a suitable density variable approximating neutral surface, and $\hat{\boldsymbol{S}}^{S_A}$ is a non-conservative production term due to biogeochimical processes.

1.2.5 Error introduced by the use of an approximately neutral surface

Considering now that we are able to describe neutral surfaces with approximately neutral surfaces defined by a density variable γ^a. At this moment, it is judicious to introduce the terms commonly used in oceanography of "isopycnal" to describe flows along density surfaces and "diapycnal" for flows through density surfaces. These terms will be used all along the study. The vertical velocity e^a through this surface is described by Figure 1.5 and can be expressed as

$$e^a = e + e^{hel} \tag{1.30}$$

where e corresponds to the transport through the surface if this surface was purely neutral. This velocity is created by irreversible processes in the ocean, that is, cabelling, thermobaricity, double-diffusion and small-scale turbulent mixing. The second member e^{hel} is created by the helical shape of neutral trajectories (see Figure 1.4) and the fact that it is impossible to construct neutral surfaces. This velocity e^{hel} through an approximately surface γ^a which transports mass, salinity, conservative temperature and all other tracers. The major point to remind is that velocity e^{hel} is not related to irreversible processes in the ocean but to the ill-defined nature of neutral surfaces.

To quantify now the quality of an approximately neutral surface in the sense of being close to neutral, it is judicious to introduce the slope difference between the neutral tangent plane and the approximately neutral surface.

$$\begin{aligned} \mathbf{s} \;=\; \nabla_n z - \nabla_a z \;&=\; \frac{g}{N^2}(\alpha^\theta \nabla_a \theta - \beta^\theta \nabla_a S_P) \\ &=\; \frac{g}{N^2}(\alpha^\Theta \nabla_a \Theta - \beta^\Theta \nabla_a S_A) \end{aligned} \tag{1.31}$$

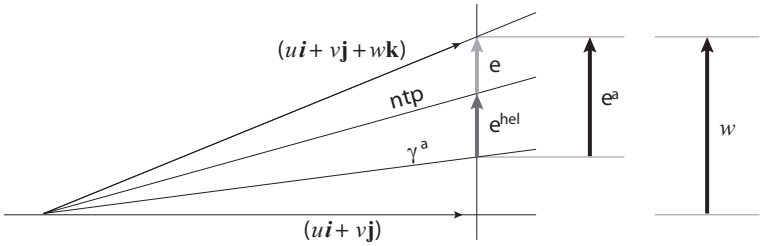

Figure 1.5: This figure shows the differences between e, e^{hel}, e^a and w. The lateral velocity $(u\mathbf{i} + v\mathbf{j})$ is directed horizontally. The three surfaces shown are the approximately neutral surface (γ^a), the neutral tangent plane (ntp) and the top-most is the lateral velocity plus w, where w includes all components leading to a flow which differs from a purely horizontal flow (the tilt of an approximately neutral surface, mixing effects and a diapycnal velocity caused by the ill-defined nature of neutral surfaces,e^{hel})[Klocker et al., 2009]

Mesoscale turbulence in evaluating the circulation in the main ocean is well described by a model of eddy diffusion. The fact that strongest exchanges occur along neutral surface in the ocean is well described the value of the lateral mixing diffusion coefficient $K = 1000\, m^2.s^{-1}$. On the contrary, it has been shown that the mean diapycnal diffusivity due to irreversible processes (corresponding to the velocity e (1.30)) is roughly $10^{-5}\, m^2 s^{-1}$ in the ocean [Stewart, 2007]. A simple calculation gives that isopycnal mixing is eight orders superior to diapycnal mixing. Therefore, the use of an approximately neutral surface to describe the flow in the ocean introduces a false diapycnal exchange (corresponding to the velocity e^{hel} (1.30)) because this surface does not coincide exactly everywhere with neutral tangent planes. It is then judicious to express this error in terms of diffusivity which will directly correspond to error introduce in the evaluation of conservation equations. It is called the fictitious diapycnal diffusivity and it can be evaluated using by the lateral mixing diffusion coefficient K times by the square of the slope difference $\mathbf{s}^2$ between an approximate neutral surface and the neutral tangent plane. According to the equation (1.31), the fictitious diapycnal diffusivity can be written

$$D^f = K.\mathbf{s}^2 = K.(\nabla_n z - \nabla_a z)^2 \tag{1.32}$$

As the mean value of diapycnal mixing is $10^{-5}\, m^2 s^{-1}$ in the ocean, it means that if one uses an approximate neutral surface whose the fictitious diffusivity D^f due to the velocity e^{hel} is smaller than $10^{-5}\, m^2 s^{-1}$, then no significant mixing error will be introduced describing the ocean flow. Afterwards, we will see in the next part that different density surfaces can be used for approaching neutral surfaces but not with the same results and accuracy it will be an important and this value will be important to characterize the potential of an approximate neutral surface to be close to neutral.

1.3 State-of-the-art of density surfaces

1.3.1 Properties of density surfaces

The birth of the theory of neutral tangent plane has seen the introduction of several density variables in order to describe correctly flow along isopycnals. Then it has been shown that density surfaces all differ in the extent of which they achieve the three desirable properties but mutually inconsistent properties:

- *being as neutral as possible*: a surface of a constant value of the density variables describes a neutral surface
- *being as quasi-material as possible*, that is being only a function of salinity and temperature. When taken the derivative, a density variable being of function of pressure or space introduce a false diapycnal mixing [McDougall and Jackett, 2005a]. The diapycnal velocity e^a (1.30) introduced by the use of a density surface γ^a can be written

$$e^a = \frac{\frac{D\gamma^a}{Dt}}{\frac{\partial\gamma^a}{\partial z}} \tag{1.33}$$

- *possessing a geostrophic streamfunction* (Montgomery streamfunction)

In fact, the nature of the equation of state does not allow to find an appropriate density surface which satisfies all three properties. That's why the choice of a density variable will depend on ones application. One density variable might give good results for an application but introduce substantial errors for another. This study will be focus only on the first point of being close to neutral, keeping in mind the quasi-material property. The last point will not be evoked afterwards.

1.3.2 Surface of potential density

Surface of constant *in situ* density were historically the first surfaces used for oceanic models. But in order to get a better approach of describing the surfaces where the strong exchanges occur, Wüst [1933] introduced the notion of potential density in order to counteract the effect of compressibility . On this type of density surface (identified with the index σ_r), the relation between lateral gradients of salinity and potential temperature can be written in the form

$$\alpha^\Theta(p_r)\nabla_{\sigma_r} = \beta^\Theta(p_r)\nabla_{\sigma_r} S_A \tag{1.34}$$

At $p = p_r$, potential density surface and neutral surface coincide exactly as it can be seen on Figure 1.6. Then, the neutral surface can be regarded as the envelope of a whole series of locally referenced potential density surfaces. The other thing which is remarkable is that neutral surfaces and potential density coincide along conservative isotherms and isohalines in three-dimensional space. Therefore, Reid and Lynn [1971] developed an approach of neutrality, even before the introduction of the concept of neutral surface, with patched potential density surfaces. Their method to form isopycnals involves using potential density referenced to a series of pressure (usually $0\,db$, $1000\,db$, $2000\,db$ and $4000, db$) in order to approximate neutral surfaces. Each potential density variable is used to described neutral tangent plane in a particular range of pressure. The problem with this approach is that these density variables do not connect well between the different layers making the surface discontinuous by nature and it is not desirable to have a discontinuous surface to describe the flow in the ocean.

Although potential density surfaces provide a reasonable approximation of neutral surfaces, they are actually inaccurate when used in applications requiring a good precision. For the moment, they are used in ocean models because of their rapidity of computing. Potential density referenced to $2000\,db$, namely σ_2, is very popular in numerical ocean models because it gives results in a short time, but this variable is far from being perfect.

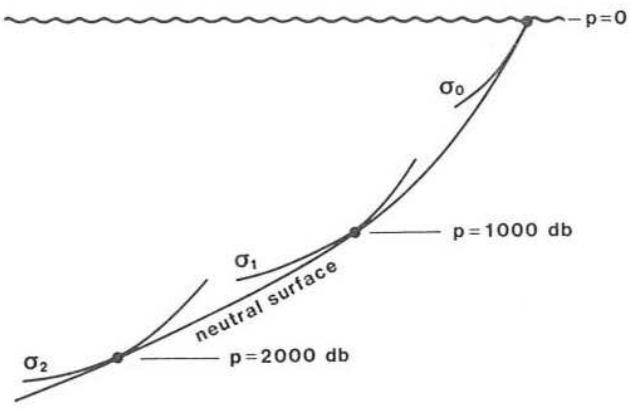

Figure 1.6: Sketch of a Neutral surface and three different potential density surfaces, referenced to 0 *db*, 1000 *db and* 2000 *db*. The Neutral surface is tangential to potential density surfaces with only at the reference pressure of those potential density surfaces. In this way, the Neutral surface can be regarded as the envelope curve of many locally referenced potential density surfaces with continually changing reference pressures.[McDougall, 1987a]

1.3.3 Surface of neutral density

Neutral density

After having defined properly the concept of neutral surface, [McDougall, 1987a] was looking for a way to describe these surfaces and led to the development of Neutral Density. The idea is to consider first that these surfaces are well defined by neutral helicity being zero everywhere $H^n = 0$. This condition can then be satisfied when there is an integrating factor $b = b(x, y, z)$, so that $b\rho(\beta\nabla S_P - \alpha\theta)$ is irrotational. Under these conditions, a scalar potential γ^n exists [Jackett and McDougall, 1997]:

$$\nabla\gamma^n = b\rho(\beta^\Theta\nabla S - \alpha^\Theta\nabla\theta) \tag{1.35}$$

so that the solution to $\nabla_n\gamma^n = 0$ is identical to the solution of $\rho(\beta^\Theta\nabla S - \alpha^\Theta\nabla\theta) = 0$. In that sense, Neutral Density is no longer a thermodynamic variable because it not only depends on salinity, temperature and pressure, but also on latitude an longitude. To summarize the relation between idealized neutral surface and Neutral Density, the following equivalences can be demonstrated:

- Neutral surfaces are orthogonal to $\rho(\beta\nabla S - \alpha\nabla\theta)$
- Helicity is zero i.e. $H = A.\nabla \times A = 0$
- Existence of the scalar potential b

To have a better idea of the integrating factor b, an approximate value can be found with the expression

$$b \approx exp\left[-g^2\rho T_b^\Theta \int_n \frac{1}{N^2}\beta^\Theta\nabla S - \alpha^\Theta\nabla\theta.d\mathbf{l}\right] \tag{1.36}$$

Then, the equation (1.35) being a system of first-order hyperbolic partial different equations can be solved by the method of characteristics. γ^n is elaborated considering that

neutral density is zero, but in the real ocean neutral surfaces are not mathematically well-defined and helicity is path-dependent, consequently γ^n is not exactly constant on local neutral tangent planes approximated by characteristics. The final stage of the process consists in averaging this error over the entire globe using an iteratively process starting with the values of initial γ^n field until reaching a steady state field. The results prove that Neutral Density is widely better in approximating neutral surfaces than potential density. Figure 1.7 represents isopycnals of γ^n, σ_2 and σ_0 along a longitudinal section of the Atlantic Ocean compared to a neutral trajectory. It can be seen that the error in evaluating neutral surface is larger using referenced potential density than neutral density, namely hundreds of meters difference for σ_2 compared to tens of meters difference for γ^n. Though, the use of γ^n is limited on labelling a world ocean dataset because the process involved is very computer intensive and requires a lot of iterations to converge. Therefore, at present γ^n cannot be used in practice in ocean models because of its dependency on time of computation. The Levitus climatology [Levitus, 1982] is the basis for the γ^n label, however it only covers the range of latitude of $-84°N \rightarrow 60°N$.

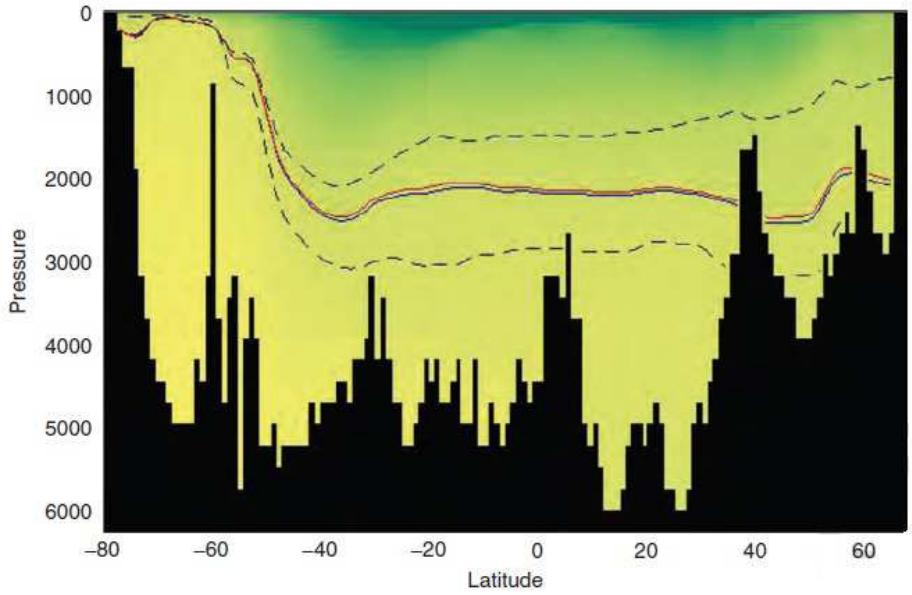

Figure 1.7: Surfaces of constant γ^n (blue solid line),σ_0 and σ_2 (dashed lines with σ_2 being the lower dashed line), and a neutral trajectory (red solid line) along $328°E$ in the Atlantic Ocean. All the surfaces coincide at $250\,dbar$ and $59°S$.[McDougall and Jackett, 2008]

Improved neutral density

γ^i is an improved version of the neutral density γ_n. It uses this last variable as an initial condition and an iterative inversion method to improve the surface. Computationally more expensive due a large number of iterations, it is more accurate than γ^n and is really close to being neutral. There is no published bibliography on the subject at present, the process is currently being developed by McDougall and Barker. The WOCE climatology [Gouretski and Koltermann, 2004] has already been labelled with γ^i and is used in this project of forming in the approximate form of neutral density γ^{GP}. But the results could be more accurate as the technology is not perfect yet for two reasons. First, the WOCE

climatology is a global average of hydrographic casts and some regions such as the Weddell Sea or the Arctic are not well described because of a lack of observational data. Secondly, the software for computing γ^i is not completely finished and some components still require improvements. Thus the results are not as good as expected, particularly in the deep part of the ocean, and regions where strong gradients of temperature and salinity occur such as those close to Antarctica and in the Labrador Sea.

1.3.4 Approximate neutral density variables

Although neutral density γ^n and γ^i gives accurate results to describe neutral surfaces, they cannot be used in practice in applications running millions of time step. That's why oceanographers tried to make approximate forms of neutral density or even define another density variable that is faster to compute. These functions have not been followed by applications because the results did not have a big improvement compared to referenced potential density σ_2, or have been limited to an ocean basin. An inventory of existing density variables aimed to be used in ocean models follows and their limits are pointed.

γ^{EW} Eden and Willebrand [1999] neutral density polynomial Constructed for a use on the North Atlantic, this function looks for achieving the second property of being quasi-material and align the vertical gradient of the neutral density with the vertical gradient of *in situ* density. In that sense, the function does not try to be neutral everywhere. Nevertheless, it gives better results in terms of neutrality than σ_2 in a similar computation time (see Figure 1.9). This is for the moment the most neutral function being able to be compute in a short time on the North Atlantic. Though, a point to denote is that the validity range of the function is limited to the dataset used for its construction and cannot be used with data at low/high level of salinity or temperature.

γ^a (or γ^{rf}) McDougall and Jackett [2005b] rational approximation of γ^n This is a rational function depending only on salinity and temperature of 16 parameters based on the approximation of γ^n. It is naturally faster and easier to compute than γ^n but it still suffers from a lack of accuracy. The fact that it ignores the hemispheric changes in water-mass characteristics make it less neutral and explains a part of its difficulty to well reproduce neutral density. Hence, there is no major improvement in approximating neutral surface compared to σ_2, and this function is far from the results of γ^n itself. For example, in terms of the volume estimates, γ^a give improvements of 23% to the σ_2 estimate, compared to 63% for γ^n (see Figure 1.8)

1.3.5 ω surfaces

Aiming to reduce the residual fictitious diapycnal diffusivity and so that it is only due to neutral helicity and not due to any other effects, the difference between the approximate density surface and neutral density surface can be minimized using a least-squares approach [Klocker et al., 2009]. Based on the dataset of neutral density, these surfaces can be improved and the slope difference with neutral surfaces reduced. The method begins

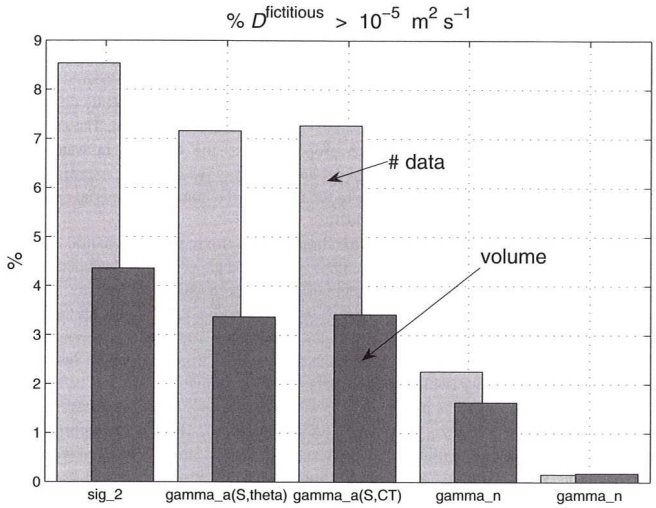

Figure 1.8: Percentages of the global ocean data for which the fictitious diapycnal is greater than $10^{-5}\,m^2s^{-1}$. The right-hand bars are for the percentages of the global ocean volume while the left-hand bars are the percentage of data pairs in the global atlas (in which the standard pressures are more closely spaced in the upper ocean than in the deep)[McDougall and Jackett, 2005b]

by defining the residue ϵ similar to the slope error $\mathbf{s}$

$$\epsilon = \beta^{\mathbf{\Theta}}\nabla_{\mathbf{a}}\mathbf{S} - \alpha^{\mathbf{\Theta}}\nabla_{\mathbf{a}}\theta = \frac{\mathbf{N^2}}{\mathbf{g}}\mathbf{s} \tag{1.37}$$

Then this residue is minimized by a least-squares method in minimizing the term

$$\left|A\Phi' - \epsilon^{init}\right|^2 \tag{1.38}$$

where A is a sparse matrix containing the equations for every grid points, Φ' is an added perturbation field as $\epsilon = \epsilon^{init} + \nabla_a\Phi'$, which will be converted into a depth change δz so as to correct the depth of the old surface. Note that the term N^2/g multiplied by the slope difference s in the expression of ϵ acts as a weight related to the stability of the water column in the least-square computation.

At present, *omega* surfaces are the best estimates possible for approximating a neutral surface. Therefore, the next step in the progress of neutral density surfaces will be computing a dataset of ω variable based on measurements. Figure 1.9 shows that it is possible to achieve with ω surfaces in the North Atlantic. On the ω-surface, there is no fictitious diapycnal diffusivity larger than $10^{-5}\,m^2s^{-1}$ with most of regions having values smaller than $10^{-10}\,m^2s^{-1}$ which is insignificant compared to the values measured in the ocean.

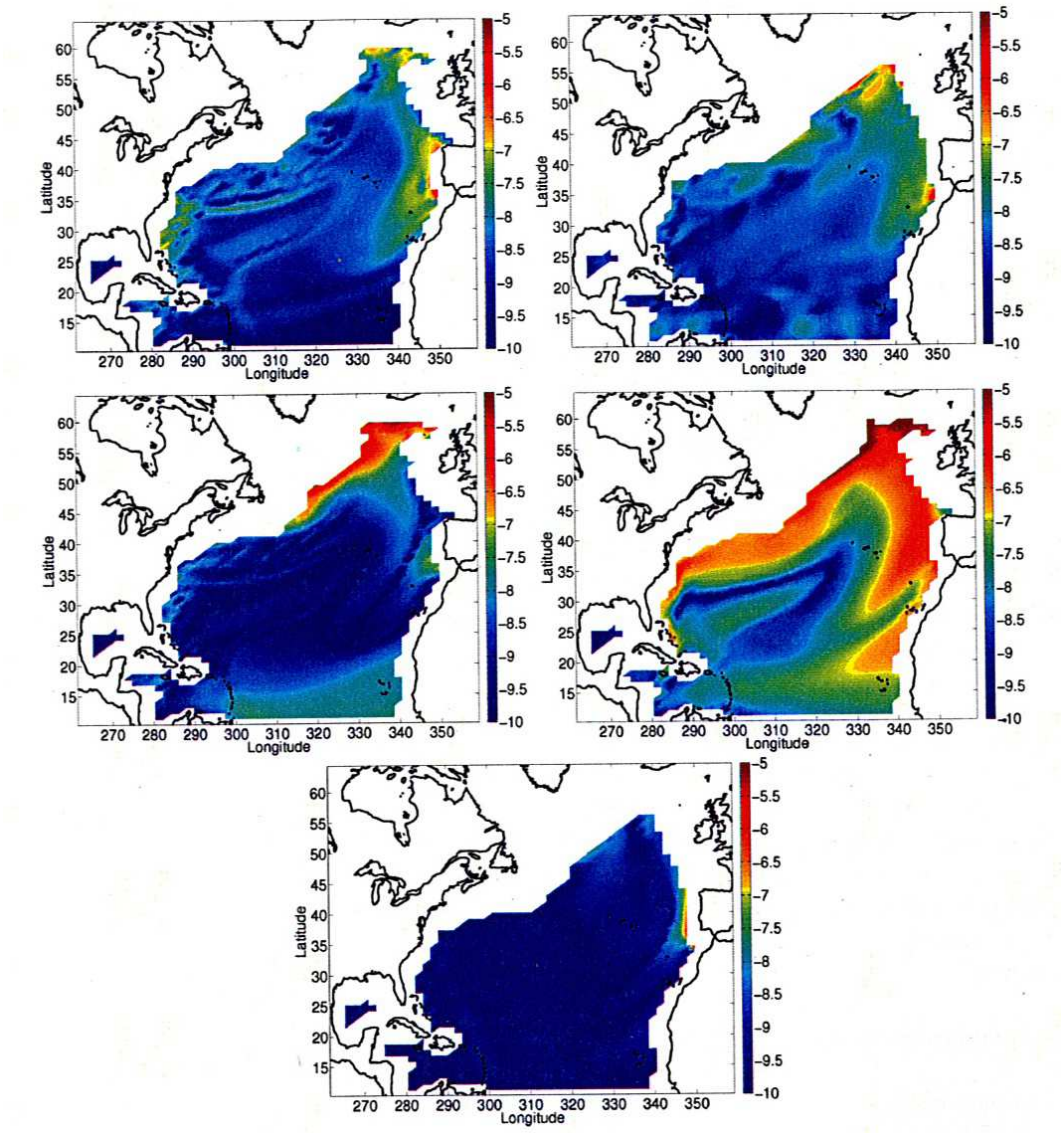

Figure 1.9: $log_{10}(D^f)$ for γ^i (top left), γ^n (top right), γ^{rf} (middle left), $\mathbf{d}\gamma^{EW}$ (middle right), and **(e)** ω(bottom). The surface chose, for these plots has an average pressure of approximately 600 $dbar$. The same colour scale is used in each plot.[Klocker et al., 2009]

Chapter 2

Method for constructing an approximate form of neutral density

2.1 The nature of the approximate form γ^{GP} of neutral density

Constructing a neutral density that is computationally efficient is needed for ocean models. To date the modellers have relied on the use of potential density referenced to 2000 *dbar*, σ_2,although this introduces significant errors when evaluating neutral surfaces. The σ_2 surfaces can often be several hundred meters away from the actual neutral surface. These errors introduce fictitious diapycnal mixing in the conservation equations that lead to non-realistic results compared to the real ocean. This demand has led to the construction of a global polynomial γ^{GP} for neutral density, based on the approximation of a γ^i labelled dataset.

Before introducing the process that has been used to form a global polynomial of neutral density γ^{GP}, it is important to clarify the specifications that the function requires. In particular, γ^{GP} is defined as a combination of polynomials, that are functions of salinity and temperature (pressure was also required for the Southern Ocean), and are joined together by weighting functions of latitude. Furthermore, these functions need to be applicable to a large range of salinities and temperatures. These specifications led to the development of multiple tools in order to obtain a good fit. These tools are described in the following sections.

The following part introduces the first version of γ^{GP}, which is a function of Practical Salinity S_P and potential temperature θ, using the old equation of state, EOS-80, for all thermodynamic computations. The tools have been developed in respect of EOS-80, a new version could easily be produced with the new equation of state, TEOS-10, by changing the thermodynamic functions inside the programs. Building a function based on EOS-80 is not a step back but is needed by ocean modellers who currently work with these outputs as their models are written in terms of EOS-80. Note that these outputs will be the basis of many studies over the next few years until the models are rewritten in terms of TEOS-10.

2.1.1 A combination of polynomials γ^{poly} function of salinity and temperature

Eden and Willebrand [1999] have shown that it was possible to obtain a polynomial that reproduces neutral surface more accurately than σ_2 on the North Atlantic (see Figure 1.9). McDougall and Jackett [2005a] tried to form a rational function, γ^a, approximating neutral density γ^n on the world, it was not very successful, and the improvement was not significant in comparison to σ_2. In the same paper [McDougall and Jackett, 2005a] pointed out the neutral limitation and explained that not considering the hemispheric change was one of the reasons of the mediocre results of γ^a. Due to the non-linearity of neutral surfaces and the limited amount of available data, a simple polynomial fit was not possible, thus we have opted to decompose the world oceans in several ocean basin and construct a neutral density polynomial γ^{poly} on each basin.

The common neutral density variable γ^n is a function of salinity, temperature, pressure, latitude and longitude. The material derivative of neutral density γ^n has been derived in McDougall and Jackett [2005a] and it has been shown that a change in pressure or a displacement $\{x, y\}$ introduces a false diapycnal velocity which is not due to natural processes in the ocean. It is then required that each of the polynomial γ^{poly} forming the global function γ^{GP} have the quasi-material property that is being only a function of potential temperature θ and Practical Salinity S_P. Nevertheless, we will see later that the function near the Antarctica in the Southern Ocean is also pressure dependent. It is very difficult to obtain a function close to being neutral without adding a pressure term. The zipping introduces the variables of latitude and longitude but these functions are chosen such that they do not introduce a strong dependence in spatial coordinates. The error introduced by the pressure and latitude terms will be discussed in the results chapter, it was necessary to accept the compromise between the two properties of a density surface, those of being neutral and quasi-material.

2.1.2 Range of validity: from fresh water to a warmer and colder ocean

As ocean models require an equation that is valid over a wider range than that found in an hydrographic atlas, γ^{GP} has been defined to be valid on a range of Practical Salinity from 0 to 40 psu. Thereby, γ^{GP} can be applied to fresh water and salinity values greater than those typically found in the actual ocean. The potential temperature range is defined from the freezing line on the salinity-temperature diagram to 40° C. Ocean models, particularly those that are being used to compute climate change, require a function that works with fresh water in order to simulate river outflow into the ocean and also deal with an ocean that is either warmer or colder than our ocean is today.

2.1.3 Datasets used and decomposition of the world oceans

Decomposing the world oceans into workable basins is not trivial and has been the fruit of long thinking and many tries. The first thought was to consider each ocean the Atlantic, the Pacific and the Indian, as a northern and a southern part. Experience has shown this was not necessary. A polynomial could fit on southward extended versions of the

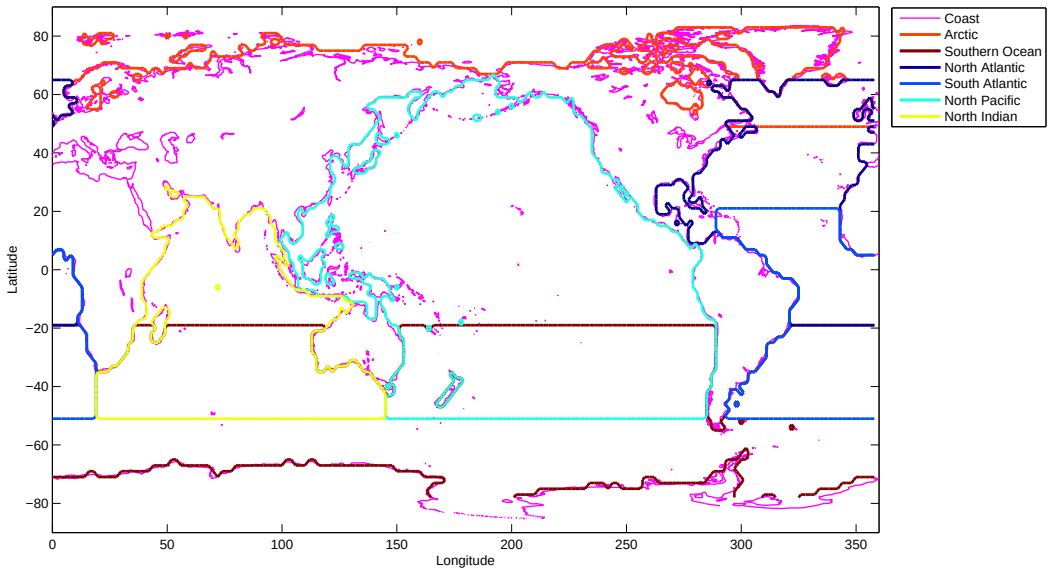

Figure 2.1: Decomposition of the world's oceans into regions used for fitting polynomials. The regions overlap to allow zipping between the functions for each basin

North Pacific and the North Indian. This required a northward extended version for the Southern Ocean. The Southern Ocean stayed a long time an object of thinking because of high gradients in temperature and salinity close to Antarctica. An example that highlights the difficulties which have been encountered is the Weddell Sea. It can be observed on Figure 2.2, that vertical gradients in temperature and salinity are large close to the surface and close to the circumpolar current by the density of their isolines. Isopycnals of γ^n follow this tendency and are concentrated in the same regions. The strong variation in neutral density compared to what happens further north where isopycnals look flat is a difficult thing to reproduce. The initial idea was to decompose the Antarctica coast into several parts. But the real problem appeared to not be here but more a competition between the deep and the shallow parts. The last decomposition of the world oceans, which was used for the fitting, is shown by Figure 2.1 and given by:

North Atlantic : from $20°S$ to $60°N$

South Atlantic : from $50°S$ to $20°N$

North Pacific : from $50°S$ to $60°N$

North Indian : from $50°S$ to the coast

Arctic Ocean : from $50°N$ to the North pole

Southern Ocean : from the South pole to $20°S$

Each ocean basin is briefly described in Appendix A and characterized by its salinity-temperature diagram. γ^{GP} isopycnals are also plotted for the range previously defined $(0/, g.kg^{-1} \leq S_P \leq 40/, g.kg^{-1}$ & $\theta_{freezing} \leq \theta \leq 40°C)$.

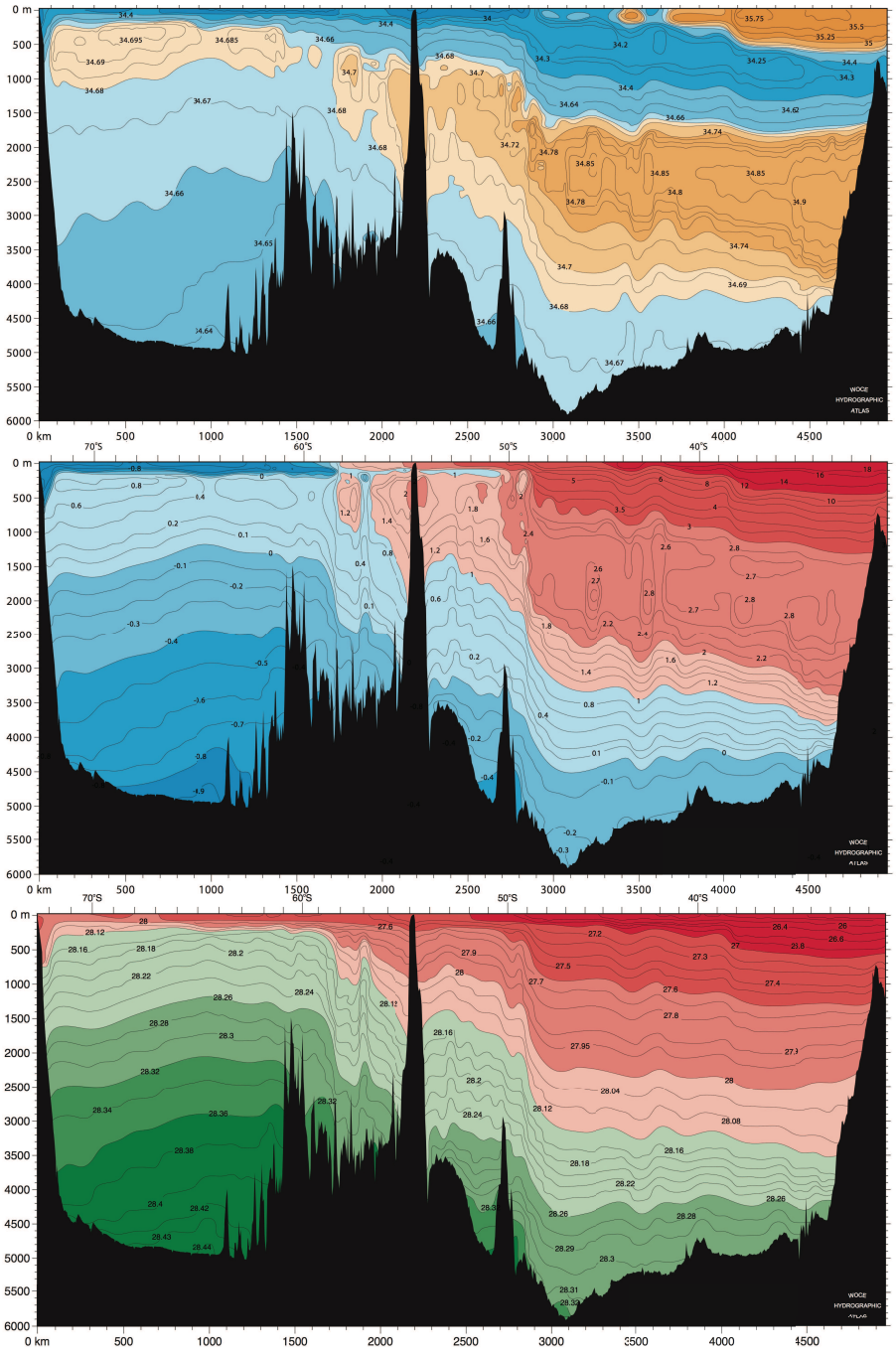

Figure 2.2: Section A23 along a latitude of 30° W of the Hydrographic Atlas of the World Ocean Circulation Experiment(WOCE). It starts from the Wedell Sea to the South Atlantic. The first graphic shows Practical Salinity, the second potential temperature, and the last is neutral density γ^n. The strength of the gradient in temperature and salinity induces a strong variation in isopycnals of neutral density. The southern shallow part of this section possess a strong gradient in neutral density compared to the northern part. [?]

2.2 Fitting method to obtain a polynomial γ^{poly} on an ocean basin

The construction of the global polynomial neutral density γ^{GP} began with the construction of a polynomial on an specified ocean basin. The major part of the work resides actually in obtaining a fit that achieves the specifications previously defined, and the global polynomial is simply a case of joining of all the polynomials γ^{poly}. Then, the process of making a γ^{poly} function on an ocean basin is actually a combination of several steps all linked together. Figure 2.3 depicts the method with its different steps and feedbacks. It can be seen that the dataset is the basis of the process, any errors in the original dataset are carried through to the final product. The dataset of Levitus climatology [Levitus, 1982] labelled with γ^n and the World Ocean Circulation Experiment (WOCE) climatology [Gouretski and Koltermann, 2004] labelled with γ^i has been used for constructing the function γ^{GP}. The first one allowed to see that it was possible to have a correct fit in each basin. Nevertheless, because of simplistic averaging and being based on small observational dataset the Levitus climatology hasn't been used to design the final form of γ^{GP}. Then, the final product has been built with the WOCE climatology. Furthermore, as the technology of γ^i is now operational (see **?** for improved results in defining neutral surfaces using γ^i), it has been used to label the WOCE climatology and obtain an accurate dataset describing neutral tangent planes.

Then, from the complete dataset an ocean basin from the previous list is extracted and is plotted on the salinity-temperature diagram. This allowed the dataset can be refined and extrapolated using two different methods, the first one based on the definition of neutral tangent plane (section 2.4.1), the second one on the definition of neutral density(section 2.4.2). The refined dataset labelled with γ^i is fitted in a least-square sense to the form the polynomial. Afterwards, to evaluate the relevancy of the fit and characterize its capability of being close to neutral surfaces, three methods are successively employed:

(i) the Root Mean Square difference and the maximum difference between the reference γ^i and the polynomial γ^{GP}

(ii) comparison between the vertical gradient along the water column of ρ_{local}, γ^{GP} and γ^i,

(iii) the evaluation of the fictitious diapycnal diffusivity D^f introduced by γ^i, σ_2 and γ^{poly}

Note that they do not achieve the same goal in the sense where (i) and (ii) characterizes how close γ^{GP} is from γ^i. (ii) allows to see if the vertical gradient of γ^{GP} is aligned with the vertical gradient of ρ. (iii) is the best method to evaluate the error which the approximate surface introduces. Note that the third is computer intensive so it is the last step of evaluating the polynomial.

A Graphic User Interface (GUI) has been developed in Matlab for this process, based on the schema of Figure 2.3. It provided the ability to centralise all the functions and have more efficient method to access to the different parameters such as the power of the polynomials and the added data. Note that the extrapolating part is another interface which has an interactive salinity-temperature diagram to add artificial data. It is described in one of the following sections.

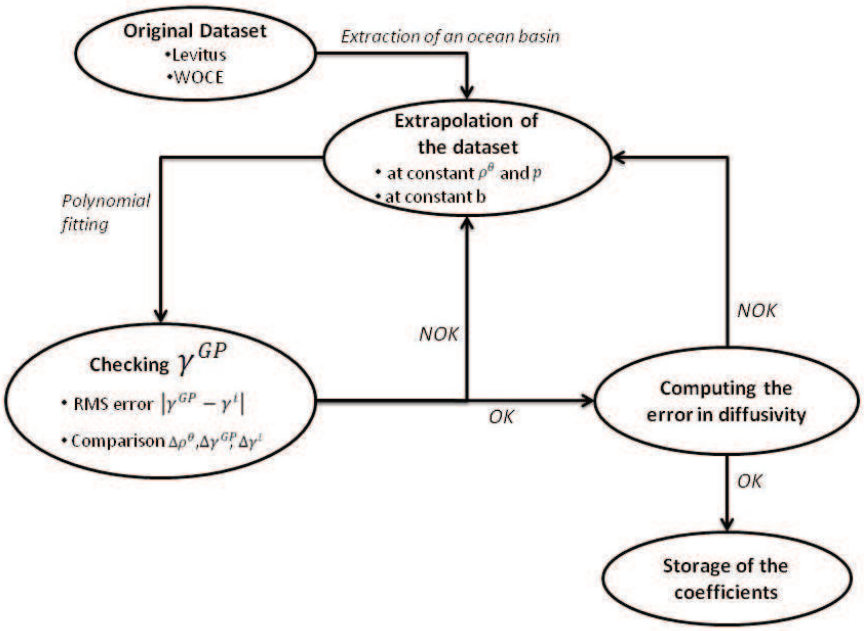

Figure 2.3: Schema describing the iterative process and the different steps used for fitting a γ label on an ocean basin. Because of an important number of parameters, loops are necessary before achieving a correct fit. (NOK=Not OK)

2.2.1 Linear system

In order to build the polynomials γ^{poly} from a dataset labelled with γ^i, we have to prescribe what sort of polynomials is required. In order to produce a function that is close to neutral, the polynomials need to depend only on salinity and temperature. Nevertheless, we will see later that some regions require an additional pressure term to give good results. It has been also decided for reasons of simplicity and sufficiency to look for polynomials with integer exponents. The linear system to solve is given by

$$K.A = \Gamma^i \tag{2.1}$$

Where the matrix K contains the unknown coefficients of the polynomials, A contains the value Practical Salinity and potential temperature at each power less han n which in other words constitute the basis vectors (note that it includes cross products). Γ^i contains the value of the reference label γ^i. Weights w can also be included in A and Γ^i in order to add one more degree of freedom in the fitting and reduce the influence of outlying data. The size of the dataset used is noted by L and it corresponds to the total number

of equations of the system.

$$
\begin{aligned}
K &= \begin{bmatrix} a_0 & a_1 & a_2 & \cdots & \cdots & a_{\frac{(n+2)(n+1)}{2}} \end{bmatrix} \\
A &= w. \begin{bmatrix} 1 & S_{P_1} & \theta_1 & S_{P_1}\theta_1 & \cdots & \cdots & {S_{P_1}}^n & \cdots & {S_{P_1}}^{n-k}{\theta_1}^k & \cdots & {\theta_1}^n \\ \vdots & \vdots & \vdots & \vdots & \ddots & \ddots & \vdots & \ddots & \vdots & \ddots & \vdots \\ 1 & S_{P_j} & \theta_j & S_{P_j}\theta_j & \cdots & \cdots & {S_{P_j}}^n & \cdots & {S_{P_j}}^{n-k}{\theta_j}^k & \cdots & {\theta_j}^n \\ \vdots & \vdots & \vdots & \vdots & \ddots & \ddots & \vdots & \ddots & \vdots & \ddots & \vdots \\ 1 & S_{P_L} & \theta_L & S_{P_L}\theta_L & \cdots & \cdots & {S_{P_L}}^n & \cdots & {S_{P_L}}^{n-k}{\theta_L}^k & \cdots & {\theta_L}^n \end{bmatrix} \\
\Gamma^i &= w. \begin{bmatrix} \gamma_1^i \\ \vdots \\ \gamma_j^i \\ \vdots \\ \gamma_L^i \end{bmatrix}
\end{aligned}
\tag{2.2}
$$

The system is solved by using the Moore-Penrose pseudo-inverse giving the solution in a least-square sense. The pseudo inverse can be computed using the Singular Value Decomposition. All of this is implemented in the MatLab function ***pinv()*** and it has been used for obtaining the solution.

2.2.2 Introduction of weights in the fitting

Some places such as the Antarctic region and the Arctic contain a lot of data with low buoyancy frequency N^2. Thus, the stability of the vertical stratification is small in these places. Such data introduce a lot of noise in the fitting. Therefore, it could seem judicious to insert a weight in the fit taking account of these low stability points and N^2 is quite appropriate to the situation.

$$
w = \frac{1}{N^2 + \epsilon} = \begin{bmatrix} \frac{1}{N_1^2+\epsilon} \\ \vdots \\ \frac{1}{N_j^2+\epsilon} \\ \vdots \\ \frac{1}{N_L^2+\epsilon} \end{bmatrix}
\tag{2.3}
$$

The weights have been tested on different ocean basins, their influence vary depending on the basin. It gave good results for certain range of pressures to the detriment of a loss of accuracy for another range. In other words, the weights were too strong and skewed the fit only in one direction. In general, it has been observed that a high value of ϵ gives more influence to the shallow waers whereas low value weights act more on the deep waters. After several tries, its use was abandoned because the improvement was not significant and difficult to control.

2.2.3 Antarctica particularity

It was difficult to obtain a correct fit close to the Antarctica using only salinity and temperature. The ice-sea interaction produces large gradients in temperature and salinity. It was not possible to reproduce this phenomenon with only a single polynomial function of

salinity and temperature on the Southern Ocean. The ocean required another polynomial to describe the shallow part close to Antarctica. In an attempt to obtain a better fit, two terms were added to the fitting:

- a pressure envelope: as the strongest gradients occur in the shallow part, (namely above 1000 meters), it was chosen to introduce a pressure term in an exponential form, $exp\left(-\frac{P}{p_0}\right)$. The advantage is that this term has negligible effect at high pressure so that it is appropriate to this fitting.
- a temperature envelope: as the strongest gradients occur in the southern side of the Antarctic Circumpolar Current, it was decided to introduce a term with an hyperbolic tangent function of temperature to simulate its shape, $th\left(\frac{\theta-\theta_0}{\tau^\theta}\right)$. It vanishes on the northern side of the Antarctic Circumpolar Current.

Thus the new linear system for the Southern Ocean becomes:

$$K.A + Q.B.exp\left(-\frac{P}{p_0}\right).th\left(\frac{\theta-\theta_0}{\tau^\theta}\right) = \Gamma^i \tag{2.4}$$

Where Q and B are similar to K and A but contain less terms. Adding a pressure term is not desired because it may produce a false diapycnal diffusivity when running in ocean models. Nevertheless, this solution gives good results to describe neutral surfaces in the Antarctica region and will see later how to quantify the introduced error using the pressure term. The constants were determined after several tries and is the result of a compromise between the quality of the results in the two parts (Antarctic coastline and the rest of the Southern Ocean). p_0 has been set to $700\,dbar$, θ_0 to $2.5°\,C$ and τ^θ to $0.65°\,C$.

2.3 Evaluation of the error

Several methods are used to characterize the quality and the accuracy of the fit. As we look for an approximate function, the first way to evaluate the error is obviously the RMS difference and the maximum difference between the label γ^i and the approximate function evaluating on grid points. It gives an idea if the fitting is going in the right direction. However it is not sufficient to evaluate the property of the function to be neutral. That's why several tools have been developed and are introduced in the following sections.

2.3.1 Comparison of the vertical gradient

The variation of the vertical gradient of γ^{poly} with increasing depth is compared to those of locally referenced potential density, and γ^i. It has been already shown that $\nabla\gamma^i = b\nabla\rho^\theta_{loc}$ and because γ^i follows the aim of being as close as possible to neutral, this factor varies in the ocean depending on space It is possible to generalize the factor b, assuming that $\nabla\gamma^{poly} = b_{poly}\nabla\rho^\theta_{loc}$ to see how γ^{poly} behaves with increasing depth. One last thing which can be plotted is the vertical gradient of γ^{poly} compared to γ^i and it gives a good insight as to how close the fit is to Neutral Density. Note that the polynomial defined by Eden and Willebrand [1999] aims to keep the scalar b close to one, in order to stay quasi-material.

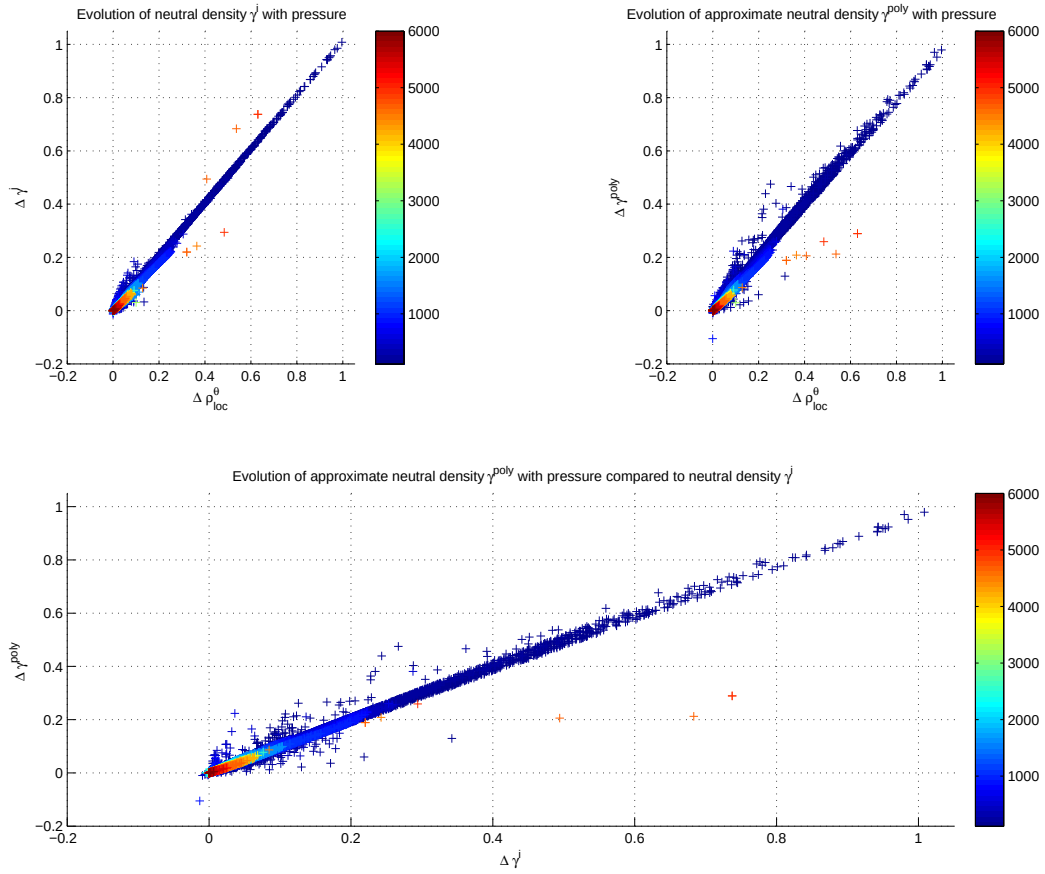

Figure 2.4: Windows plotting the evolution with depth of the vertical gradient of γ^i (left up) γ^{poly}(right up) in comparison with the evolution of the vertical gradient of ρ^{θ}_{loc}. The plot at the bottom is the evolution of the vertical gradient γ^{poly} compared to γ^i. The dataset used is the North Atlantic ocean basin extracted from the WOCE climatology labelled with improved neutral density. The results are plotted for the the last polynomial in date $\gamma^{poly\,NA}$.

2.3.2 Fictitious diffusivity evaluation

Evaluating the false diapycnal diffusivity sometimes called fictitious diffusivity is the best way to see how far a density function is from being neutral. It has been seen in the first chapter (equation (1.31)) that the diffusivity can be computed by the lateral diffusion coefficient $K = 1000\, m^2.s^{-1}$ multiplied by the square of a slope difference s^2 between the approximate neutral surface and the neutral tangent plane.

To compute the fictitious diffusivity, multiple programs had to be developed. The heart of the code is a program allowing the determination of the intersection of a neutral tangent plane on a neighbouring cast starting from a bottle. A first algorithm produced by David R. Jackett has been made more efficient. The new process is as follows:

- One looks for the simple approximation of a neutral tangent plane by finding the closest pressure in the neighbouring cast by minimizing the difference between the pressure of the bottle and the pressure of a bottle in the neighbouring cast. This

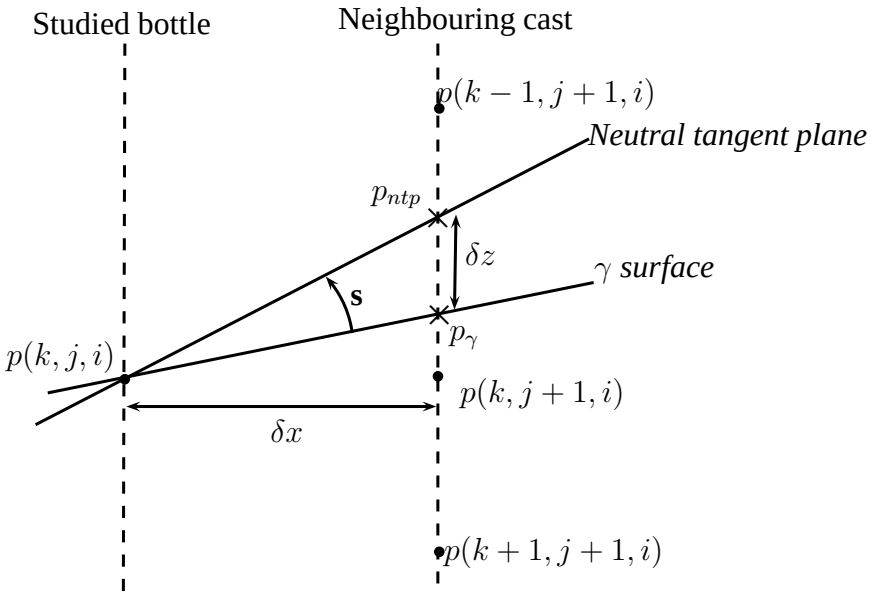

Figure 2.5: Slope difference between a density surface and the neutral tangent plane. Each intersection p_{ntp} and p_γ is determined by finding the two bottles of the neighbouring cast between which the density variable of the studied bottle (ρ_l^θ for neutral tangent plane, and γ^{poly} for the approximate neutral density) is included. The position between the two bottle is then approximate using a Newton-Rahpson method.

will be the starting point for the next part.

- Then, one studies the difference in local potential density between the bottle and a bottle of the neighbouring cast. According to the sign, one looks for the denser or less dense point. In this way, one finds an area where the local potential density of the studied bottle is included between two bottles of the neighbouring cast.
- The crossing point is finally approximated by a Newton-Raphson method.

This program is more efficient than the original version because the Newton-Raphson resolution required searching the entire neighbouring cast for each bottle on the starting cast wich was very time consuming. Performing on the Levitus [Levitus, 1982] dataset of 33 pressure layers, with a resolution of 4° in latitude and 4° in longitude, 133650 points, the computation was seven times faster than the original version.

Once the intersection has been found, the difference in pressure between the approximate neutral surface and the neutral tangent plane δp is converted into a depth difference δ_z. With δ_x the distance between the studied bottle and the neighbouring cast, the slope difference is then computed with the simple geometric relation:

$$\mathbf{s} = \frac{\delta_z}{\delta_x} \tag{2.5}$$

Figure 2.3.2 describes the formation of the slope difference after having solved the intersection between the studied bottle and the neighbouring cast.

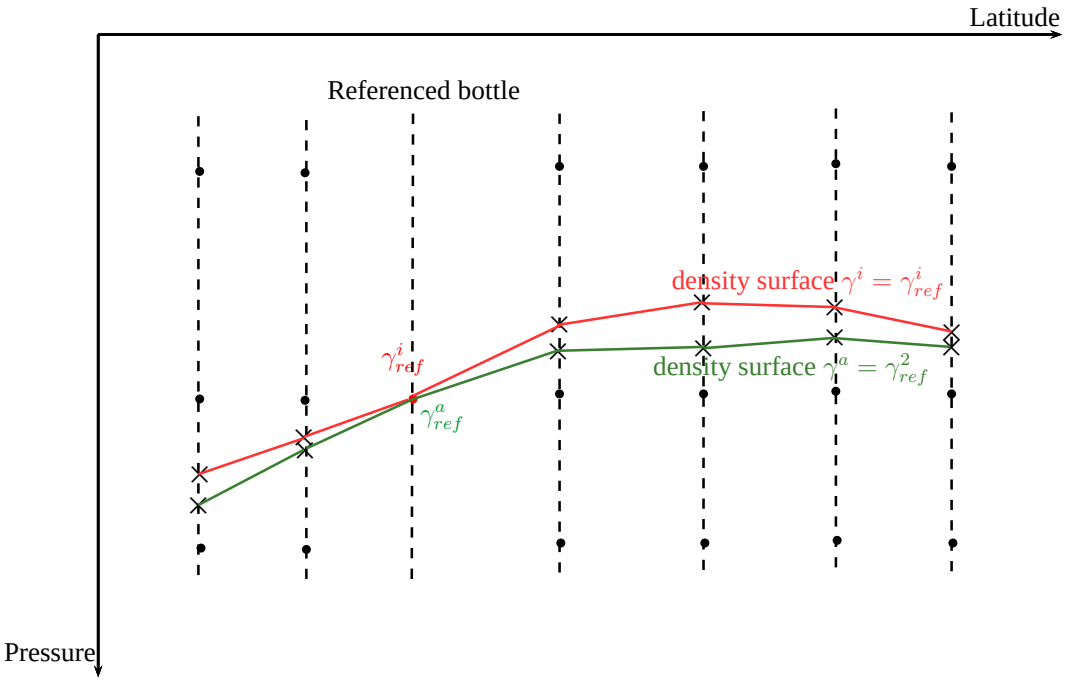

Figure 2.6: Neutral Density surfaces of constant γ^i and approximate neutral density γ^a (γ^{poly} or σ^2), starting from the same referenced bottle. The intersection with the neighbouring casts is found by the same program used to determine the slope difference (section 2.3.2). The two surfaces coincide exactly at the reference bottle.

2.3.3 Difference in pressure between different density surfaces

An algorithm similar to the diffusivity program has been developed to find the intersection of a density surface with all the casts of the dataset. The density surface starts from a referenced bottle, the intersections of this specific value with all the casts of the dataset are determined using the same algorithm as in the slope evaluation (section 2.3.2). The surface is built by joining all these intersections. It allows us to evaluate the error in depth that the use of the approximate surface introduces. Figure 2.3.3 shows the building of the surface of γ^i which is close to neutral surface and an approximate surface γ^a. By construction, the two surfaces coincide at the referenced bottle.

2.4 Data extrapolation

Trying to make a fit only with the data provided by a dataset (WOCE climatology or Levitus) does not give robust results when used in ocean models. It is sufficient to look at the shape of γ^{poly} isopycnals on the salinity-temperature diagram to realize that the validity field is narrow. Areas exist where isopycnals have too much degree of freedom because they are void of any data to constrain the fit. In order to increase the validity range of the γ^{poly} function and allow it to describe a scale larger than the actual ocean, a way to add some data in these regions had to be found. One particular goal is to have correct isopycnals near values of Pracictal Salinity of $0/, g.kg^{-1}$ in order to be able to describe fresh water. Two ways have been developed to achieve these aims and are introduced in the following sections.

2.4.1 Extension in a neutral way

The first method is based on the thought experiment of displacing a point along a constant line of potential density and at constant pressure. In this particular case, potential density coincides exactly with local potential density because of the constant pressure. Once the temperature-salinity point has been formed (at constant potential density), the new point is labelled with the same value of γ^i. It means that we consider that γ^i is constant along a neutral surface and this hypothesis seems judicious when γ^i obviously aims to reproduce neutral tangent planes. Consequently, adding some data with this principle allows us to constrain the extended fit γ^{poly} in the neutral sense.

This iterative process is shown by Figure 2.7. Taking a bottle of the dataset, the first step is to compute its potential density $\rho^\theta = \rho(S_P, \theta, p)$. Then, we choose a step in potential temperature $\Delta\theta$ in an arbitrary way to create a new bottle and we label it with the same potential density and pressure. The change in salinity is therefore computed using the inverse function.

$$S_P + \Delta S_P = S_P(\rho^\theta, \theta + \Delta\theta, p) \tag{2.6}$$

The final point is the labelling of the created bottle by the same γ^i value. The inverse function is based on the method used in the function ***gsw_SA_from_rho()*** from the Gibbs Seawater (GSW) Oceanographic Toolbox [McDougall and Barker, 2011]. As it has been designed for the new equation of state TEOS-10 [IOC et al., 2010], a version has been developed to be used with the old equation of state EOS-80. The value of salinity is found using the iterative method called the Newton-McDougall method [**?**], which is a modification of the standard Newton method. The iterative process can be written using the specific volume $v = 1/\rho$:

$$\begin{aligned}
&\text{Initial condition:} \quad S_P^1 = S_P^0 - \frac{v(S_P^0, \theta^{ref}, p^{ref}) - v^{ref}}{\left.\dfrac{\partial v}{\partial S_P}\right|_{\theta,p}^{est}} \\
&\text{for } i \geq 0, \quad S_P^{2i+2} = S_P^{2i} - \frac{v(S_P^{2i}, \theta^{ref}, p^{ref}) - v^{ref}}{v'^i} \\
&\qquad\qquad S_P^{2i+3} = S_P^{2i+2} - \frac{v(S_P^{2i+2}, \theta^{ref}, p^{ref}) - v^{ref}}{v'^i} \\
&\qquad\qquad with\ v'^i = \left.\frac{\partial v}{\partial S_P}\right|_{\left(1/2(S_P^{2i}+S_P^{2i+1})\right), \theta^{ref}, p^{ref}}
\end{aligned} \tag{2.7}$$

This recent method achieves convergence order $\sqrt{2}+1$ against 2 for the standard one. In this particular case, only two iterations are sufficient to find the value of S_P with an error under 8.10^{-13}, which is equivalent to machine precision.

What is remarkable with the method of extending data along a surface of constant locally referenced potential density is that it can be used to constrain the slopes of isopycnals. Where Eden and Willebrand [1999] defined a minimum condition based on the partial derivative of their density variable γ^{EW}, we are able to constrain isopycnals using this technique over a particular area on the salinity-temperature diagram. In respect of the notation partial derivative of potential density, the gradient γ^{poly} can be written

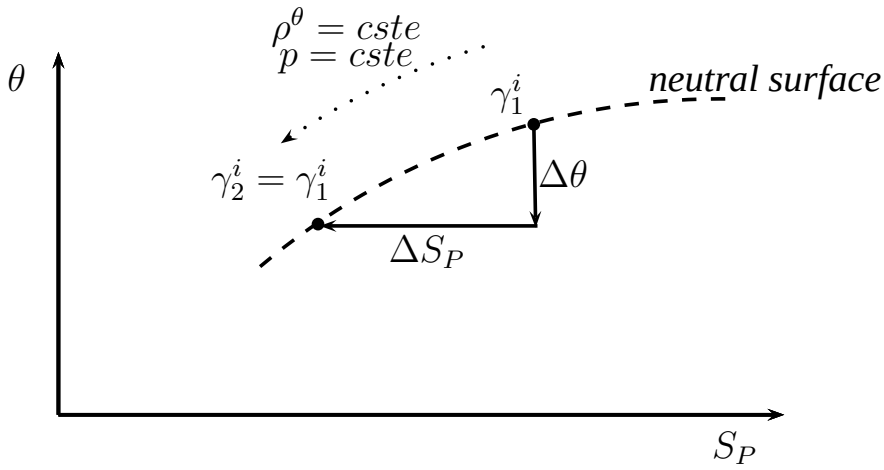

Figure 2.7: Displacement of a point along a neutral surface in the salinity-temperature diagram and labelling with the same value of γ^i in order to create new data points. The step in temperature $\Delta\theta$ is arbitrarily chosen and the step in salinity ΔS_P is derived by an inverse method.

with $\alpha^{poly} = -\frac{1}{\gamma^{poly}}\frac{\partial\gamma^{poly}}{\partial S_P}$ and $\beta^G = \frac{1}{\gamma^{poly}}\frac{\partial\gamma^{poly}}{\partial\theta}$ so that the two following equations can be written.

$$\begin{aligned}\nabla(ln\,\rho_l^\theta) &= \beta^\theta\nabla S_P - \alpha^\theta\nabla\theta \\ \nabla(l\,n\gamma^{poly}) &= \beta^{poly}\nabla S_P - \alpha^{poly}\nabla\theta\end{aligned} \tag{2.8}$$

By definition, if the point is displaced along a neutral tangent plane $\beta^\theta\nabla_n S_P - \alpha^\theta\nabla_n\theta = 0$. If γ^{poly} is also considered constant along this surface, then $\beta^{poly}\nabla_n S_P - \alpha^{poly}\nabla_n\theta = 0$. As this is true for every variation of S_P and θ, this implies that the slopes are equal, that is $\alpha^{poly} = \alpha$ and $\beta^{poly} = \beta$. This method gives good results and allow the use of a high power for the polynomial in an attempt to improve its accuracy. This method has its limitations, it can be used to extrapolate isopycnals to increasing salinity, but when applied to decreasing salinity, the isopycnals tend to converge in a small area as shown on Figure 2.7. Therefore, this method has been used intensively in the right quadrant but carefully in the left quadrant of the salinity-temperature diagram.

2.4.2 Extension at constant b for the shallow and deep parts

The second method is based on the mathematical definition of γ^i. **?** remind us that for an ocean $\{S_P, \theta, p, longs, lats\}$ the neutral stratification problem has a solution if we can find a scalar variable $b(x, y, z)$ satisfying

$$\nabla\gamma = b\rho(\beta\nabla S_P - \alpha\nabla\theta) = b(\nabla\rho - \rho\kappa\nabla p) \tag{2.9}$$

If the pressure is maintained constant, the gradient in γ is therefore directly related to the gradient in density. Considering few layers near the surface, the pressure can be considered constant and a mean value of b can be determined by the change in potential density. As b is only dependent on spatial coordinates, it is a characteristic of a region in the ocean and can vary according to the ocean basin. At depth, the mean b, $\overline{b}$, is computed using the change in locally-referenced potential density. Regarding the shallow

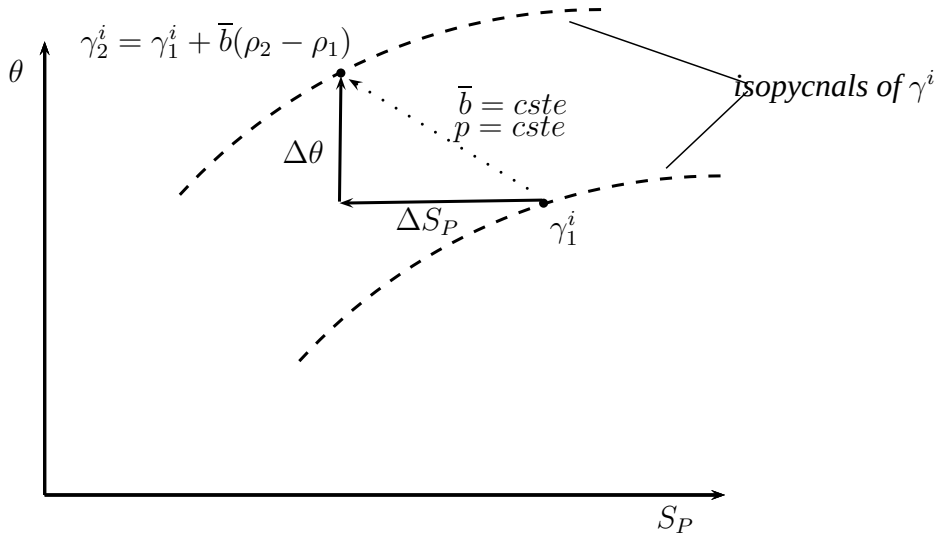

Figure 2.8: Displacement of a point labelled with γ_1^i on the salinity-temperature diagram and finding the corresponding isopycnal using a constant value of b and at constant pressure. The step in salinity ΔS_P and in temperature $\Delta\theta$ are chosen arbitrarily. The sketch describes the principle for the shallow data extrapolation, the process is similar for the deep data

part, the horizontal gradient has been used to compute $\overline{b}$. In practice, it is computed on several pressure levels and the averaging is done on the results. Figure 2.8 shows the process. Taking a bottle of the dataset, as in the previous method, the first step begin with the computation of its potential density $\rho^\theta = \rho(S_P, \theta, p)$. Then, we choose both a step in potential temperature $\Delta\theta$ and in salinity ΔS_P, once again in an arbitrary way, and create a new bottle. The change in potential density is therefore computed $\rho^\theta + \Delta\rho^\theta = \rho(S_P + \Delta S_P, \theta + \Delta\theta, p)$ in order to label this artificial bottle with γ^i. Using a mean value of b, $\overline{b}$, the change in gamma is defined by

$$\Delta\gamma = \overline{b}\Delta\rho^\theta \tag{2.10}$$

2.4.3 Interactive salinity-temperature diagram

In order to refine the dataset, another GUI interface was created in MatLab. The original idea was to be able to quickly select a part of the dataset and extrapolate it. This allows the user to select water masses using a filter (pressure, latitude, longitude, and γ^i), extrapolate without creating artificial water masses using the method of constant locally referenced density (Section 2.4.1). Second technique was also added a filter in neutral density for use on the shallow or deep parts of the data (Section 2.4.2). The use of interactive sidebars provide visualisation and easy access on the added data.

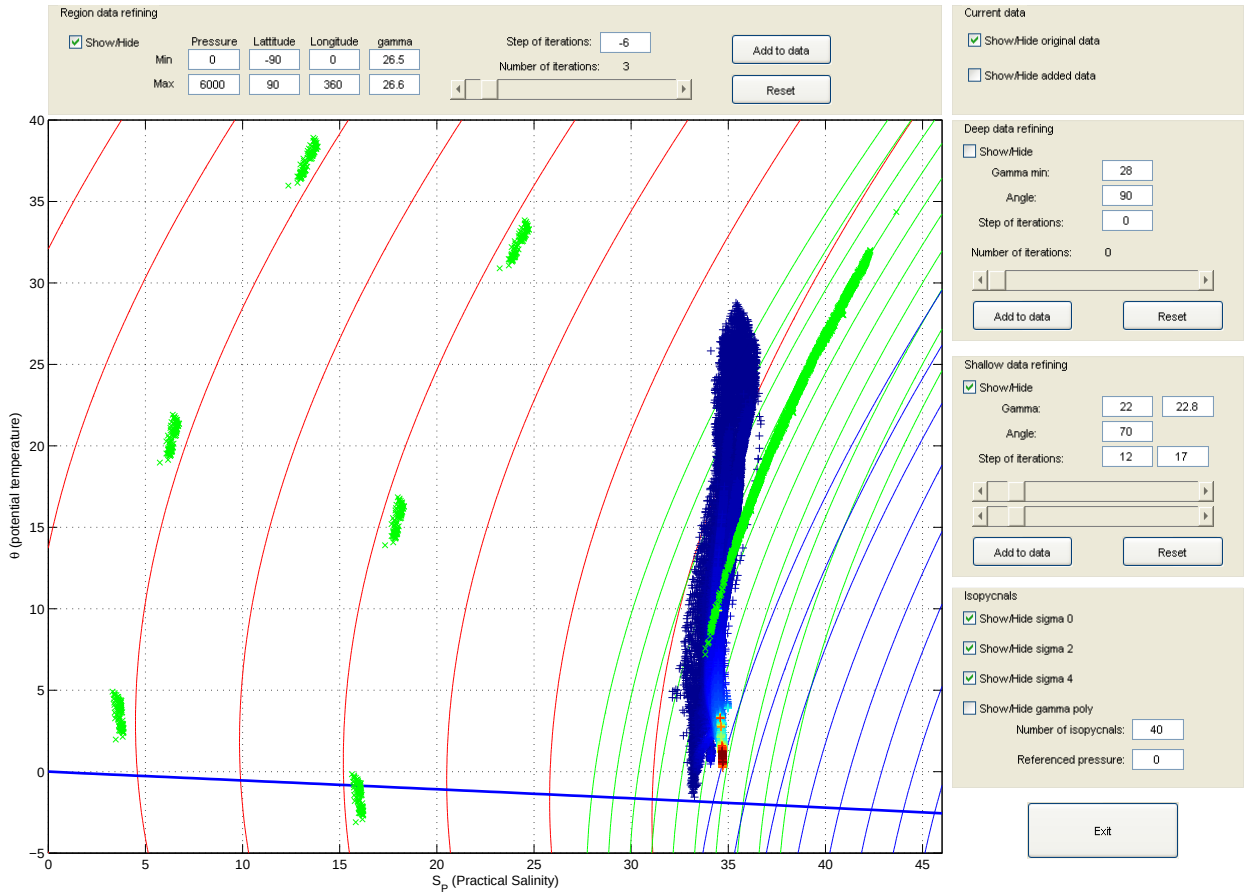

Figure 2.9: MatLab GUI designed for plotting and extrapolating the data of an ocean basin on the salinity-temperature diagram. The data of the North Pacific (WOCE climatology) is plotted on the salinity-temperature diagram. The data is colourized by pressure, (blue for low pressure and red for high pressure). The blue line at the bottom represents the freezing line at $p = 0$. Isopycnals of σ_0(red), σ_2(green) and σ_4(blue) are plotted on particular region of the diagram. The green data on the left is extrapolated using at constant value of b in the shallow data(Section 2.4.2). The green data on the right is extrapolated in a neutral way (Section 2.4.1).

2.5 Zipping method

It is difficult to obtain an accurate fit on the all the world oceans, γ^{GP} has been decomposed into polynomials on each ocean basin. In order to form a global function, these polynomials must be able to communicate between the different basins. The horizontal decomposition between the Atlantic, Indian and Pacific can be obtained using characteristic functions based on the natural frontier made by the coastline. Three horizontal junctions have been constructed between ocean basins:

- Arctic ocean and North Atlantic: splitting at $50°N$ with a range of variation of $20°$
- North Atlantic and South Atlantic: splitting at the equator with a range of variation of $20°$

- Southern ocean: splitting at $40°S$ with the Pacific, Indian and South Atlantic ocean, with a range of variation of $20°$

Weighting functions with a sinusoidal form were used to make these joints. The southern weighting function can be expressed under the form:

$$w_{south}(\lambda) = \chi_{[-90°,\lambda_{min}[} + \chi_{[\lambda_{min},\lambda_{max}]}.\cos\left(\pi\frac{\lambda-\lambda_{min}}{\lambda_{max}-\lambda_{min}}\right) \tag{2.11}$$

Where $\chi_{[a,b[}$ is a characteristic function and is equal to 1 when $a \leq \lambda < b$ and 0 when $b \leq \lambda$. λ_{min} and λ_{max} are respectively the southern and northern boundaries of the zipping. The northern weighting function is simply $w_{north} = 1 - w_{south}$. Figure 2.10 shows the shape of the weighting function for the South Atlantic. This sort of function has been especially chosen because of the smoothness of its gradients. Note that adding this weighting in spatial coordinates introduces a dependence in space for the final form of γ^{GP} so that the approximate neutral density looses the property of being quasi-material, i.e. being a function only of salinity and temperature. Figure 2.11 shows that the derivative of weighting function has its maximum at the center of zipping regions and is zero outside.

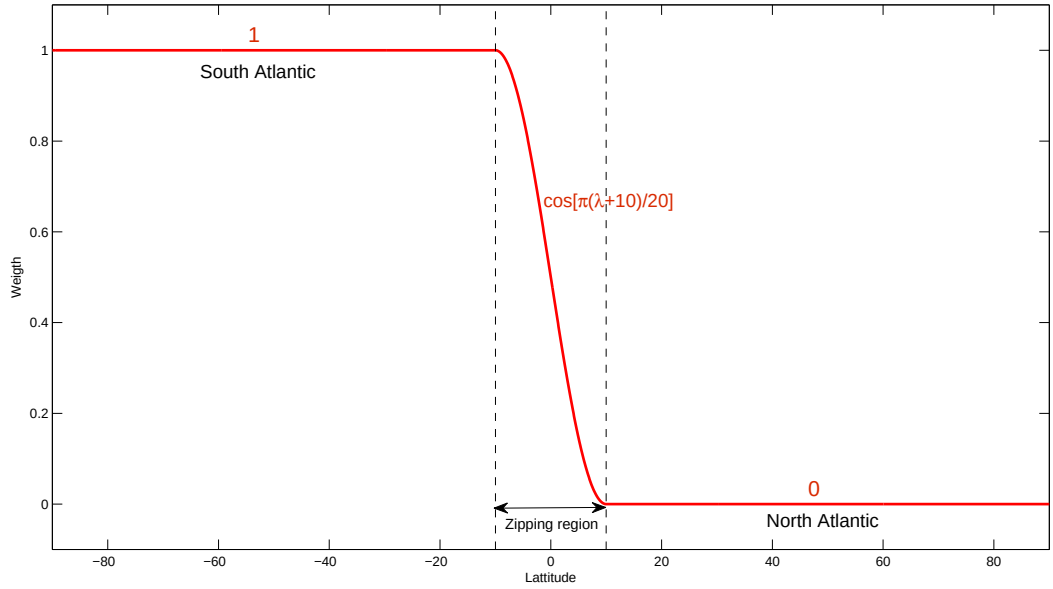

Figure 2.10: Weigthing function between North and South Atlantic. γ^{polySA} is multiplied by this function. South of $-10°$, the function is equal to one. North of $10°$, it is equal to zero. On the zipping area it changes in a sinusoidal way, the tangent on the edges is equal to one in order to avoid discontinuities.

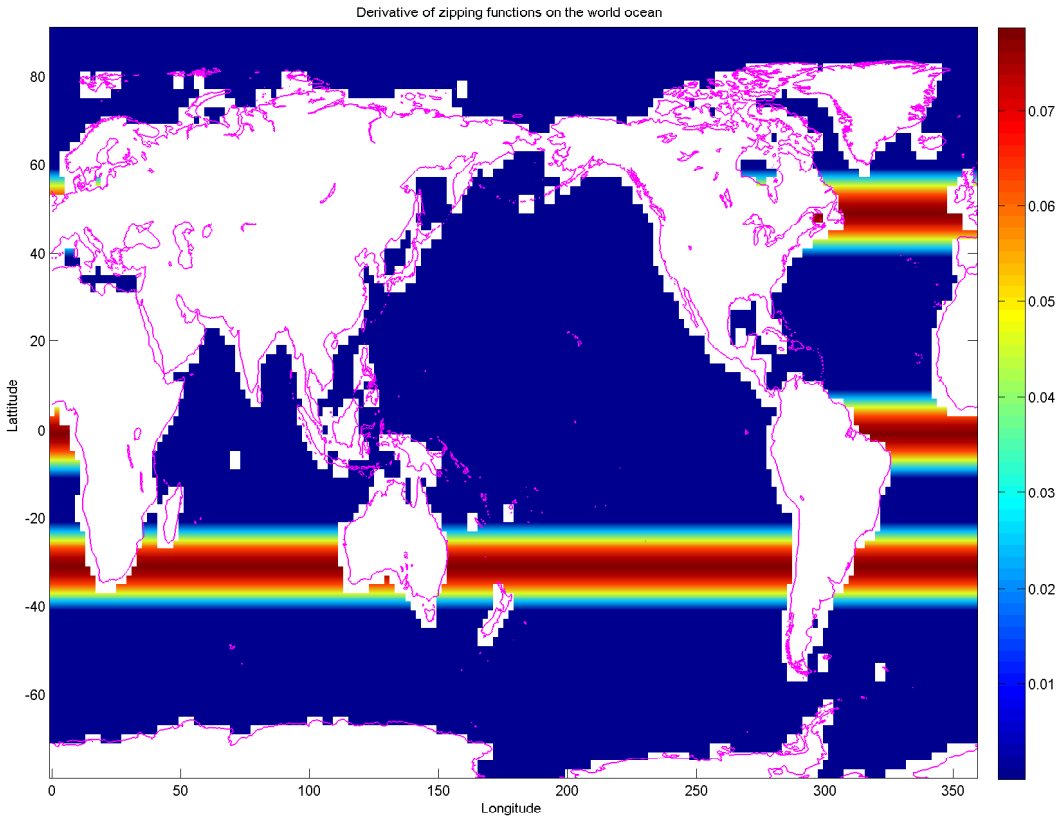

Figure 2.11: World map of the derivative of weighting functions. It shows the different zipping regions between the ocean basins. The derivative is maximum in the middle of the zipping area and reaches zero on the edges to limit strong dependence in latitude

Chapter 3

Delivered product and results

3.1 γ^{poly} on ocean basins on the WOCE climatology

All of the methods and the toolbox developed in the second chapter have been applied to build polynomials γ^{poly} for each ocean basin approximated γ^i computed on the WOCE climatology. It was found that the amount of false diapycnal mixing (i.e. the error in the fit) was strongly dependant on the quality of the original labelled dataset. Three surfaces of constant pressure were chosen to describe the shallow ($505\,db$), the middle ($2534\,db$) and the deep ($4069\,db$) parts of the ocean. The fictitious diapycnal diffusivity is plotted on these three surfaces for neutral density γ^i and potential density referenced to $2000\,db$ σ_2 (see Figures 3.2 and 3.3). γ^{poly} aims to describe more accurately neutral surfaces than σ^2 in order to replace it in ocean models. It is then important to be able to quantify the improvement of γ^{poly} compared to σ^2. It is also judicious to be able to compare how close γ^{poly} is from γ^i in terms of being neutral. In the following sections, we will use the common term in oceanography of water mass which is distinctive body of water characterized by ranges of temperature and salinity and having a common formation history.

After considerable effort it was decided that the data in the Arctic was of very low quality. Gouretski and Koltermann [2004] indicate that there are very few oceanographic observations in this region. This is not surprising since much of the Arctic circle remains frozen for most of the year which makes it very difficult for scientist to sample the ocean. Analysis of the γ^i dataset revealed that it contained a lot of false diapycnal mixing which caused the fit to be very unneutral. Consequently, at present, it is not possible, to build neutral density γ^{poly} on the Arctic ocean because of the lack of workable data. A new climatology has to be done and labelled with γ^i before trying to make a polynomial fit. The coefficients of the polynomials whose the results are introduced in this chapter are available in Appendix A.

3.1.1 North Atlantic

This study began with the North Atlantic where a previous polynomial function of neutral density γ^{EW} already exists [Eden and Willebrand, 1999]. Their function was built in a different way compared to our fitting process. They tried to make the vertical gradient of this neutral density variable close to the vertical gradient of *in situ* density. However, the function gives good results in terms of being close to neutral as Figure 3.1 shows. γ^{EW}

has 69% decrease in fictitious diffusivity less than $10^{-5}m^2s{-}1$ compared to σ_2 whereas γ^i gives improvements of 87%. The function does not achieve the specification of working on a wide range of salinities. Figure 3.4 shows that the validity range is only $32 \rightarrow S_P \rightarrow 36$ and $\theta_{freezing} \rightarrow \theta \rightarrow 27°C$ which is not sufficient to be used in ocean models.

The first version of γ^{poly} was built by extending the data using the technique describing in section 2.4.1 (i.e. displacing data at constant locally referenced potential density and constant pressure). Its isopycnals have good shapes on the high salinity section of the salinity-temperature diagram as shown in Figure 3.4, note that the validity range is already wider than γ^{EW}. It also gives an improvement of 62% in diffusivity less than $10^{-5}\,m^2s{-}1$ compared to σ_2 (see Figure 3.1). Nevertheless, this function does not achieve the property of being valid at low salinity values. The isopycnals on the salinity-temperature diagram of γ^{poly} of Figure 3.4 are not well defined in the Practical Salinity range from 0 to 30.

In order to increase the validity range of γ^{poly}, the second method of data extrapolation taking a constant value of b was used (section 2.4.2). Adding few points from the original dataset constrained the shape of the isopycnals and gave the results of $\gamma^{poly}(shape)$ on the salinity-temperature diagram (Figure 3.4). The consequences of adding data in this way are important to the accuracy of the fit. It has also increased the amount of data with $D^f > 10^{-5}\,m^2.s^{-1}$ by 33% compared to the previous version. The improvement compared to σ_2 has dropped to 42%. We will see in a further section that the loss is not as significant in other ocean basins and that it is possible to obtain good extended isopycnals without degrading the quality of the function of being close to neutral. It is difficult in the North Atlantic because of the Labrador Sea where gradients in salinity and temperature are important. On the salinity-temperature diagram (Figure 3.4) the shallow water has salinities and temperature that are very close to those of the deep water which causes the isopycnals to converge. Moreover, γ^i is not very accurate in the deep part as we can see on Figure 3.2.

The polynomial selected for the global version of γ^{GP} is $\gamma^{poly}(shape)$ because it has the required properties for our neutral density approximation. Other results are given by Figure 3.5 which shows that the diffusivity greater than $10^{-5}\,m^2.s^{-1}$ is concentrated to the shallow parts of the Labrador Sea. Ocean processes are difficult to reproduce in this region without having a better γ^i labelled dataset. γ^{poly} is even better than γ^i at depth as there is less data with D^f larger than $10^{-5}\,m^2.s^{-1}$.

Figure 3.5 also shows that the difference between a γ^i surface of $28.05\,kg.m^3$ and a σ_2 surface of $37.019\,kg.m^3$ is roughly $100\,m$ whereas the difference between this same γ^i surface and le γ^{poly} surface is not more than $10\,m$ in the North Atlantic. Note that both γ surfaces do not have exactly the same value. Therefore, the error in depth might be less than $10\,m$ for the exact value.

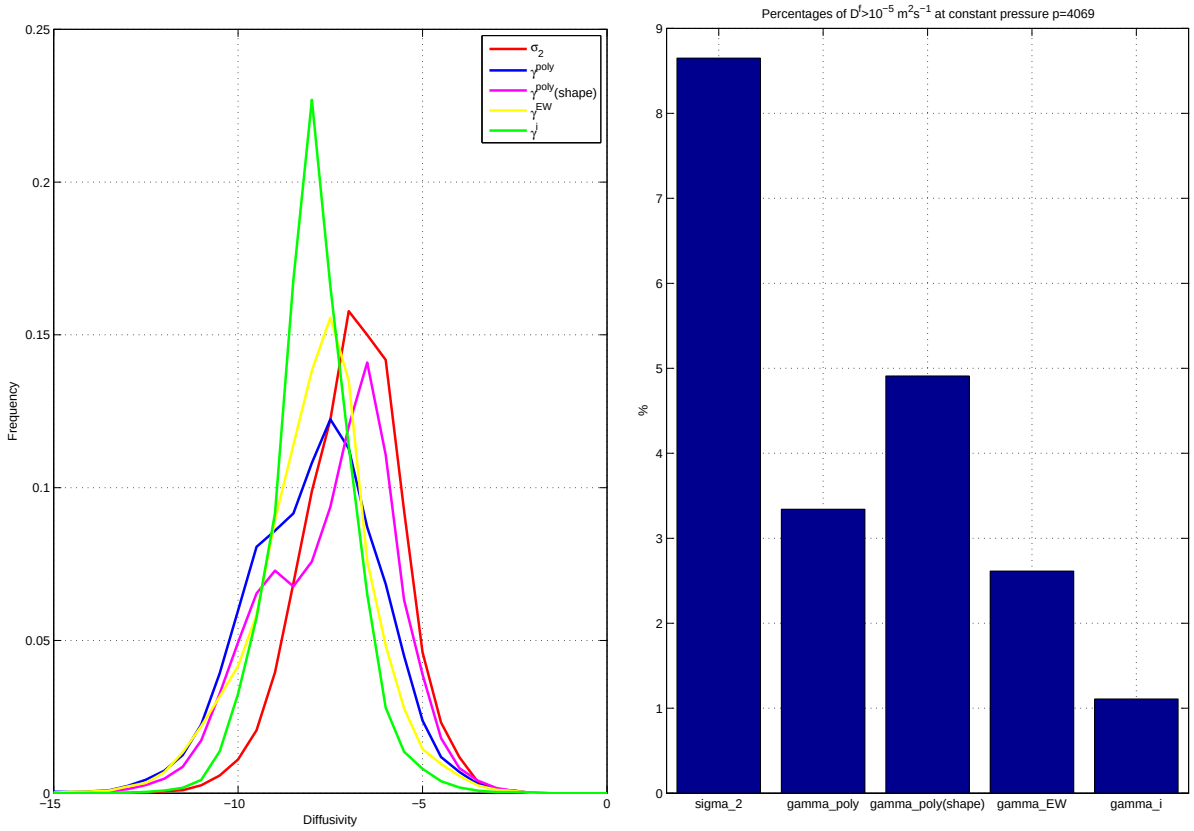

Figure 3.1: On the left, frequency of the decimal logarithm of the fictious diapycnal diffusivity D^f on the North Atlantic. On the right, percentage of fictitious diapycnal velocity greater than $10^{-5}\,m^2.s^{-1}$ on the North Atlantic. The results are compared between σ_2, γ^i, γ^{EW}, a first version of γ^{poly}, and $\gamma^{poly}(shape)$ with extension to low salinities

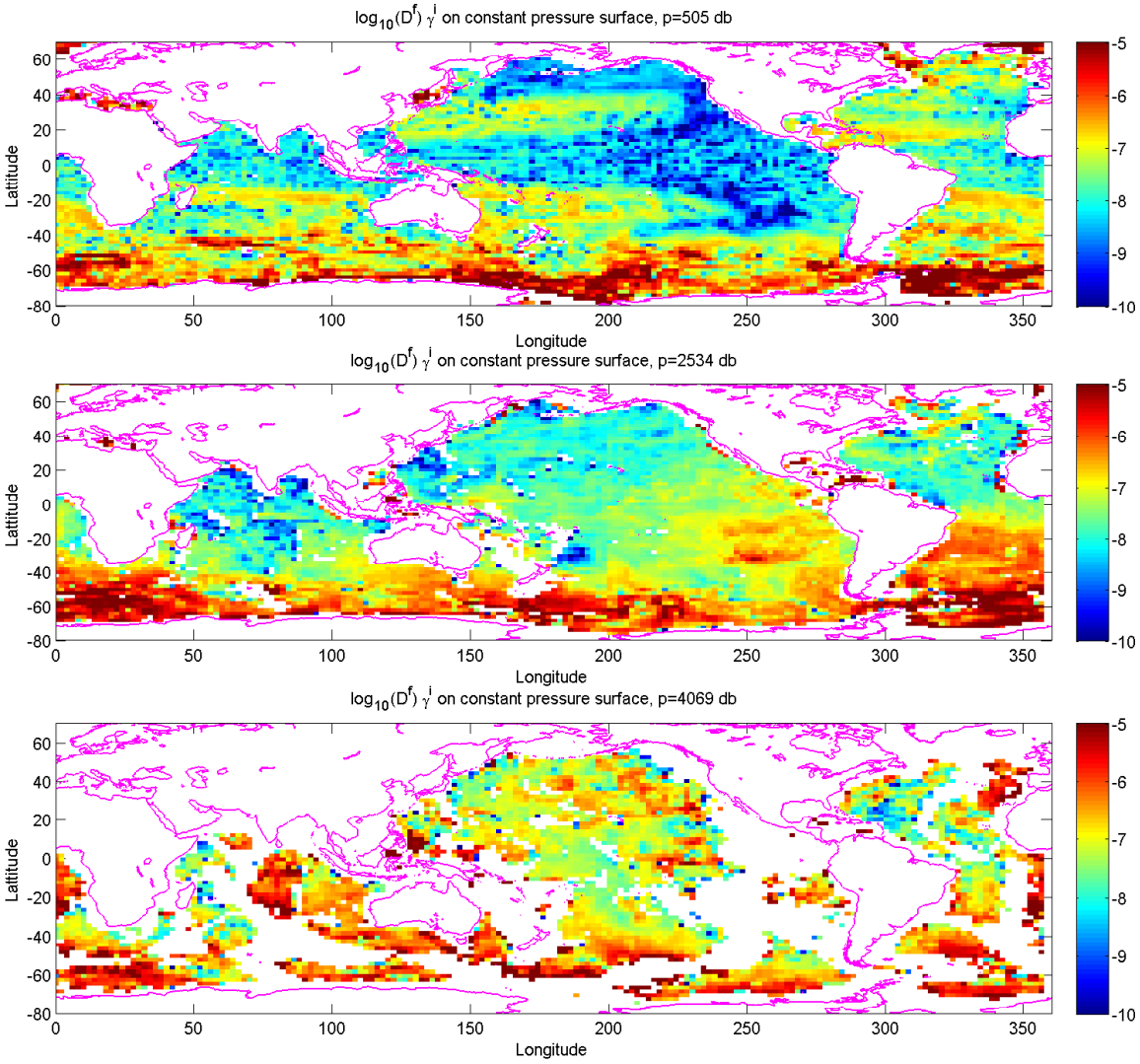

Figure 3.2: Reference maps of the decimal logarithm of the fictitious diffusivity D^f on three constant pressure surfaces of 505, 2534 and 4069 *dbar* (from the top to the bottom) for γ^i computed on the WOCE dataset and used for the fitting.

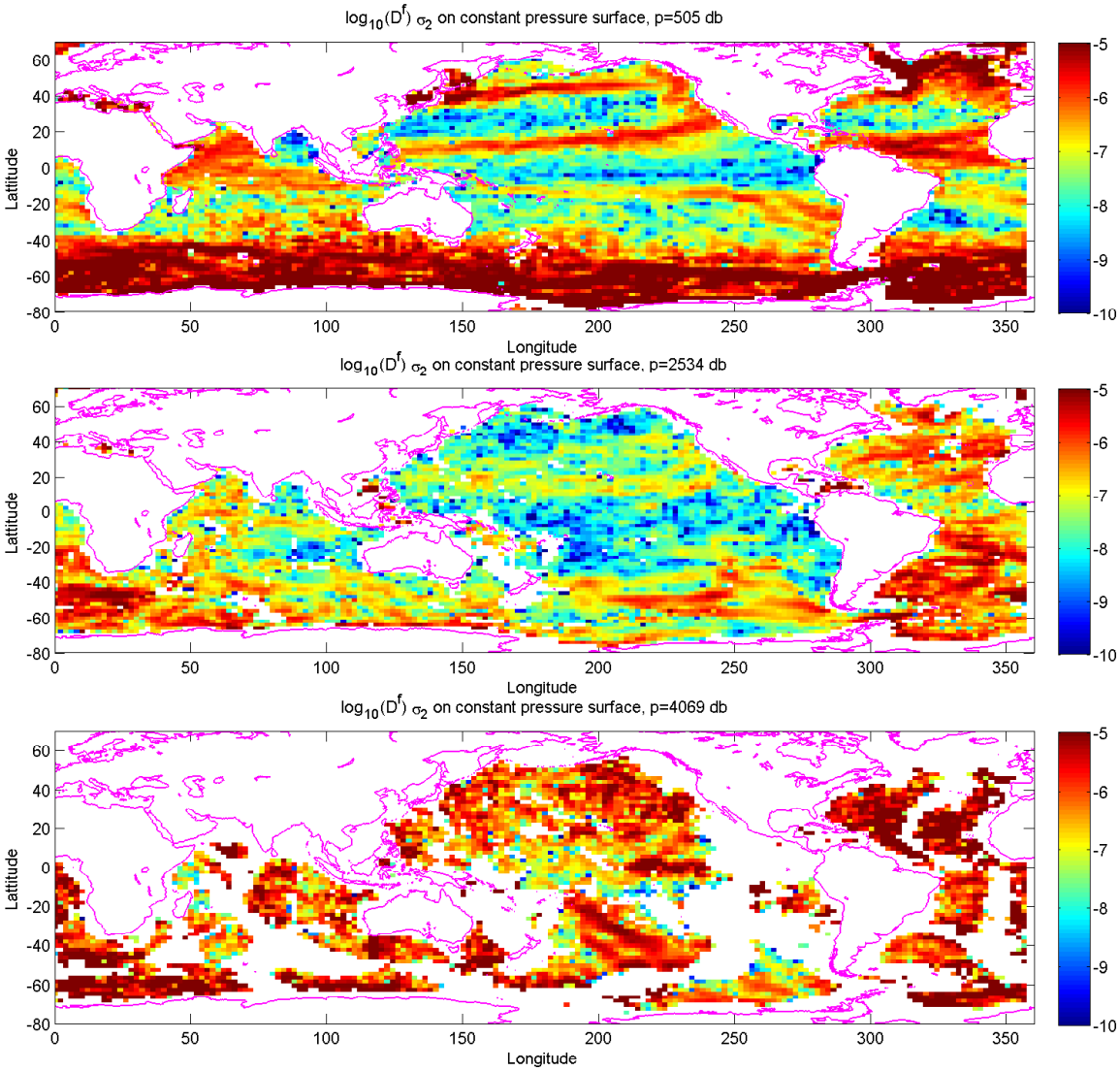

Figure 3.3: Reference maps of the decimal logarithm of of fictitious diffusivity D^f on constant pressure surface of 505, 2534 and 4069 *dbar* (from the top to the bottom) for σ_2 computed on the WOCE dataset.

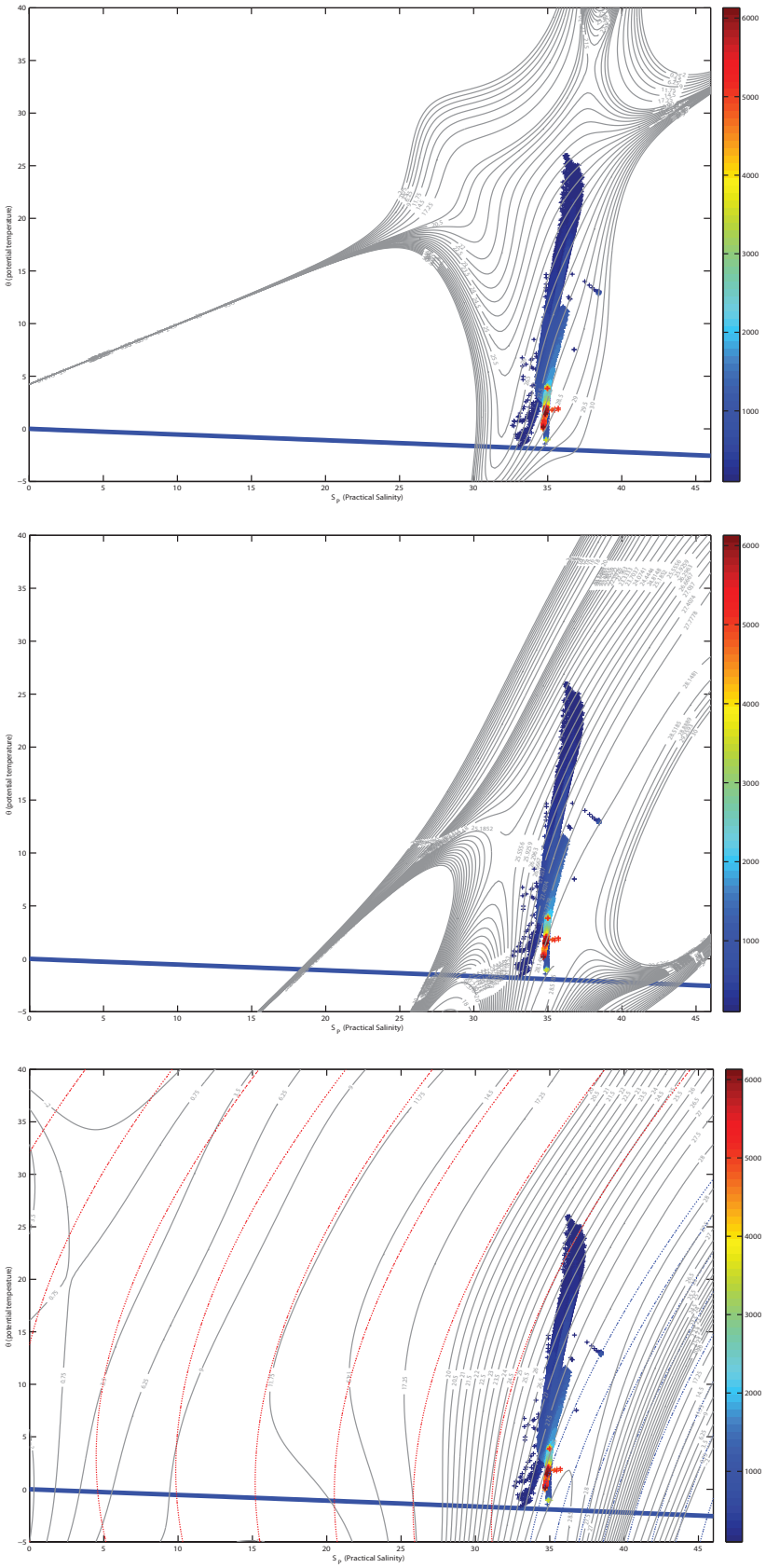

Figure 3.4: Comparison of the shape of isopycnals for the North Atlantic dataset on the salinity-temperature diagram between γ^{EW} (top), a first version of γ^{poly}(middle), and $\gamma^{poly}(shape)$ with extension to low salinities (bottom)

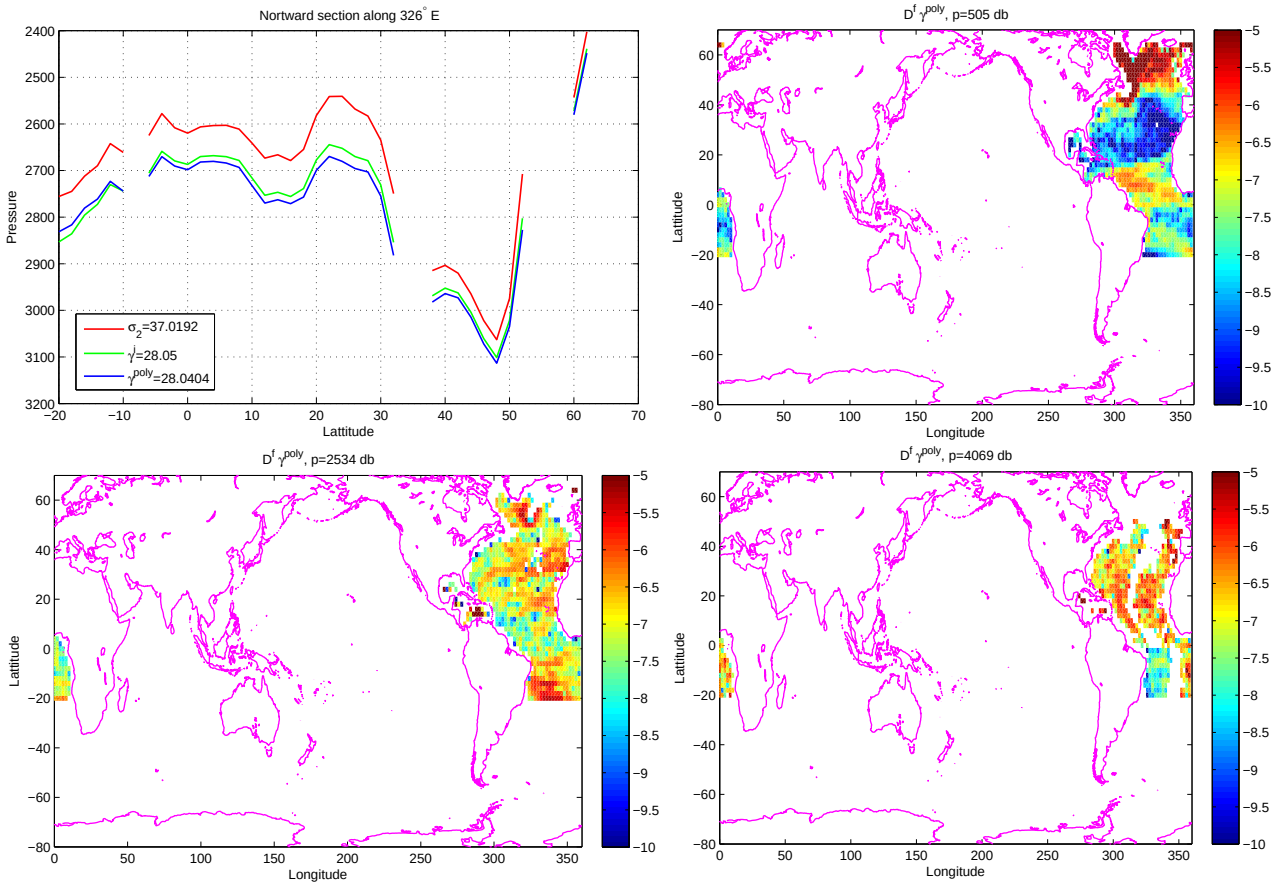

Figure 3.5: The decimal logarithm of the fictitious diapycnal diffusivity D^f of γ^{poly} on the North Atlantic ocean is plotted on three surfaces of constant pressure 505 (top right), 2534 (bottom left), and 4069 db (bottom right). The top left panel depicts the three density surfaces of γ^i, σ_2 and γ^{poly} plotted along a North-South section describing the same neutral surface.

3.1.2 South Atlantic, North Pacific and North Indian

The γ^{poly} fits for the South Atlantic, North Pacific and North Indian proved to be extremely successful (Figures 3.6, 3.7 and 3.8). The decrease in the amount of false diapycnal diffusivity greater than $10^{-5}\,m^2s{-}1$ of γ^{poly} when compared with σ_2 is 57%, 67% and 73% respectively. In comparison, γ^i is better by 78%, 72% and 82% compared to σ_2 on these basins. It can be seen on surfaces of constant pressure(Figures 3.6, 3.7 and 3.8) that γ^{poly} is close to neutral (in the sense that $D^f < 10^{-5}\,m^2.s^{-1}$). Most of error occurs in the shallow waters and along the frontier of the Antarctic Circumpolar Current. As water masses in these basins are different from those in the Southern Ocean, it follows that the fits for the South Atlantic, North Pacific and North Indian are worse in the Southern Ocean. A polynomial was designed for the Southern Ocean such that when all of the γ^{poly} functions are combined, the error observed on the circumpolar current on the southern boundaries of the South Atlantic, North Pacific and North Indian Oceans is minimised.

When plotted on a nort-south section, the γ^{poly} surface is closer to the γ^i surface than σ^2. The isopycnals are plotted on salinity-temperature diagrams in Appendix A on

Figures A.2, A.3 and A.4, and it can be seen that the functions γ^{poly} are valid up to low salinities and values of potential temperature up to $40°C$.

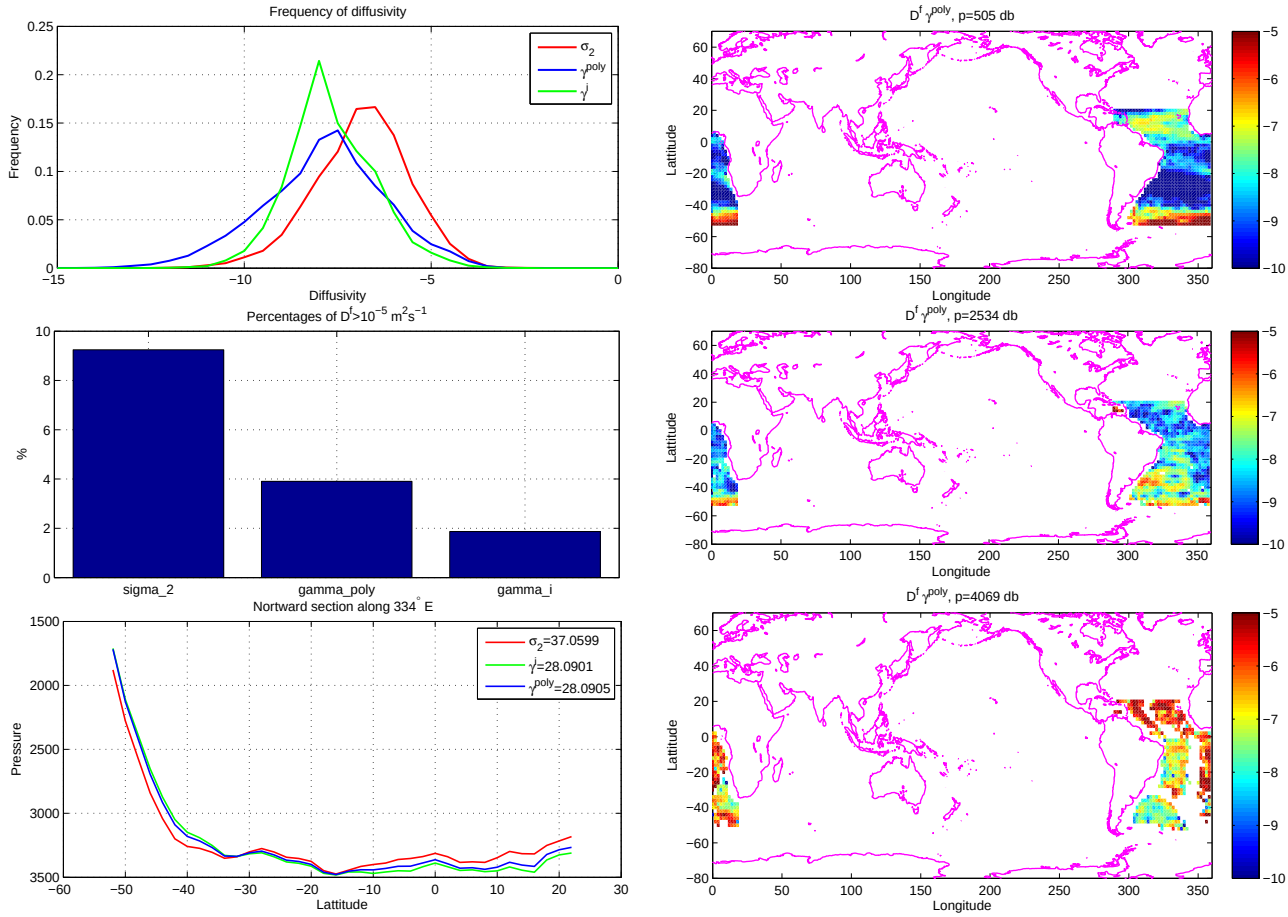

Figure 3.6: South Atlantic ocean results. Frequency of the decimal logarithm of the fictitious diapycnal diffusivity D^f (top left) and percentage of fictitious diapycnal velocity greater than $10^{-5}\,m^2.s^{-1}$ (middle left) compared between γ^i, σ_2 and γ^{poly}. The three density surfaces of γ^i, σ_2 and γ^{poly} are plotted on a North-South section along $334°E$ describing the same neutral surface (bottom right). The decimal logarithm of the fictitious diapycnal diffusivity D^f of γ^{poly} is plotted on three surfaces of constant pressure (505, 2534, and 4069 db) (left side).

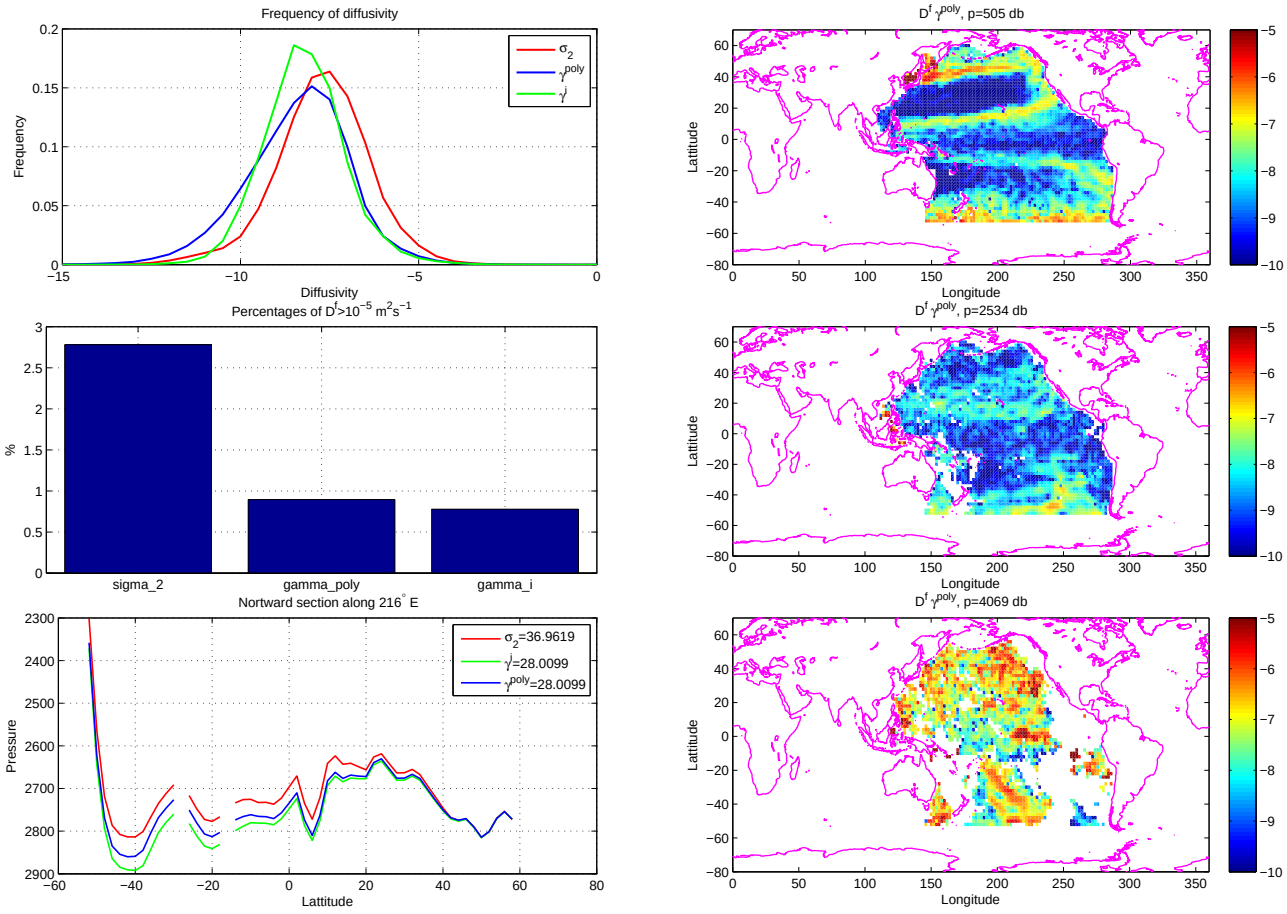

Figure 3.7: North Pacific ocean results. Frequency of the decimal logarithm of the fictitious diapycnal diffusivity D^f (top left) and percentage of fictitious diapycnal velocity greater than $10^{-5}\,m^2.s^{-1}$ (middle left) compared between γ^i, σ_2 and γ^{poly}. The three density surfaces of γ^i, σ_2 and γ^{poly} are plotted on a North-South section along $216°E$ describing the same neutral surface (bottom right). The decimal logarithm of the fictitious diapycnal diffusivity D^f of γ^{poly} is plotted on three surfaces of constant pressure (505, 2534, and 4069 db) (left side).

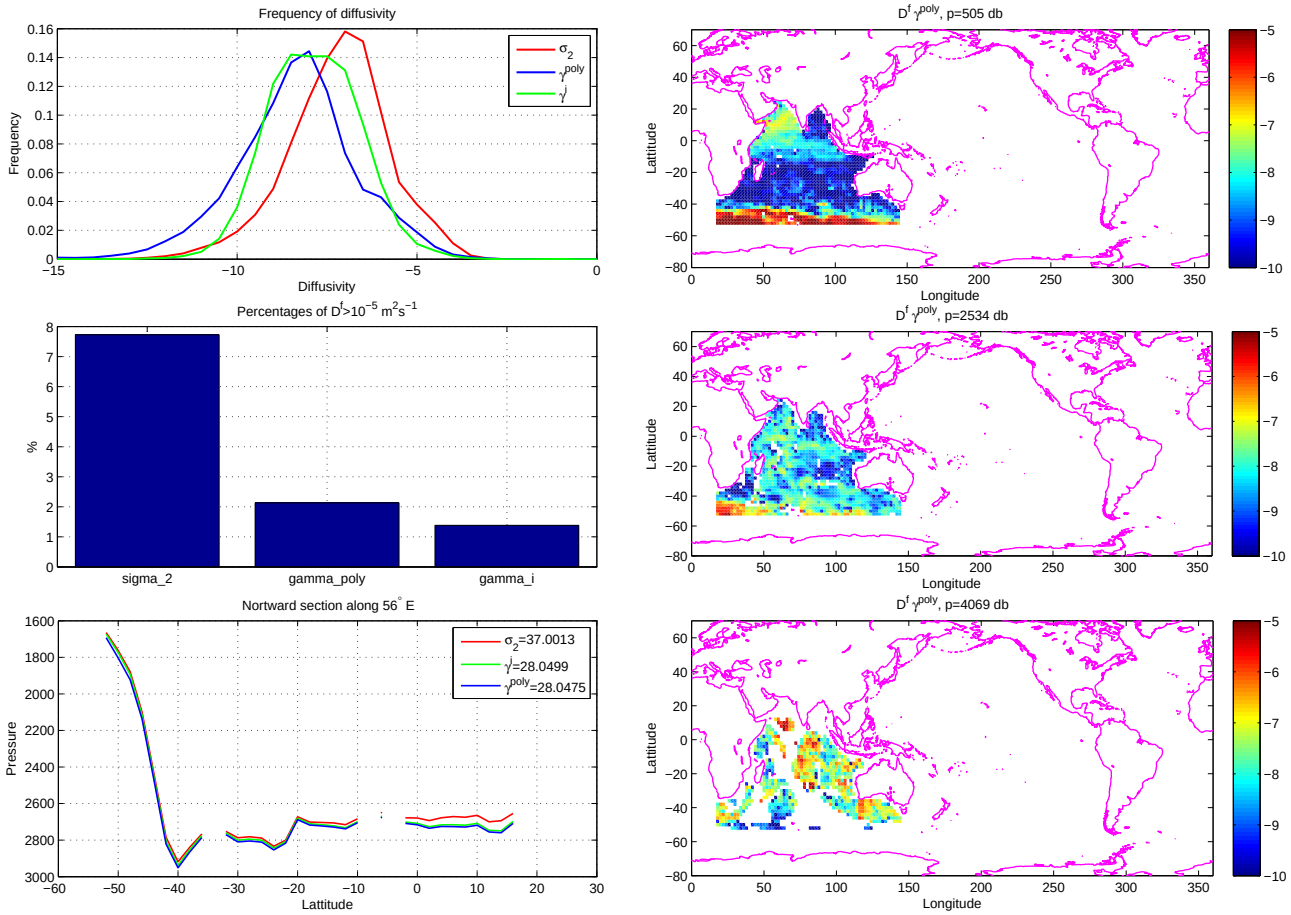

Figure 3.8: North Indian ocean results. Frequency of the decimal logarithm of the fictitious diapycnal diffusivity D^f (top left) and percentage of fictitious diapycnal velocity greater than $10^{-5}\,m^2.s^{-1}$ (middle left) compared between γ^i, σ_2 and γ^{poly}.The three density surfaces of γ^i, σ_2 and γ^{poly} are plotted on a Nort-South section along $56°E$ describing the same neutral surface (bottom right). The decimal logarithm of the fictitious diapycnal diffusivity D^f of γ^{poly} is plotted on three surfaces of constant pressure (505, 2534, and 4069 db) (left side).

3.1.3 Southern Ocean

Figures 3.2 and 3.3 show that the Southern Ocean is the region where the fictitious diapycnal diffusivity is the strongest and it is greater than $10^{-5}\,m^2.s^{-1}$ in a lot of places. Even γ^i is not as close to being neutral compared to the other regions in the world (Figure 3.2). In order to achieve a reasonable fit it was necessary to add a pressure dependent function to the fit. The disadvantage of adding pressure is that γ^{poly} looses its quasi-material property.

The global error and the percentage of diffusivity superior to $10^{-5}\,m^2.s^{-1}$ are shown in Figure 3.9. γ^{poly} has an improvement of 28% compared to σ_2 whereas γ^i is 72% better. The fictitious diffusivity is better in the shallow waters for γ^{poly} than it is for σ^2 but is still a long way from the results of γ^i. The dependency is due to the fact that γ^i does not describe neutral surfaces perfectly in this region and γ^{poly} tries to fit this label. Also, the pressure plot at $2534\,db$ shows that the diffusivity greater than $10^{-5}\,m^2.s^{-1}$ is concentrated on the Weddell Sea and this corresponds to where γ^i fails to accurately

approximate neutral surfaces. Something noticeable is that γ^{poly} is able to better describe the deep water than γ^{i}. The bottom left plot of Figure 3.9 shows the pressures along a North South section at $198°E$. It contains the three types of density surface considered here (σ_2, γ^{i} and γ^{poly}), note that these surfaces all coincide at $(28°E, 58°S)$ and a pressure of $606\,db$. It can be seen that both γ^{i} and γ^{poly} are quite close together whereas σ_2 is roughly $200\,m$ shallower in the south yet is in excess of $200\,m$ deeper in the north.

The shape of the isopycnals are shown on salinity-temperature diagrams in appendix A for referenced pressure of $0\,db$ and $4000\,db$ (Figure A.5 and A.6). Because γ^{poly} depends on pressure in the Southern Ocean, isopycnals for shallow water and deep water has been plotted. Note that at $0\,db$, isopycnals are valid at low salinity which indicates that the γ^{poly} fit is valid for fresh water. A variation in the shape is observed around values of potential temperature of $2°C$ which is due to the tangent hyperbolic envelop to describe the frontier of the circumpolar current.

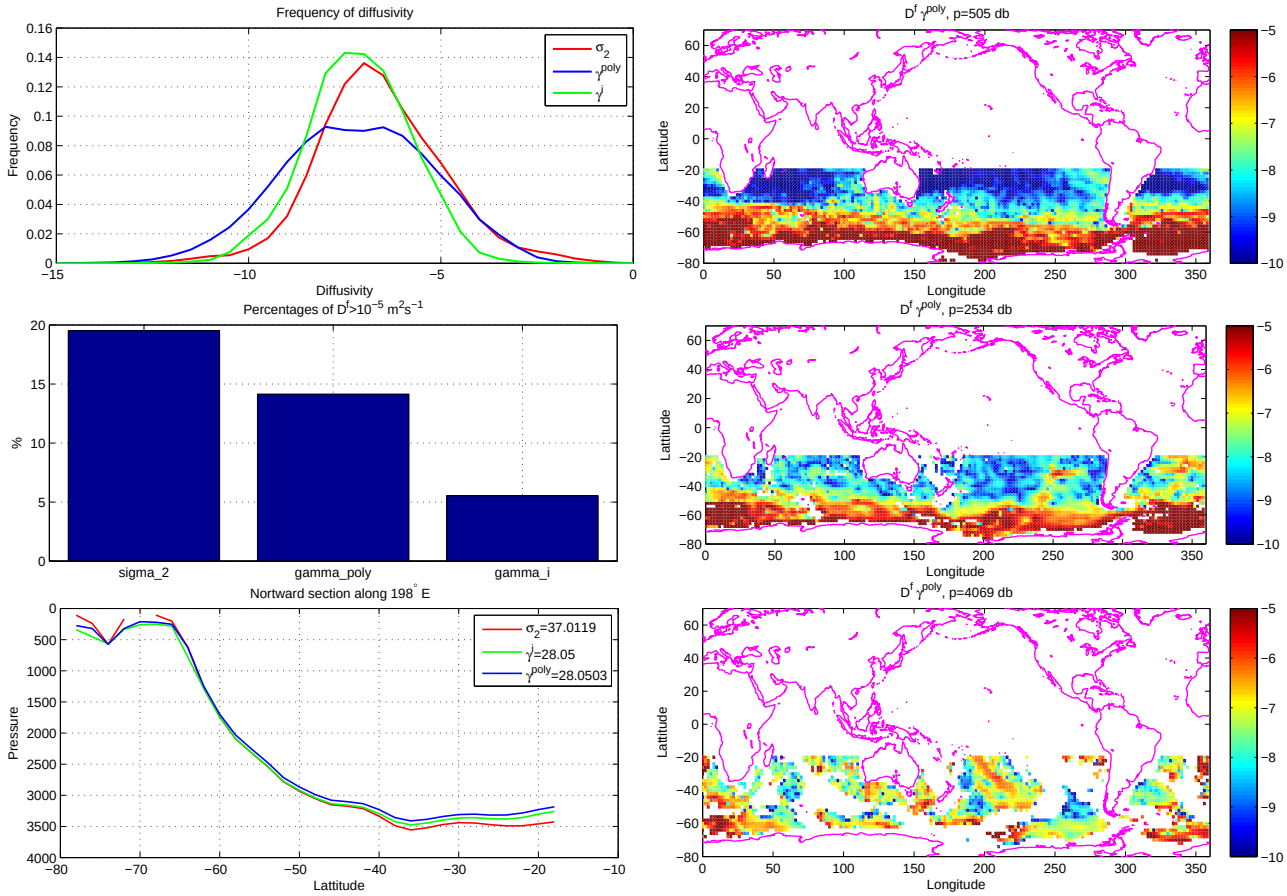

Figure 3.9: Southern Ocean results. Frequency of the decimal logarithm of the fictitious diapycnal diffusivity D^f (top left) and percentage of fictitious diapycnal velocity greater than $10^{-5}\,m^2.s^{-1}$ (middle left) compared between γ^{i}, σ_2 and γ^{poly}.The three density surfaces of γ^{i}, σ_2 and γ^{poly} are plotted on a North-South section describing the same neutral surface (bottom right). The decimal logarithm of the fictitious diapycnal diffusivity D^f of γ^{poly} is plotted on three surfaces of constant pressure (505, 2534, and $4069\,db$) (left side).

3.2 γ^{GP} applied to the world oceans

Once all polynomials γ^{poly} have been constructed on each ocean basin and it has been seen that they describe neutral surfaces better than σ_2, the last step is to combine all these functions to form γ^{GP}. This has been be achieved through the use of the zipping functions introduced in section 2.5. One could think that the results will be similar to those from each of the ocean basin when they were studied independently. However, the zipping introduced variations of the surface slope which have an impact on the neutrality of the global polynomial γ^{GP}. The following sections highlight the error introduced by the combining of the polynomials and suggests an explanation of the origin of this error.

γ^{GP} was tested the WOCE climatology used for the fitting and on a snapshot the ocean model MOM4 where it gave results better than σ_2 in terms of fictitious diapycnal diffusivity. In the following sections, the Arctic Ocean and the Mediterranean Sea are not included in the results of global diffusivity because a correct polynomial does not exist on these regions. A better dataset is required to obtain γ^{poly} functions for these regions. We did attempt to use the North Atlantic γ^{poly} function for these two regions, however we note that the resulting fictitious diapycnal diffusivity is very large which is to be expected as the water masses are quite different.

3.2.1 WOCE climatology

The WOCE climatology [Gouretski and Koltermann, 2004] was used for building all the γ^{poly} functions. Consequently, the global polynomial γ^{GP} was tested first on this dataset. Figure 3.10 shows that the mean value of fictitious diapycnal diffusivity D^f is less high than σ_2. The area under the curve of diffusivity of γ^{poly} greater than $10^{-5}\,m^2.s^{-1}$ is smaller than for σ_2, but higher than for γ^i. In comparison to σ_2, it represents an improvement of 30.3% for γ^{GP} against 71.3% for γ^i.

The consequences of the zipping can be observed with the picture of the bottom of Figure 3.11 which describes a level of constant pressure at $4069\,db$. Bands of fictitious diapycnal diffusivity that are larger than those observed in the surrounding areas are present on the zipping regions, with diffusivity sometimes greater than $10^{-5}\,m^2.s^{-1}$. Unfortunately, it generates non negligible errors in diapycnal diffusivity and decreases the overall quality of the function. If we are able to reduce the harmful effect of the zipping, γ^{GP} will become more accurate and be able to correctly describe neutral physics. Note that the zipping only introduces fictitious diapycnal diffusivity greater than $10^{-5}\,m^2.s^{-1}$ in the deep layers. Figure 3.11 shows that in the shallow part the introduced error is not significant.

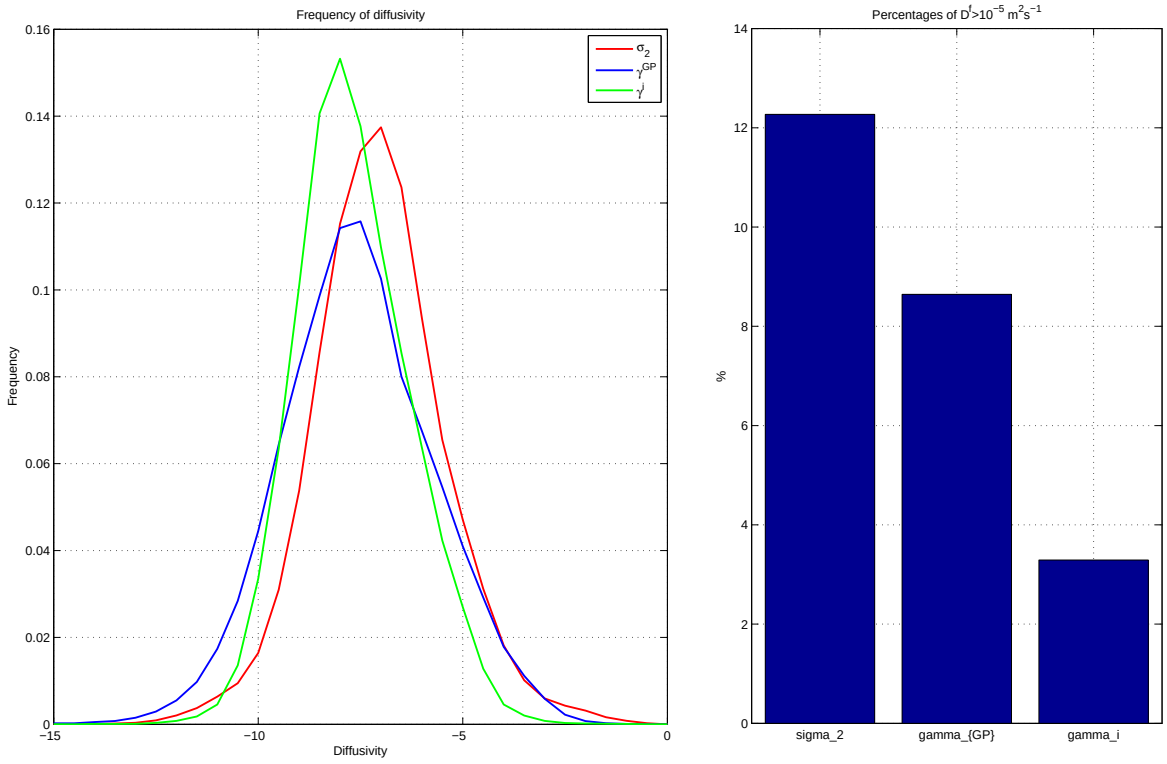

Figure 3.10: On the left, frequency of the decimal logarithm of the decimal logarithm of the fictious diapycnal diffusivity D^f. On the right, percentage of fictitious diapycnal velocity greater than $10^{-5}\,m^2s{-}1$. The results are compared between σ_2, γ^{GP} and γ^i on the WOCE climatology used for the polynomial construction

3.2.2 Test on the ocean model MOM4

The original goal was to design a function that can be used in ocean models. In order to test γ^{GP}, we applied the function on a snapshot extracted from the MOM4 oceanic model. The Modular Ocean Model (MOM) is a numerical representation of the ocean's hydrostatic primitive equations. It is designed primarily as a tool for studying the global ocean climate system, but with recent enhance capabilities for regional and coastal applications. MOM4 is the latest version of the GFDL ocean model whose origins date back to the pioneering work of Kirk Bryan and Mike Cox in the 1960s-1980s. It is developed and supported by researchers at NOAA's Geophysical Fluid Dynamics Laboratory (GFDL).

The results on this snapshot are shown in Figure 3.12 the distribution of diffusivity for γ^{GP} is centred around lower diffusivity value compared to σ_2 (namely 10^{-8} for γ^{GP} and 10^{-7} for σ_2). This also represents 45% improvement in terms of diffusivity greater than $10^{-5}\,m^2.s^{-1}$ compared to σ_2. Figures 3.13, 3.14 and 3.15 show maps of the distribution of fictitious diapycnal diffusivity on the world oceans at depths near 450, 2600, and 3880 m. The regions that have strong salinity and temperature gradients are better described by γ^{GP} than σ_2. It can be seen in Figure 3.13 that the Sea of Okhotsk, the Southern Ocean, the North Atlantic tropical regions and the Arabian Sea are significantly lower in diffusivity for γ^{GP} than for σ^2. The Labrador Sea and the Weddell Sea are the parts of the ocean that are still difficult for γ^{GP} to describe. We know that the dataset and the

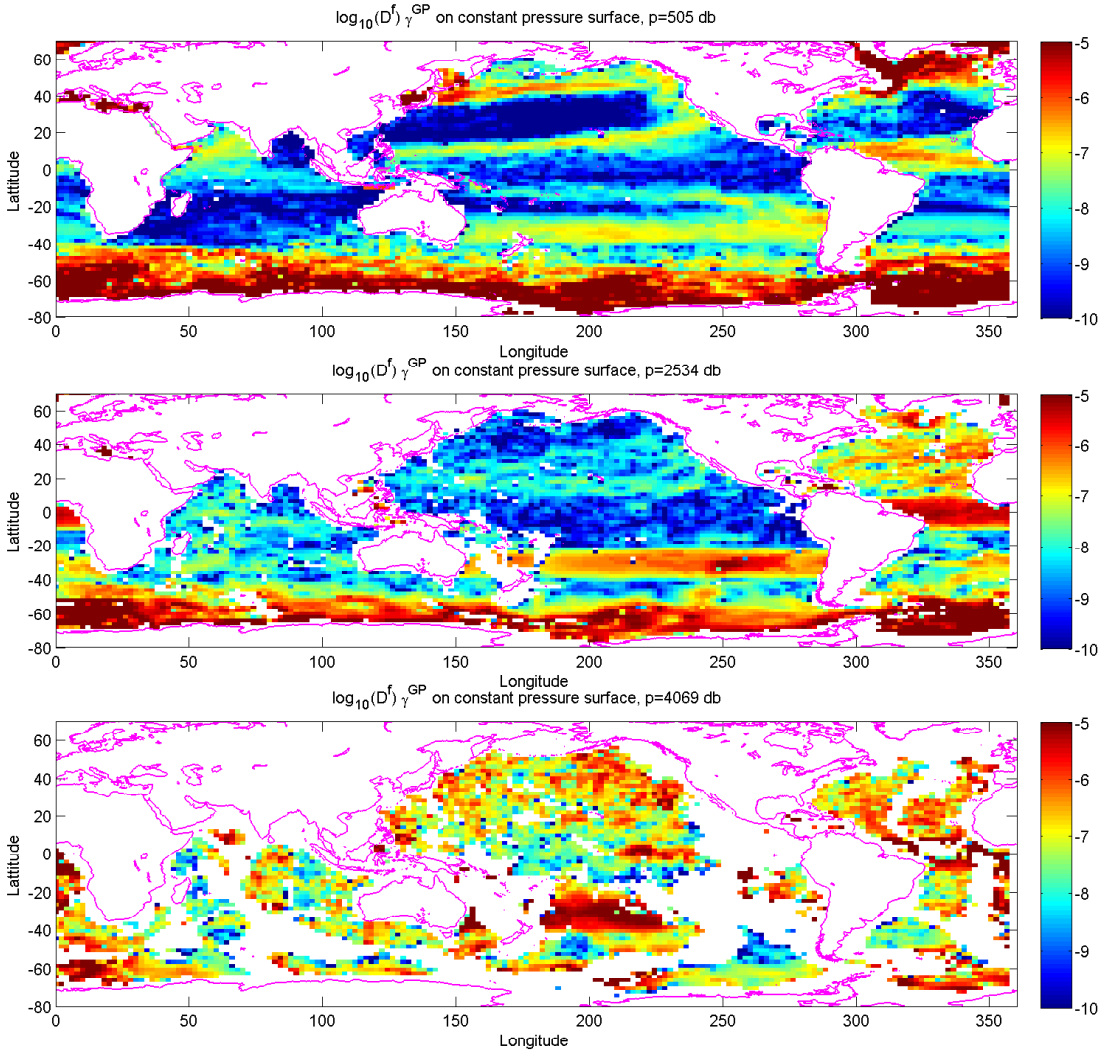

Figure 3.11: Map of the decimal logarithm of the fictitious diffusivity D^f at constant pressure of 505, 2534 and 4069 *dbar* (from the top to the bottom) for γ^{GP} computed on the WOCE dataset used for the fitting.

γ^i label used for constructing the polynomials were not as accurate in these regions as they were in the rest of the ocean. On Figure 3.14 we can see the effect of the zipping where it results in bands of large fictitious diapycnal diffusivity. The error in diffusivity stays under $10^{-5}\,m^2.s^{-1}$ for the majority of the ocean. Figure 3.15 shows that γ^{GP} gives better results than σ_2 in terms of being close to neutral at depth, in particular in the North Pacific. Nevertheless, the effect zipping becomes more important at this depth and it introduces diffusivity greater than $10^{-5}\,m^2.s^{-1}$.

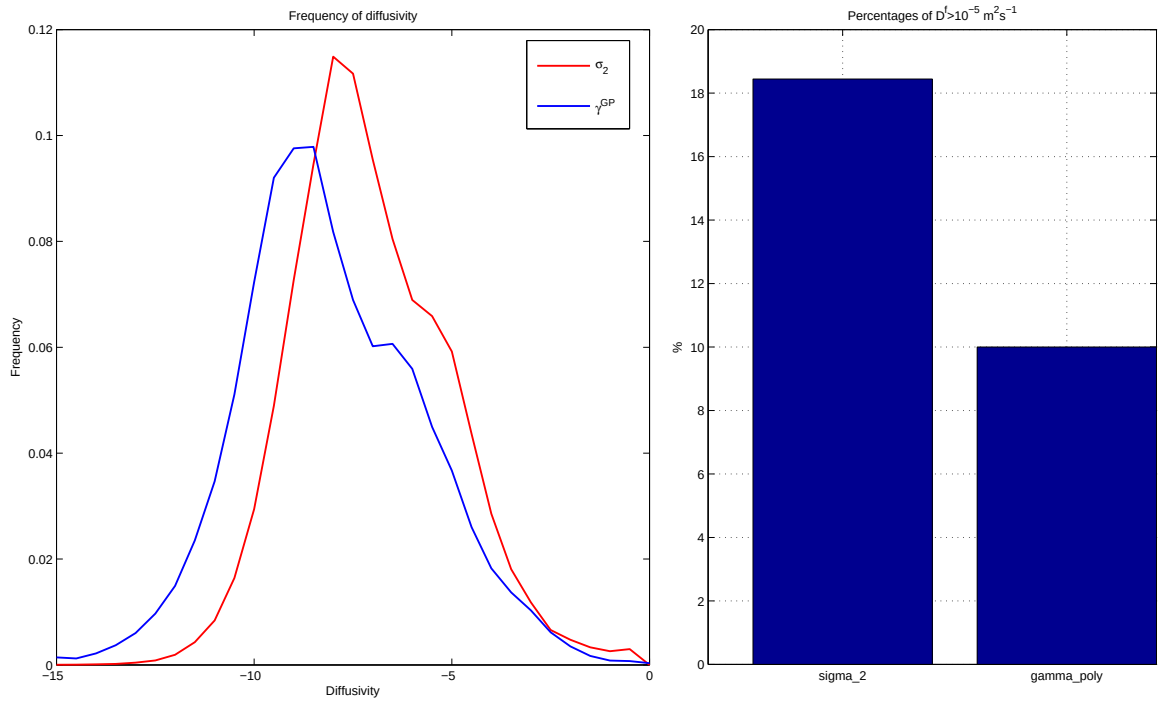

Figure 3.12: On the left, frequency of the decimal logarithm of the fictious diapycnal diffusivity D^f. On the right, percentage of fictitious diapycnal velocity greater than $10^{-5}\,m^2.s^{-1}$. The results are compared between σ_2 and γ^{GP} on a snapshot of the ocean model MOM4

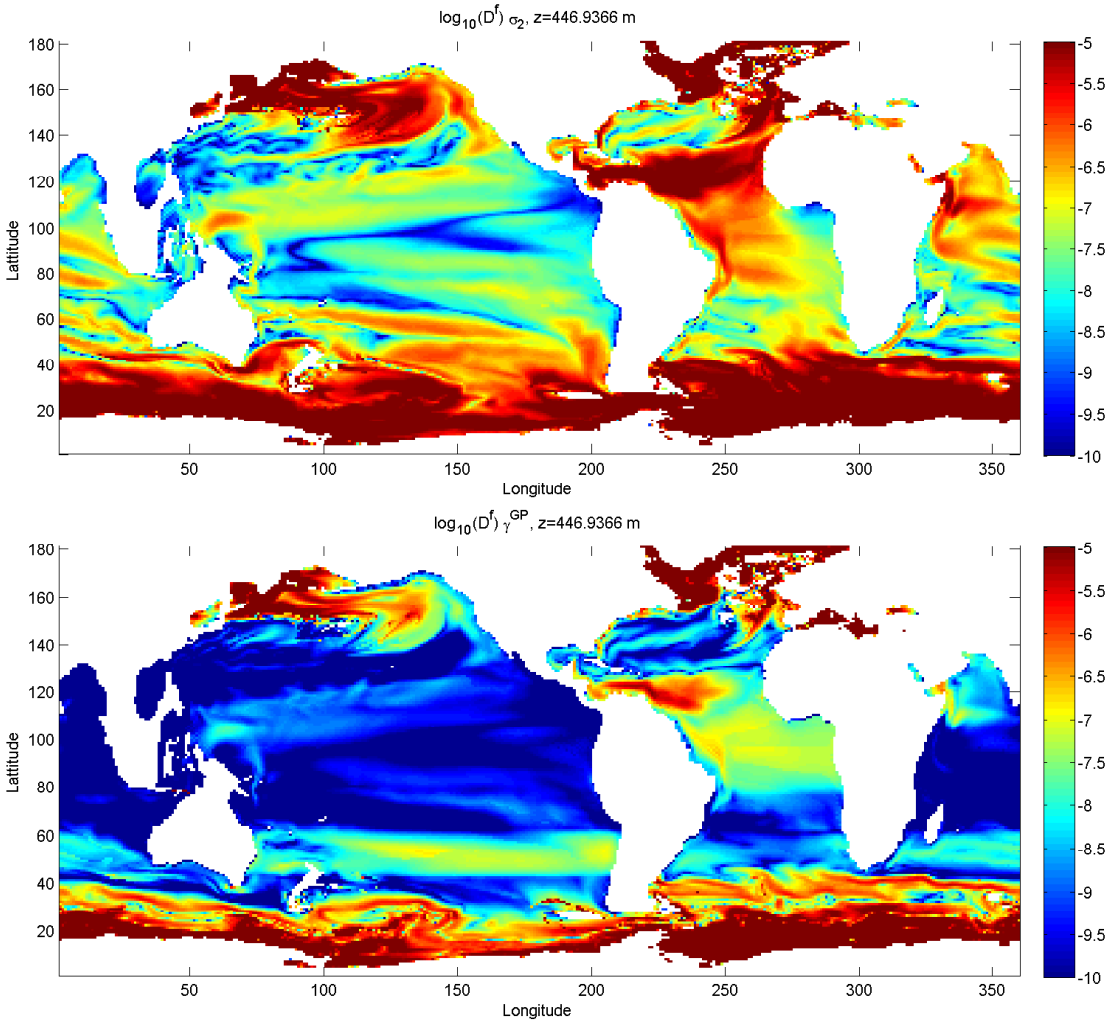

Figure 3.13: Comparison between σ_2(top) and γ^{poly}(bottom) of the decimal logarithm of the fictious diapycnal diffusivity D^f plotted on at constant pressure 446 db

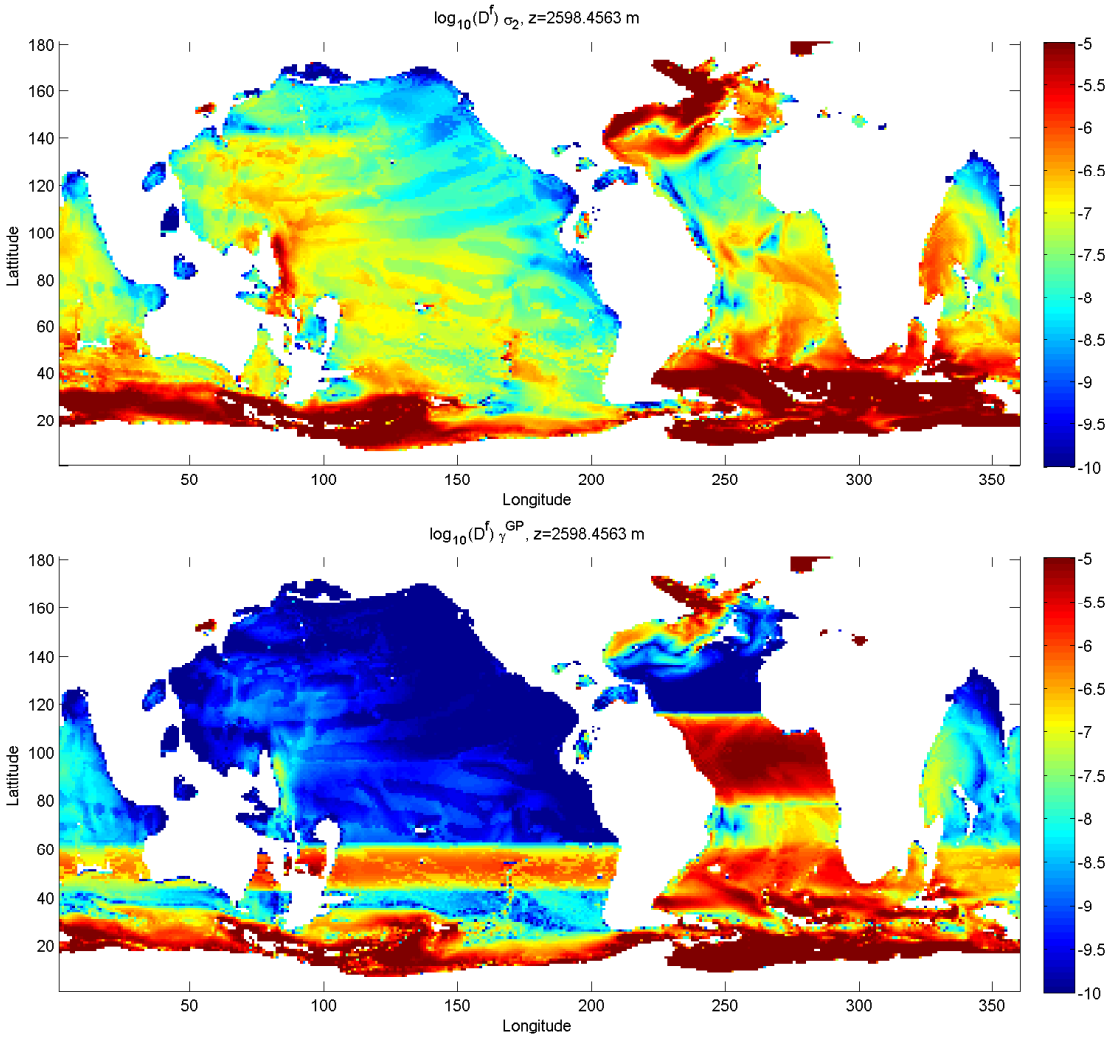

Figure 3.14: Comparison between σ_2(top) and γ^{poly}(bottom) of the decimal logarithm of the fictious diapycnal diffusivity D^f plotted on at constant pressure 2598 db

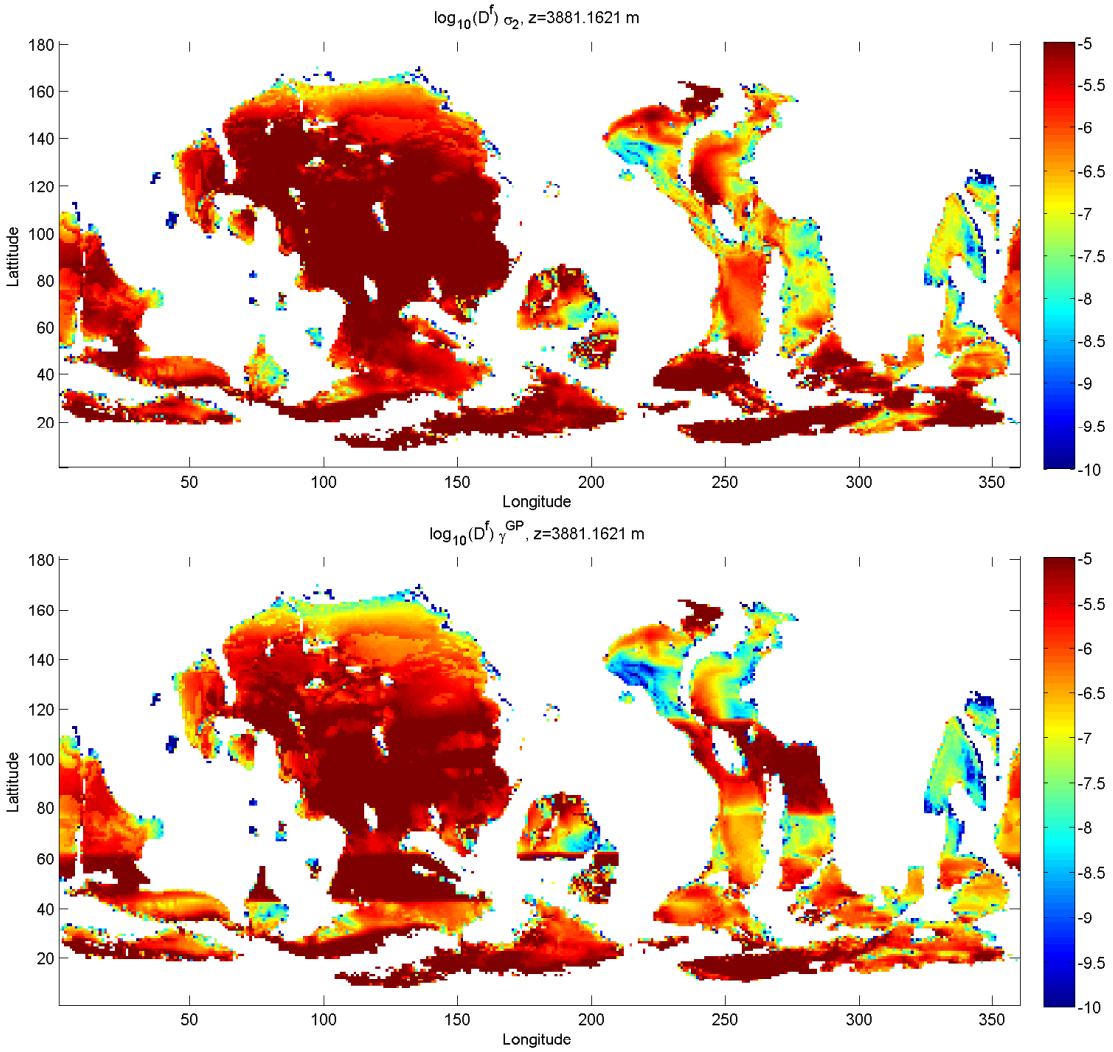

Figure 3.15: Comparison between σ_2(top) and γ^{poly}(bottom) of the decimal logarithm of the fictious diapycnal diffusivity D^f plotted on at constant pressure 3881 db

3.3 Zipping issues

We found that the zipping regions sometimes introduce significant errors which generate fictitious diapycnal diffusivity values greater than $10^{-5}\,m^2.s^{-1}$. It was noticed that this phenomenon occurs principally in depth and reduces the quality of the global polynomial γ^{GP}. This section offers an explanation for the origin of these errors and suggests a possible solution to correct it in order to obtain a more accurate γ^{GP} function. Due to time constraints we did not have the possibilty to test these solutions, we offer them for future investigations.

3.3.1 Theoretical explanation of the introduction of a fictitious diffusivity by the zipping

In order to explain the effect that the zipping has on γ^{GP}, we can consider that γ^{GP} is only a combination of a southern polynomial $\gamma^{poly\,S}$ and a northern polynomial $\gamma^{poly\,N}$, joined by a weighting function w:

$$\gamma^{GP} = w\gamma^{poly\,S} + (1-w)\gamma^{poly\,N} \tag{3.1}$$

and the partial derivative of γ^{GP} with respect to latitude λ can be written:

$$\frac{\partial \gamma^{GP}}{\partial \lambda} = (\gamma^{poly\,S} - \gamma^{poly\,N})\frac{dw}{d\lambda} \tag{3.2}$$

If $\gamma^{poly\,S}$ and $\gamma^{poly\,N}$ correctly describe a neutral surface, i.e. $\nabla_n \gamma^{poly\,S} = 0$ and $\nabla_n \gamma^{poly\,N} = 0$, then the gradient of γ^{GP} along a neutral surface is:

$$\nabla_n \gamma^{GP} = (\gamma^{poly\,S} - \gamma^{poly\,N})\frac{dw}{d\lambda}\nabla_n \lambda \tag{3.3}$$

Hence, if $\gamma^{poly\,S}$ and $\gamma^{poly\,N}$ correctly describe a neutral surface with different values the variation of γ^{GP} along a neutral surface is non zero and depends on two parameters which are the value of the offset $(\gamma^{poly\,S} - \gamma^{poly\,N})$ and the derivative of the weighting function $\frac{dw}{d\lambda}$.

Inversely, if $\gamma^{poly\,S}$ and $\gamma^{poly\,N}$ are equal to the same value but do not describ the same neutral surface (Figure 3.16), which can be interpreted as a difference in depth. It induces a strong variation on the resulting surface γ^{GP} whose the shape is similar to the weighting function. Therefore, on the zipping area the slope changes suddenly and is no longer parallel to the slope of the γ^i surface which is close to being neutral.

If this phenomenon happens principally at depth, it could due to the fact that γ^i label is not enough close to being perfectly neutral in depth. It may also arise because the data at depth is condensed to a very small range of salinities and temperatures compared to the data in shallow waters. Note that γ^i varies slowly with depth (i.e. $\frac{\partial \gamma^i}{\partial p}$ is small) and a small error on fitting γ^i as $0.001\,m^3.s^{-1}$ can result in a non-negligible error in depth of $50\,m$.

3.3.2 Suggestion of solutions to decrease the zipping effect

Two solutions can be considered in an attempt to reduce the error introduced by the zipping. The first is to increase the overlap of the regions and base the fit of at the

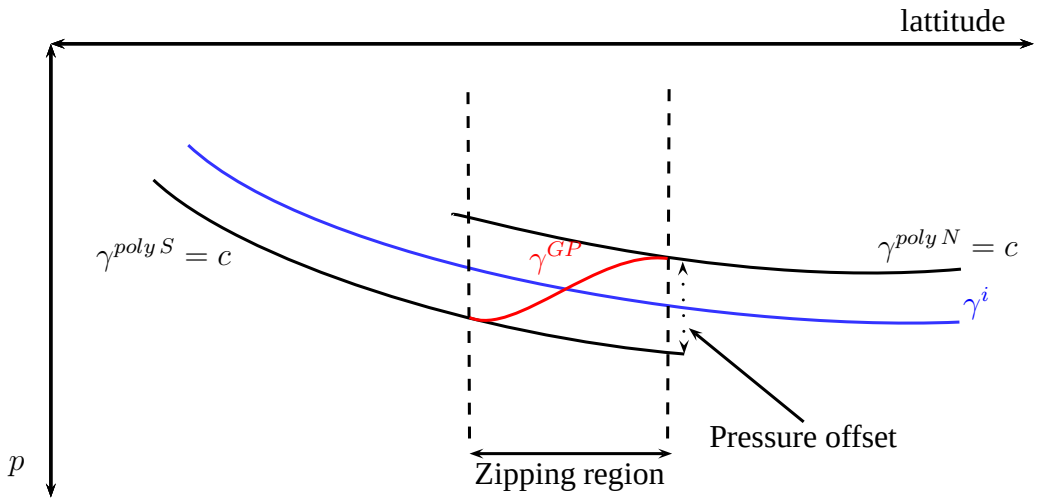

Figure 3.16: This schema describes the zipping between the northern polynomial $\gamma^{poly\,N}$ and the southern polynomial $\gamma^{poly\,S}$. The two neutral density functions $\gamma^{poly\,N}$ and $\gamma^{poly\,S}$ have the same γ value c and yet describe two different neutral surfaces (black) which are approximations of the neutral surface described by γ^i (blue). The existence of an offset in pressure in the zipping region induce a sudden change on the slope of the resulting surface γ^{GP}. The offset times by the weighting function creates this local shape on the global surface γ^{GP} (red) making it less close to being neutral.

polynomials on bigger ocean basins. This would increase the amount of data at depth which would improve the accuracy of the fit in that region. It is possible that it could decrease the offset between the northern and the southern polynomials. Note that a finer climatology labelled with a new more accurate version of neutral density γ^i, should also reduce the magnitude of the offset. The second method is to make the zipping regions larger so that the derivative of the weighting functions will be smoother. This last solution would introduce, into the final function, a stronger dependence in latitude which is not desirable.

Conclusion

The development of the neutral surface theory allowed an accurate description of surfaces where the strong exchanges occur in the ocean. It was shown that the non-linearities of the equation of state do not allow neutral helicity to be zero everywhere in the ocean and this complicates the construction of neutral surfaces. The ill-defined nature of neutral surfaces led to the development of Neutral Density in order to approximate these surfaces. Neutral Density γ^n or improved Neutral Density γ^i gives an accurate description of neutral surfaces. However, their computation is time-consuming because they involve the use of an iterative process, this makes them impractical for use in ocean models. Models typically use potential density referenced to 2000 db, σ_2 which is fast to compute but introduces significant errors if it is assumed that they approximate neutral surfaces. Thus, ocean modellers require a Neutral Density function that is both computationally efficient and accurate in order to describe these surfaces.

The global polynomial neutral density γ^{GP} was designed as a series of polynomials γ^{poly} it was found that one is needed for each ocean basin to correctly describe an approximate form of improved Neutral Density γ^i. The world oceans were divided into six oceanic basins in the following way, the Arctic Ocean, the North Atlantic Ocean, the South Atlantic Ocean, the North Pacific Ocean, the North Indian Ocean and the Southern Ocean. Each γ^{poly} function was fitted on the WOCE climatology that had been labelled with γ^i. Two methods were developed to extrapolate the data, increase the validity range of γ^{poly} and provide workable functions: (i) extension in a neutral way at constant pressure and (ii) constant potential density extension at constant b based on the definition of Neutral Density. The first proved to be extremely successful in increasing the validity range of the function to high salinities and high temperatures. The second was used only to extrapolate low salinities using a mean value of b in shallow waters, as the γ^i label at depth did not accurately describe neutral surfaces, it was not possible to employ this method in deep waters without propagating the errors contained in the γ^i dataset. The RMS and maximum errors, and the variation of the vertical gradient with depth were used as an initial indication of the quality fit. The computation of the fictitious diapycnal diffusivity and the construction of density surfaces were then used to qualify how γ^{poly} was closed to being neutral. Each of the γ^{poly} functions were combined to form γ^{GP} with aid of sinusoidal weighting functions. They were designed such that they were equal to zero or one outside the zipping region and their derivative was equal to zero at the edges.

Construction of each of the polynomials to achieve the specifications of being neutral and having a wide validity range (i.e. $0 \leq S_P \leq 40$ & $\theta_{freezing} \leq \theta \leq 40$) was difficult to obtain with the current dataset. The WOCE climatology is based on very sparse observational data along the Antarctic coastline and in the Arctic Ocean, this did not provide sufficient accuracy to obtain an accurate estimation of the special distribution

$D^f > 10^{-5}\,m^2.s^{-1}$	σ_2	γ^{poly}	γ^i
North Atlantic	8.5%	5%	1%
South Atlantic	9.5%	4%	2%
North Pacific	3%	1%	0.5%
North Indian	8%	2%	1.5%
Southern Ocean	19.5%	14%	5.5%
World oceans	12.2%	8.5%	3.5%
MOM4	18.3%	10%	-

Table 3.1: Percentages of fictitious diapycnal diffusivity greater than $10^{-5}\,m^2.s^{-1}$ compared between σ_2,γ^i, and γ^G.

of salinity and temperature. This combined with the fact that the γ^i technology is not finalised resulted in us needing to form a compromise when extending the validity range of the fit and staying close to being neutral. However, it was shown that the polynomials γ^{poly} gave satisfactory results on each ocean basin. There was an reduction of 30% in the Southern Ocean and at least 40% in the other oceanic basins in terms of diapycnal diffusivity greater than $10^{-5}\,m^2.s^{-1}$ compared to σ_2. (Table **??**). The polynomials fits on the basins of the North Atlantic and the Southern Ocean were the most difficult to make, they were also the regions where the maximum possible improvements can be made when compared to σ_2. In the zipping regions where the polynomials overlapped the amount of total amount of fictitious diapycnal diffusivity larger than $10^{-5}\,m^2.s^{-1}$ increased. The effect of this was to reduce the quality of γ^{GP} in terms of being neutral by being only better than σ_2 by 30%. This magnitude of the error is neglectable in shallows waters but increases with depth and has values larger than $10^{-5}\,m^2.s^{-1}$ in deep waters. It is possible that this error in the junction of two neighbouring basins could come from the fact each of the polynomials may have the same value of γ^{poly} yet could be describing two slightly different neutral surfaces. Also, the quality of the dataset and the accuracy of the γ^i label could be the cause of these errors.

The results were encouraging and show that it was possible to achieve an accurate polynomial approximation of Neutral Density that describes neutral surfaces better than σ_2, even if the dataset and the neutral density label were not very accurate. Performed on a snapshot of the ocean model MOM4, γ^{GP} gave an improvement of 45% compared to σ_2 and demonstrated its capability to replace σ_2 in ocean models. We believe that a more accurate γ^{GP} will be able to be produced when the isopycnal atlas of Barker and McDougall, and the γ^i code are finalised. These products are crucial for the construction of a reliable γ^{poly} in the Arctic, Labrador Sea and the Weddell Sea. Another possible application of γ^{GP} is that it could be the method employed to label future Neutral Density software outputs.

Bibliography

C. Eden and J. Willebrand. Neutral density revisited. *Deep-sea Research Part II*, 46(1-2): 33–54, 1999. doi: 10.1016/S0967-0645(98)00113-1.

V.V. Gouretski and K.P. Koltermann. 2004: Woce global hydrographic climatology. Tech. Rep. 35, Bundesamtes für Seeschifffahrt Hydrographie, 2004.

F. S. Graham and T. J. McDougall. Quantifying the non-conservative production of conservative temperature, potential temperature and entropy. In preparation, 2012.

IOC, SCOR, and IAPSO. *The international thermodynamic equation of seawater-2010: Calculation and use of thermodynamic properties*. Intergovernmental Oceanographic Commission, manuals and guides no. 56 edition, 2010.

D. R. Jackett and T. J. McDougall. A neutral density variable for the world's oceans. *Journal of Physical Oceanography*, 27(2):237–263, February 1997. doi: 10.1175/1520-0485(1997)027<0237:ANDVFT>2.0.CO;2.

A. Klocker, T. J. McDougall, and D. R. Jackett. A new method for forming approximately neutral surfaces. *Ocean Science*, 5(2):155–172, 2009.

S. Levitus. Climatological atlas of the world ocean. NOAA Prof. Paper No. 13, Govt. Printing office, Wahington DC, USA, 1982. 173 pp.

T. J. McDougall. The vertical motion of submesoscale coherent vortices across neutral surfaces. *Journal of Physical Oceanography*, 17(12):2334–2342, December 1987a. doi: 10.1175/1520-0485(1987)017<2334:TVMOSC>2.0.CO;2.

T. J. McDougall. Neutral surfaces. *Journal of Physical Oceanography*, 17(11):1950–1964, November 1987b. doi: 10.1175/1520-0485(1987)017<1950:NS>2.0.CO;2.

T. J. McDougall. Neutral surfaces in the ocean - implications for modeling. *Geophysical Research Letters*, 14(8):797–800, August 1987c. doi: 10.1029/GL014i008p00797.

T. J. McDougall. Neutral-surface potential vorticity. *Progress In Oceanography*, 20(3): 185–221, 1988. doi: 10.1016/0079-6611(88)90002-X.

T. J. McDougall. Potential enthalpy: A conservative oceanic variable for evaluating heat content and heat fluxes. *Journal of Physical Oceanography*, 33(5):945–963, May 2003. doi: 10.1175/1520-0485(2003)033<0945:PEACOV>2.0.CO;2.

T. J. McDougall and P.M. Barker. *Getting started with TEOS-10 and the Gibbs Seawater (GSW) Oceanographic Toolbox*. SCOR/IAPSO WG127, 2011. doi: ISBN978-0646-55621-5.

T. J. McDougall and D. R. Jackett. An assessment of orthobaric density in the global ocean. *Journal of Physical Oceanography*, 35(11):2054–2075, November 2005a. doi: 10.1175/JPO2796.1.

T. J. McDougall and D. R. Jackett. The material derivative of neutral density. *Journal of Marine Research*, 63(1):159–185, January 2005b. doi: 10.1357/0022240053693734.

T. J. McDougall and D. R. Jackett. *Encyclopedia of Ocean Sciences (Second Edition)*, chapter Neutral Surfaces and the equation of state, pages 25–31. Elsevier Ltd, 2008.

F. J. Millero, R. Feistel, D. G. Wright, and T. J. McDougall. The composition of standard seawater and the definition of the reference-composition salinity scale. *Deep-sea Research Part I-oceanographic Research Papers*, 55(1):50–72, January 2008a. doi: 10.1016/j.dsr.2007.10.001.

F. J. Millero, J. Waters, R. Woosley, F. Huang, and M. Chanson. The effect of composition on the density of indian ocean waters. *Deep-sea Research Part I-oceanographic Research Papers*, 55(4):460–470, April 2008b. doi: 10.1016/j.dsr.2008.01.006.

R. B. Montgomery. Circulation in the upper layers of the southern north atlantic, deduced with the use of isentropic analysis. *Pap. Phys. Oceanogr. Meteor*, 6:55pp, 1938.

R. Pawlowicz, D. G. Wright, and F. J. Millero. The effects of biogeochemical processes on oceanic conductivity/salinity/density relationships and the characterization of real seawater. *Ocean Science*, 7(3):363–387, 2011. doi: 10.5194/os-7-363-2011.

R. J. Perkins. Atmospheric dynamics. In *Ecole Centrale Lyon, 3rd year lesson*, 2011.

J. L. Reid and R. J. Lynn. On the influence of the norwegian-greenland and weddell seas upon the bottom waters of the indian and pacific oceans. *Deep-sea Research*, 18: 1063–1088, 1971.

R.H. Stewart. *Introduction to Physical Oceanography*. 2007.

Unesco. *Algorithms for computation of fundamental properties of seawater*. Number 44 in Unesco technical papers in marine science. 1983.

G. Wüst. Das bodenwasser und die gliederung der atlatischen tiefsee. *Wiss. Ergebn. Dtsch. Atlant. Exped. "Meteor"*, 6(I):1–107, 1933.

Appendix A

Polynomials γ^{poly} on each ocean basin

This appendix publishes the coefficients of the first version of the global polynomial of neutral density γ^{GP}. The polynomials γ^{poly} are defined on the North Atlantic, the South Atlantic, the North Pacific, the North Indian and the Southern Ocean. The coefficients are given in term of polynomials function of Practical Salinity and potential temperature $\widehat{\gamma^{poly}} = \widehat{P}\left(\widehat{S_P}, \widehat{\theta}\right)$ with the normalization:

$$\begin{aligned} \widehat{S_P} &= \frac{S_P}{42} \\ \widehat{\theta} &= \frac{\theta}{42°C} \end{aligned} \tag{A.1}$$

To obtain the correct value of γ^{poly} the following operation is also needed

$$\gamma^{poly} = \widehat{\gamma^{poly}} * 20\, kg.m^{-3} - 20\, kg.m^{-3} \tag{A.2}$$

The function γ^{poly} is different for the Southern Ocean because it includes an additional pressure term. Then, this function is written:

$$\hat{\gamma}^{poly\,SO}\left(\widehat{S_P}, \widehat{\theta}, \widehat{p}\right) = \widehat{P}\left(\widehat{S_P}, \widehat{\theta}\right) + \widehat{Q}\left(\widehat{S_P}, \widehat{\theta}\right).exp\left(-\widehat{p}\right).th\left(\frac{\widehat{\theta} - \widehat{\theta_0}}{\widehat{\tau^\theta}}\right) \tag{A.3}$$

with the properties:

$$\begin{aligned} \widehat{p} &= \frac{p}{700\, db} \\ \widehat{\theta_0} &= 0.0625 \\ \widehat{\tau^\theta} &= 0.0163 \end{aligned} \tag{A.4}$$

These isopycnals given by these polynomials are plotted on the salinity temperature diagram as well as the dataset of the basin which was used to build the function. The scale goes from 0 to 46 in Practical Salinity and from -5 to 40 in potential temperature. The freezing line is drawn in blue. The isopycnals of $sigma_0$ and $sigma_4$ are also plotted for low an high salinities respectively and gives a reference for the shape of the isopycnals close to being neutral in these areas of the salinity-diagram.

North Atlantic polynomial coefficients

$\hat{P}$	1	θ	θ^2	θ^3	θ^4	θ^5	θ^6
1	0.868250629754601	0.0324341891674178	1.72145961018658	-3.47469967954487	5.56029166412630	-3.84846537069737	-0.156149127884621
S_P	4.40022403081395	-9.92256348514822	-12.9562244122766	10.1143932959310	-0.868664167905995	5.58313794099231	
${S_P}^2$	-6.45929201288070	66.9856908160296	7.73752363817384	-26.0173602458275	-8.16468531808416		
${S_P}^3$	-19.3531532033683	-125.546334295077	36.2272244269615	22.6867313196590			
${S_P}^4$	66.0796772714637	70.6874394242861	-36.2275575056843				
${S_P}^5$	-54.5838313094697	0.189417034623553					
${S_P}^6$	10.8620520589394						

North Atlantic on salinity-temperature diagram

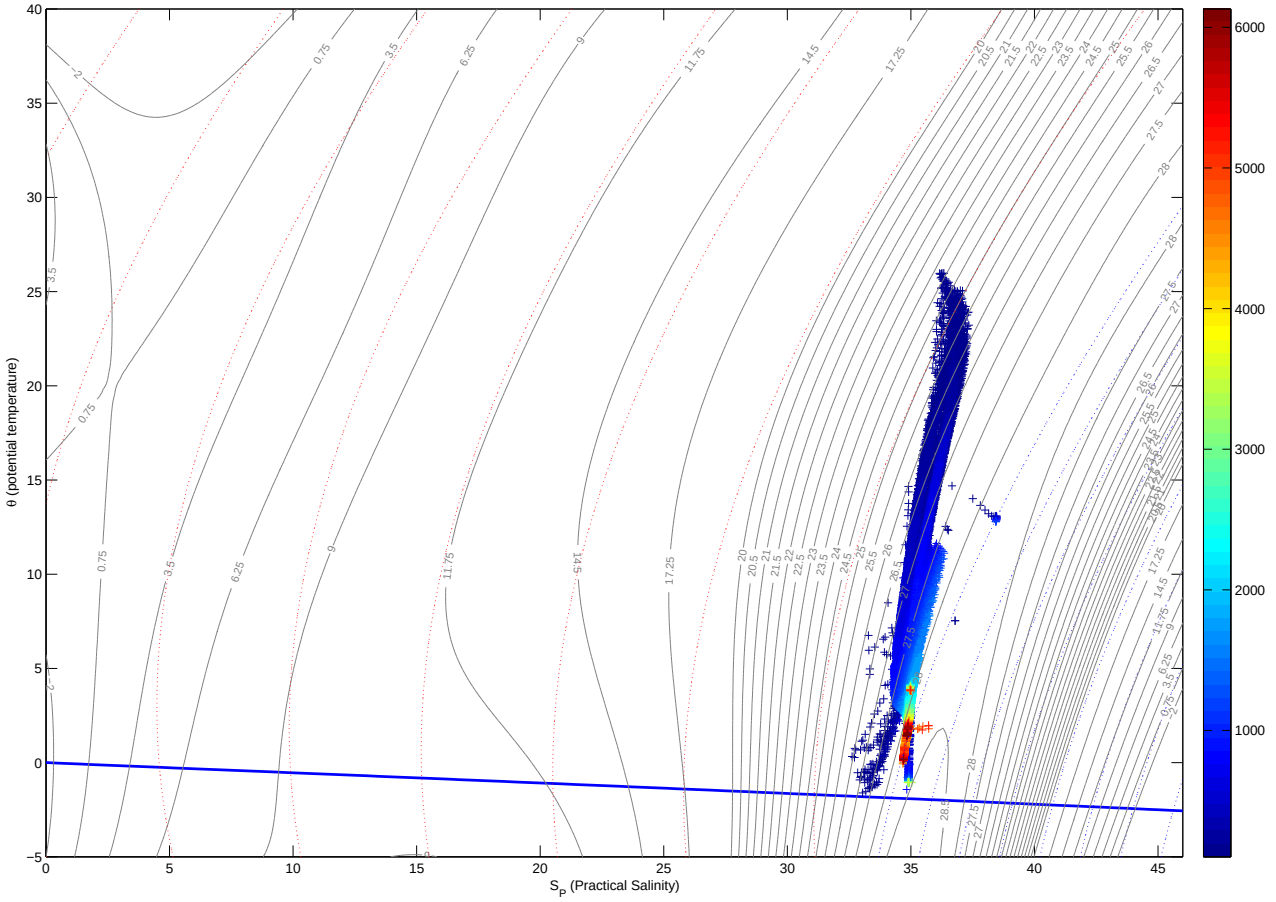

Figure A.1: Hydrographic data used to build γ^{poly} on the North Atlantic plotted on the $S_P - \theta$ diagram, coloured by pressure. Isopycnals of γ^{poly} are plotted from $-2\,kg.m^{-3}$ to $30\,kg.m^{-3}$ (grey). Isopycnals of σ_0 are also plotted for low salinities (red dot) and σ_4 for high salinities (blue dot). The freezing line is drawn by the solid blue line at pressure $p = 0\,db$.

South Atlantic polynomial coefficients

$\hat{P}$	1	θ	θ^2	θ^3	θ^4	θ^5	θ^6
1	0.970176813506429	0.270391840513646	-0.702511207122356	-0.342569734311159	-3.14312850717262	2.73778893334855	1.25587481738340
S_P	0.755382324920216	-3.30869686476731	10.6725319826530	14.6648969886981	-12.1368518101468	-8.73093192235768	
${S_P}^2$	10.0570534575124	-3.60728647124795	-61.0511562956348	5.18263256656924	28.7899447141466		
${S_P}^3$	-29.0124086439839	61.1208402591733	74.4131690710915	-35.0297276945571			
${S_P}^4$	22.1708651635369	-106.892619745231	-15.8597461367756				
${S_P}^5$	13.0718524535924	51.7078062701412					
${S_P}^6$	-15.8634717978759						

South Atlantic on salinity-temperature diagram

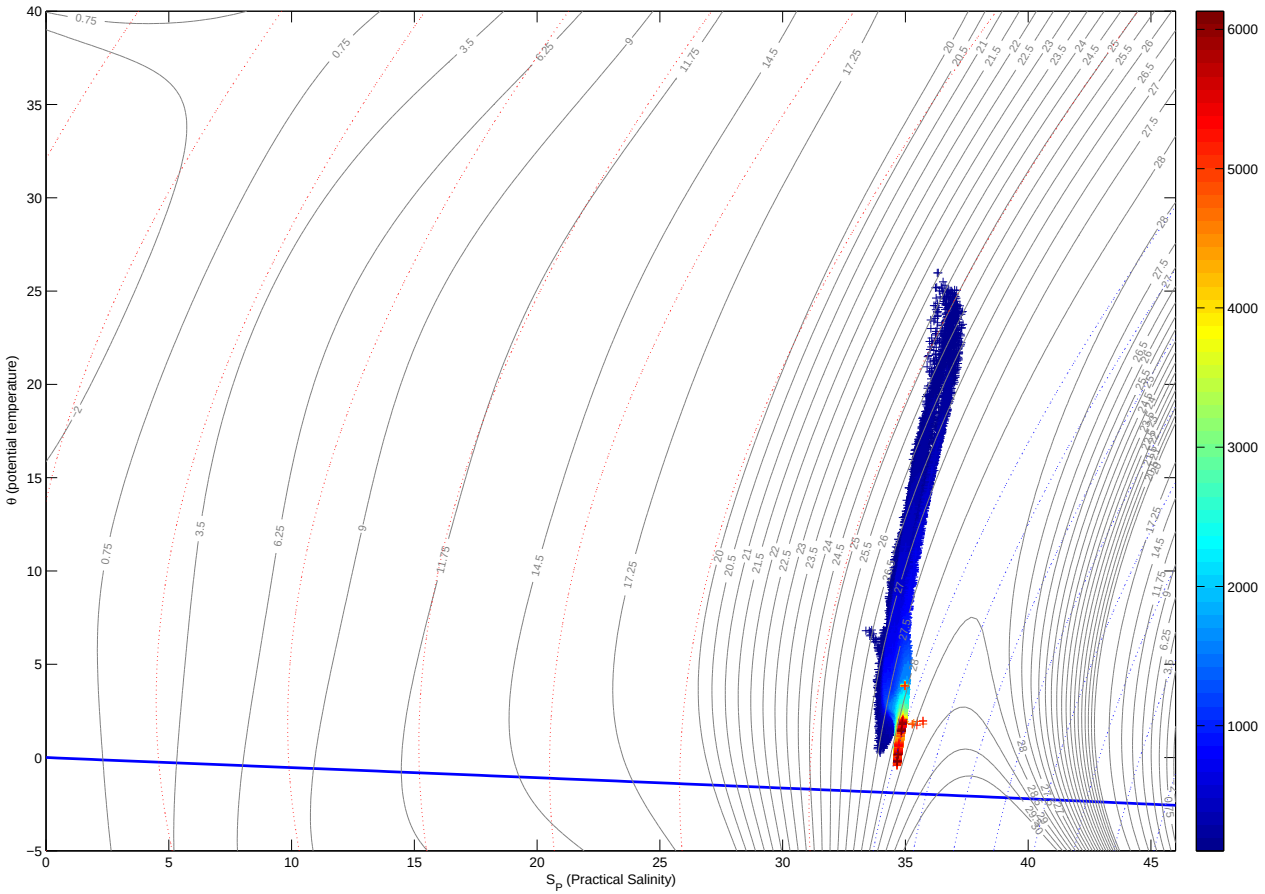

Figure A.2: Hydrographic data used to build γ^{poly} on the South Atlantic plotted on the $S_P - \theta$ diagram, coloured by pressure. Isopycnals of γ^{poly} are plotted from $-2\,kg.m^{-3}$ to $30\,kg.m^{-3}$ (grey). Isopycnals of σ_0 are also plotted for low salinities (red dot) and σ_4 for high salinities (blue dot). The freezing line is drawn by the solid blue line at pressure $p = 0\,db$.

North Pacific polynomial coefficients

$\hat{P}$	1	θ	θ^2	θ^3	θ^4	θ^5	θ^6
1	0.990419160678528	0.0545075600726227	0.673362062889351	-3.35534931941803	-1.19356232779481	3.51016478240624	0.0505878919989799
S_P	1.10691302482411	-1.81027781763969	6.94431859780735	23.1248810527697	-16.0450914593959	-5.58077135773059	
${S_P}^2$	5.48298954708578	-11.1211267642241	-63.9113580983532	-8.43447476300482	25.1352444814321		
${S_P}^3$	-9.59966716439147	86.4094941684553	95.6825154064427	-21.9219942747555			
${S_P}^4$	-15.7911318241728	-145.889251358860	-34.7983038993856				
${S_P}^5$	48.3336456682489	72.6259160928028					
${S_P}^6$	-28.5141488621899						

North Pacific on salinity-temperature diagram

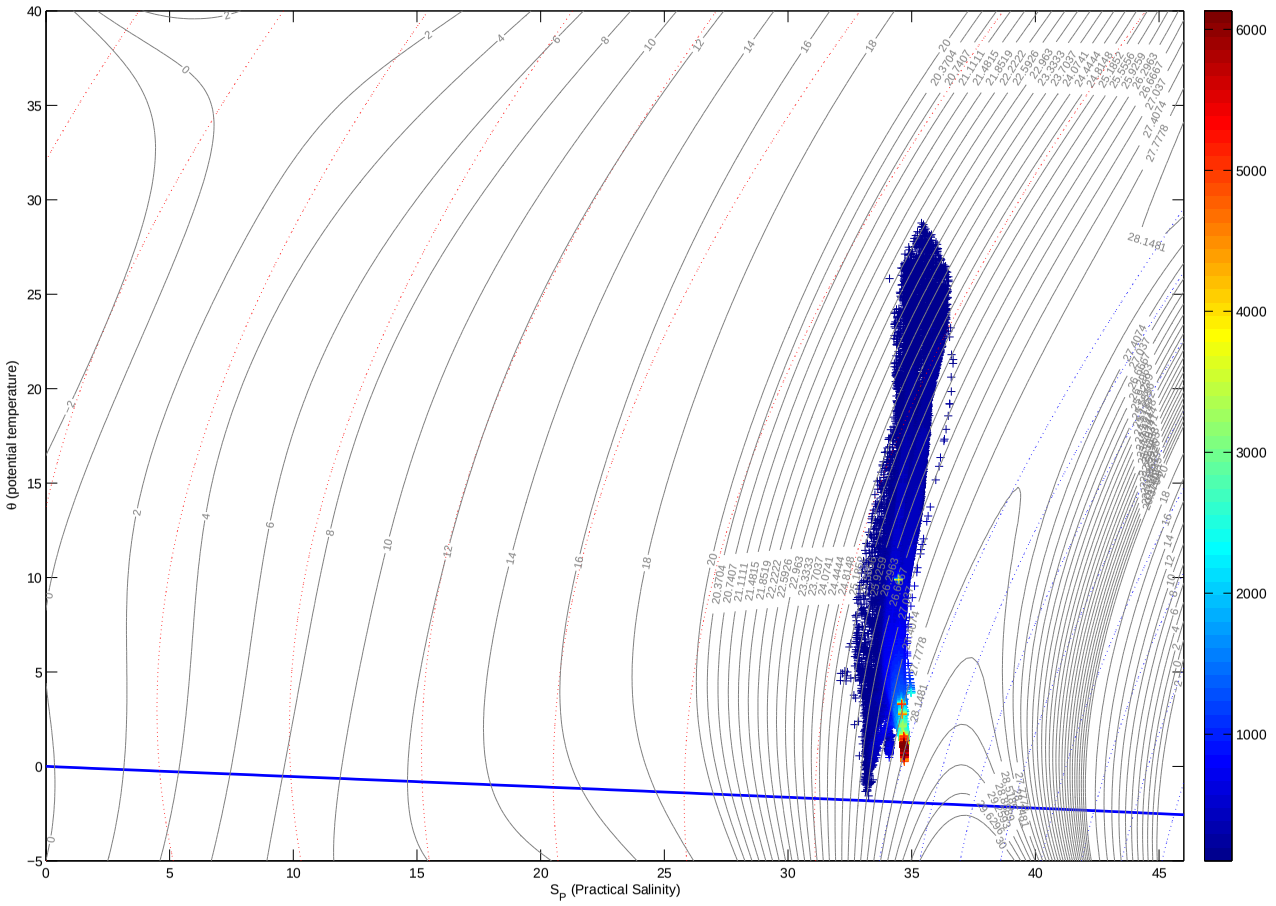

Figure A.3: Hydrographic data used to build γ^{poly} on the North Pacific plotted on the $S_P - \theta$ diagram, coloured by pressure. Isopycnals of γ^{poly} are plotted from $-2\,kg.m^{-3}$ to $30\,kg.m^{-3}$ (grey). Isopycnals of σ_0 are also plotted for low salinities (red dot) and σ_4 for high salinities (blue dot). The freezing line is drawn by the solid blue line at pressure $p = 0\,db$.

North Indian polynomial coefficients

$\hat{P}$	1	θ	θ^2	θ^3	θ^4	θ^5	θ^6
1	0.915127744449523	0.276709571734987	-1.29591003712053	3.75322031850245	-5.64931439477443	0.738499368804742	1.42081034484842
S_P	2.52567287174508	-5.95006196623071	-0.628267986663373	14.5023693075710	4.04000477318118	-6.93690276392252	
${S_P}^2$	-0.531583207697361	23.8940719644002	-39.2270069641610	-30.0525851211887	13.2992863063285		
${S_P}^3$	-6.52652369460365	0.341647815015304	88.0985881844501	0.754772283610568			
${S_P}^4$	1.92080379786486	-64.7046763005989	-43.1528176185231				
${S_P}^5$	20.3803121236886	46.5646683140094					
${S_P}^6$	-16.6137493655149						

North Indian on salinity-temperature diagram

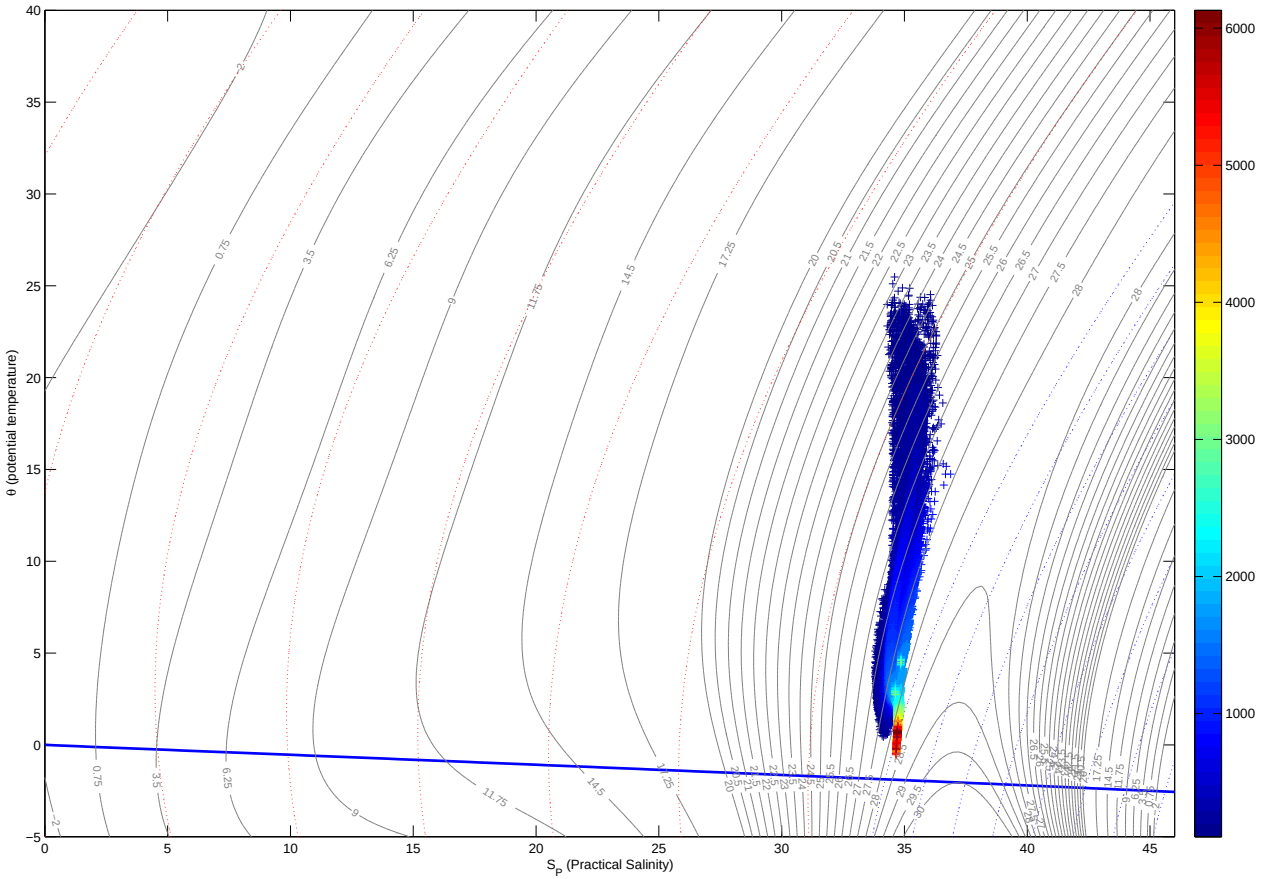

Figure A.4: Hydrographic data used to build γ^{poly} on the North Indian plotted on the $S_P - \theta$ diagram, coloured by pressure. Isopycnals of γ^{poly} are plotted from $-2\,kg.m^{-3}$ to $30\,kg.m^{-3}$ (grey). Isopycnals of σ_0 are also plotted for low salinities (red dot) and σ_4 for high salinities (blue dot). The freezing line is drawn by the solid blue line at pressure $p = 0\,db$.

Southern Ocean polynomial coefficients

$\hat{P}$	1	θ	θ^2	θ^3	θ^4	θ^5	θ^6
1	0.874520046342081	2.05462556912973	-9.03290825881587	21.4780019724540	-21.0132492641922	4.26251346968625	1.44257249650877
S_P	-1.64820627969497	-8.27848721520081	0.949958161544143	-11.7794732139941	31.2611766088444	-10.8585153444218	
${S_P}^2$	28.0996269467290	34.8904015133508	-4.44794543753654	-32.9544488911897	1.95823443401631		
${S_P}^3$	-91.0872821653811	-50.0511970208864	44.5061015983665	11.9380310360096			
${S_P}^4$	133.921771803702	7.85544471116596	-27.7122792678779				
${S_P}^5$	-85.1619212879463	13.4683704071999					
${S_P}^6$	17.2136374200161						

$\hat{Q}$	1	θ	θ^2	θ^3	θ^4
1	0.209190309846492	-3.06518655463115	39.0265896421229	-215.306225218700	20.1983279379898
S_P	-1.92636557096894	2.96183396117389	-53.6710556192301	264.211505260770	
${S_P}^2$	9.06344944916046	3.87221350781949	3.68258441217306		
${S_P}^3$	-15.3989635056620	-3.14460332260582			
${S_P}^4$	8.31163564170743				

Southern Ocean on salinity-temperature diagram

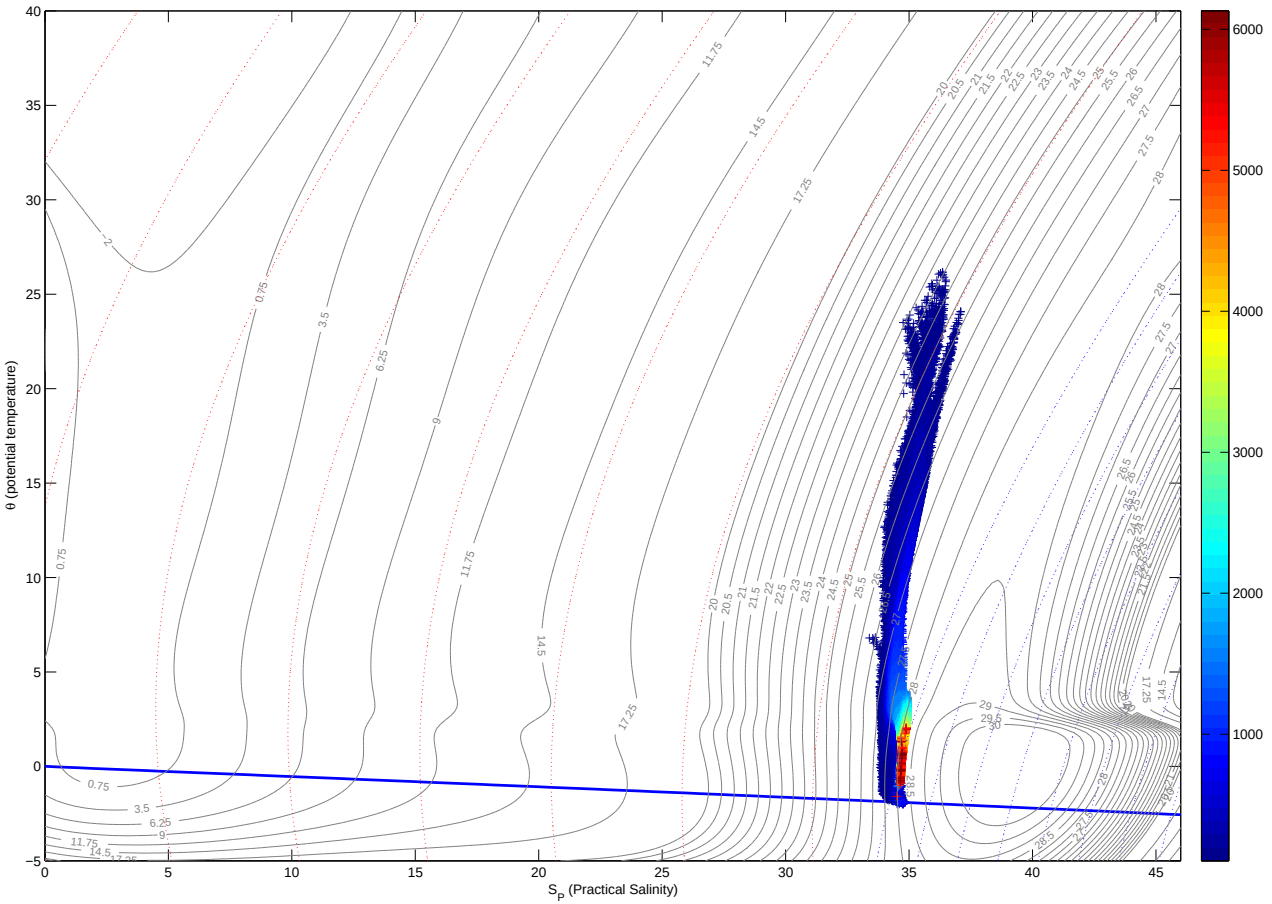

Figure A.5: Hydrographic data used to build γ^{poly} on the Southern Ocean plotted on the $S_P - \theta$ diagram, coloured by pressure. Isopycnals of γ^{poly} are plotted from $-2\,kg.m^{-3}$ to $30\,kg.m^{-3}$ at a referenced pressure of $0\,db$(grey). Isopycnals of σ_0 are also plotted for low salinities (red dot) and σ_4 for high salinities (blue dot). The freezing line is drawn by the solid blue line at pressure $p = 0\,db$.

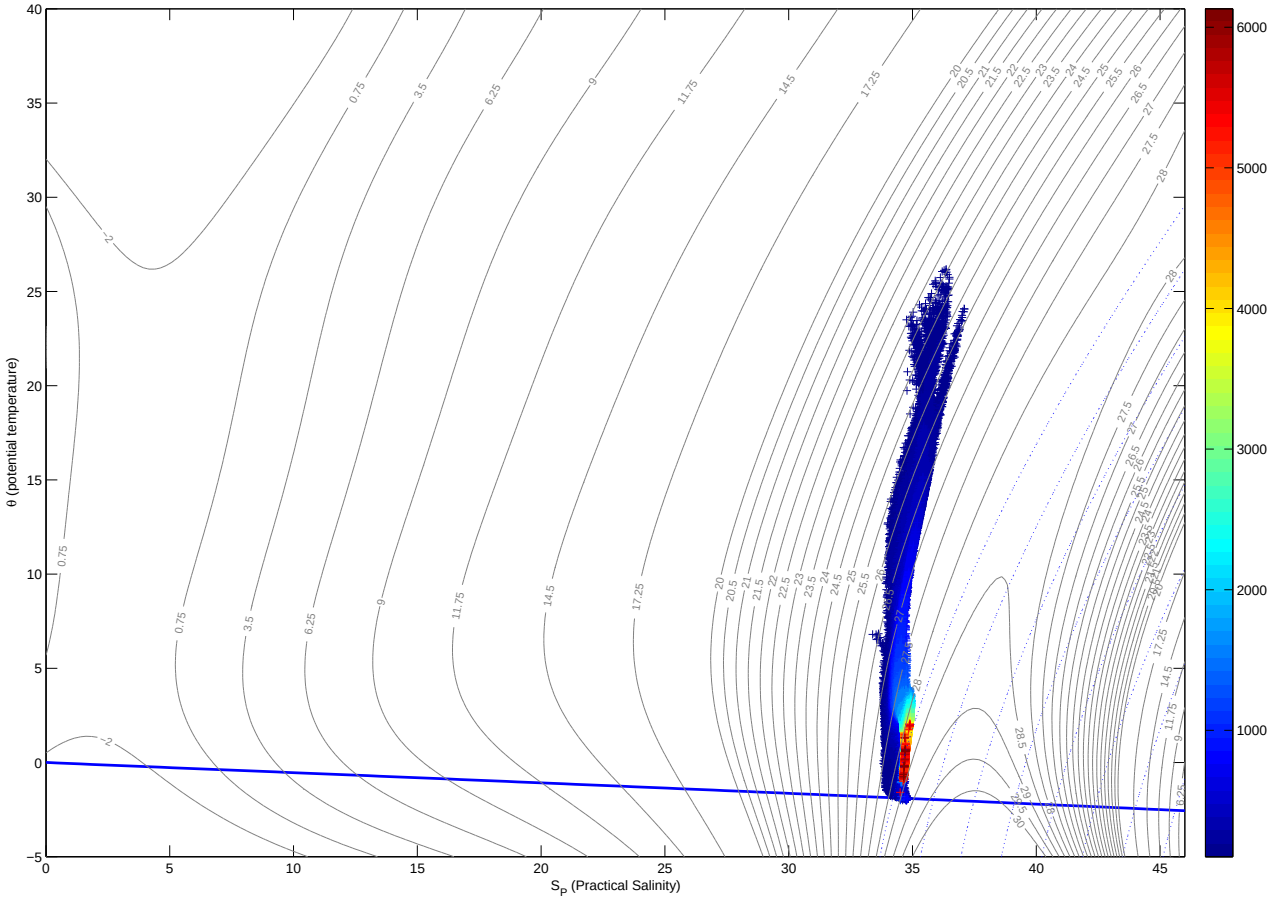

Figure A.6: Hydrographic data used to build γ^{poly} on the Southern Ocean plotted on the $S_P - \theta$ diagram, coloured by pressure. Isopycnals of γ^{poly} are plotted from $-2\,kg.m^{-3}$ to $30\,kg.m^{-3}$ at a referenced pressure of $4000\,db$(grey). Isopycnals of σ_4 are also plotted for high salinities (blue dot). The freezing line is drawn by the solid blue line at pressure $p = 0\,db$.

Appendix B

List of symbols

Quantity	Symbol	Units	Comments
Absolute pressure	P	Pa	When absolute pressure is used it should always be in Pa, not in $M\,Pa$ nor in $dbar$.
Sea pressure	p	$dbar$	Equal to $P - P_0$ and expressed in $dbar$ not Pa.
Reference pressure	p_r	$dbar$	The value of the sea pressure p to which potential temperature or potential density are referenced.
One standard atmosphere	P_0	Pa	exactly $101\,325\,Pa$
Standard Ocean Reference Salinity	S_{SO}	$g.kg^{-1}$	$35.165\,04\,g.kg^{-1}$ corresponding to the standard ocean Practical Salinity of $35\,g.kg^{-1}$
Practical Salinity	S_P	1	Defined by the range 2 <= S_P <= 42 by PSS-78
Reference Salinity	S_R	$g.kg^{-1}$	Reference Composition Salinity (or Reference Saliniy for short) is the Absolute Salinity of seawater samples that have Reference Composition. At $S_P = 35$, S_R is exactly $35.165\,04\,g.kg^{-1}$ while in the range 2 <= S_P <= 42, $S_R = \frac{35.16504\,g.kg^{-1}}{35} S_P$
Absolute Salinity	S_A	$g.kg^{-1}$	$S_A = S_R + \delta S_A$
Absolute Salinity Anomaly	δS_A	$g.kg^{-1}$	$\delta S_A = S_A - S_R$
In situ temperature	t	$°C$	
Absolute Temperature	T	K	$T = 273.15 + t$
Potential temperature	θ	$°C$	
Conservative Temperature	Θ	$°C$	Θ is exactly potential enthalpy divided by c_p^0

A constant 'specific heat', for use with Conservative Temperature	c_p^0	$J.kg^{-1}.K^{-1}$	$c_p^0 = 3991.86795711963\, J.kg^{-1}.K^{-1}$
Specific potential enthalpy	h^0	$J.kg^{-1}$	Specific enthalpy referenced to zero sea pressure.
Thermal expansion coefficient with respect to potential temperature	α^θ	K^{-1}	$-\frac{1}{\rho}\left.\frac{\partial\rho}{\partial\theta}\right\|_{S_P,p}$
Saline contraction coefficient at constant potential temperature	β^θ	1	$\frac{1}{\rho}\left.\frac{\partial\rho}{\partial\theta}\right\|_{\theta,p}$
Isentropic and isohaline compressibility	κ	$dbar^{-1}$	$\frac{1}{\rho}\left.\frac{\partial\rho}{\partial p}\right\|_{S_P,\theta}$
Buoyancy frequency	N	s^{-1}	$N^2 = -\frac{g}{\rho}\frac{\partial\rho}{\partial z}$
Neutral helicity	H^n	m^{-1}	$H^n = \beta^\theta T_b^\theta \nabla p.\nabla S_P \times \nabla\theta$
In situ density	ρ	$kg.m^{-3}$	
Density anomaly	σ	$kg.m^{-3}$	$\rho - 1000\, kg.m^{-3}$
Potential density	ρ^θ	$kg.m^{-3}$	$\rho\left(S_P, \theta\left[S_P, t, p, p_r\right], p, p_r\right)$ where p_r is a referenced pressure
Potential density anomaly referenced to a sea pressure of $O\, dbar$	σ_0	$kg.m^{-3}$	$\rho\left(S_P, \theta\left[S_P, t, p, 0\, dbar\right], p, 0\, dbar\right) - 1000\, kg.m^{-3}$
Potential density anomaly referenced to a sea pressure of $2000\, dbar$	σ_2	$kg.m^{-3}$	$\rho\left(S_P, \theta\left[S_P, t, p, 0\, dbar\right], p, 2000\, dbar\right) - 1000\, kg.m^{-3}$
Potential density anomaly referenced to a sea pressure of $4000\, dbar$	σ_4	$kg.m^{-3}$	$\rho\left(S_P, \theta\left[S_P, t, p, 0\, dbar\right], p, 4000\, dbar\right) - 1000\, kg.m^{-3}$
Neutral Density	γ^n	$kg.m^{-3}$	A density variable whose isosurfaces are to be approximately neutral, i.e. $\alpha^\theta \nabla_{\gamma^n}\theta \approx \beta^\theta \nabla_{\gamma^n} S_P$
Improved Neutral Density	γ^i	$kg.m^{-3}$	An improved version of γ^n which is independent of a reference data set.
γ^a	γ^a	$kg.m^{-3}$	A γ-variable approximated with a rational function.
γ^{EW}	γ^{EW}	$kg.m^{-3}$	A γ-variable with a function fitted to the North Atlantic.
ω	ω	$kg.m^{-3}$	Density surfaces which are designed to be approximately neutral, i.e. $\alpha^\theta \nabla_\omega \theta \approx \beta^\theta \nabla_\omega S_P$

Neutral density polynomial on a ocean basin	γ^{poly}	$kg.m^{-3}$	A γ-variable with a polynomial fitted on a particular ocean basin
Neutral density Global Polynomial	γ^{GP}	$kg.m^{-3}$	A γ-variable with polynomials which are the combination of the γ^{poly} functions.
Gradient on a neutral tangent plane	∇_n		
Gradient on a continuous "density" surface	∇_a		
Slope error between a continuous "density" surface and the neutral tangent plane	$\mathbf{s}$	1	$\mathbf{s} = \nabla_\mathbf{n}\mathbf{z} - \nabla_\mathbf{a}\mathbf{z}$
Density gradient error between a continuous "density" surface and the neutral tangent plane	ϵ	m^{-1}	$\epsilon = \frac{N^2}{g}\mathbf{s}$
Epineutral diffusivity	K	$m^2.s^{-1}$	
Dianeutral diffusivity	D	$m^2.s^{-1}$	
Fictitious diapycnal diffusivity	D^f	$m^2.s^{-1}$	$D^f = K\mathbf{s^2}$
Diapycnal velocity through a neutral tangent plane	e	$m.s^{-1}$	
Diapycnal velocity through a continuous "density" surface	e^a	$m.s^{-1}$	
Diapycnal velocity due to the spatial effects of neutral helicity	e^{hel}	$m.s^{-1}$	